SAHC

Study of the seismic performance of traditional masonry buildings in the “Barceloneta” neighbourhood of Barcelona.

Stavri Gjergji Burda

Spain | 2020

ADVANCED MASTERS IN STRUCTURAL ANALYSYS OF MONUMENTS AND HISTORICAL CONSTRUCTION

Master’s Thesis

Stavri Gjergji Burda

Study of the seismic performance of traditional masonry buildings in the “Barceloneta” neighbourhood of Barcelona

UNIVERSITAT POLITÈCNICA DE CATALUNYA

University of Minho

Spain | 2020

DECLARATION

Name:	Stavri Burda
Email:	stavriburda@gmail.com

Title of the Msc Dissertation:	Study of the seismic performance of traditional masonry buildings in the “Barceloneta” neighborhood of Barcelona
Supervisor(s):	Professors Pedro Roca Fabregat and Cossima Cornado Bardon
Year:	2019-2020

I hereby declare that all information in this document has been obtained and presented in accordance with academic rules and ethical conduct. I also declare that, as required by these rules and conduct, I have fully cited and referenced all materials and results that are not original to this work.

I hereby declare that the MSc Consortium responsible for the Advanced Masters in Structural Analysis of Monuments and Historical Constructions is allowed to store and make available electronically the present MSc Dissertation.

University:	Universitat Politècnica de Catalunya
Date:	21/07/2020
Signature:	_____

This page is left blank on purpose.

ACKNOWLEDGEMENTS

Foremost, I would like to express my deepest gratitude to both my advisors Prof. Pere Roca and Cossimo Corrando for their lead, support, in-depth knowledge, and insightful comments.

Besides my both advisors, I would like to thank, two valuable friends, Ernesto Inzunza Araya and Darion Vecchio which have proven to be very good friends and have provided unconditional support to me during my studies.
My professional career, of 5 years, gave me the opportunity to work and study more in-depth in the field of preservation. The way in which the past and the future can be interwoven and impact our present still fascinates me. Being able to build our present based on the past, especially in the preservation field, is one of the main drivers in my work.

Joining SAHC Master in the field of building heritage conservation is one of the best decisions in my professional career.
The in-depth information, analysis, and knowledge that I gained during 11 months of studying have shaped me with better tools for the future field - preserving projects yet to come.

And finally, I want to thank all my friends and especially my family, without the support of whom this journey would have been much more difficult.

This page is left blank on purpose.

ABSTRACT

This study is focused on the evaluation of the seismic performance of la Barceloneta neighborhood typology to estimate and assess the expected damage if hit by an earthquake. The main aim is to calculate, using the Vulnerbility index methodology, and nonlinear kinematic analysis to draw results based on which it is defined whether the neighborhood is safe or further investigation is required.

The historic neighborhood of la Barceloneta, in Barcelona, is characterized by its straight narrow streets, that lead to the sea. Its perfect location along the Barceloneta beach makes it a very popular neighborhood. The neighborhood was initially designed and built with 2-story houses during the 18th century, to accommodate the residents of the neighborhood La Ribera, who had to move due to the demolition ordered by Felipe v to build Parc de la Ciutadella. Nowadays only a few houses from the original design have survived, most of them are four, five, and six stories.

Unreinforced masonry buildings are among the most vulnerable structures in the Mediterranean region, a region with high seismic activity.

A state-of-the-art investigation was done in the field of seismic vulnerability evaluation in large scale and nonlinear kinematic analysis of masonry structures to define the best techniques to perform the seismic evaluation of la Barceloneta.

The analysis uses vulnerability index method evaluation based on GNDTII level approach (GNDT, 1994) which is adopted for the Portuguese context.

During the vulnerability index analysis, 14 parameters that characterize the building's type of structure, level of connection, and quality of resisting systems are evaluated.
Each parameter is distributed in classes from a to d, a for the highest quality while d for the lowest. These parameters are equivalent to numbers which in the end are multiplied with the weight coefficient that expresses the importance in the structure. The final result, the expected damage in case of an earthquake, is expressed in percentage.

The second analysis method used is the nonlinear kinematic analysis, which studies the activation of local mechanisms in masonry structures to determine the capacity of the element. The evaluation of the performance point is carried out based on well-known standards such as Eurocode 8 (2004), Spanish seismic code (NCSE-02, 2002), Atc (1996), and (NTC 2018).
The model geometry, according to drawings, was considered to represent well the typology of la Barceloneta house. In total 12 types of structures were identified based on the number of stories and their position in the aggregate. For each of the possible local mechanisms were defined. In corner buildings' types, 15 mechanisms were identified, while for attached buildings amongst a row just 8. The capacity of the corner buildings was lower compared to buildings amongst a row. All in all, the most vulnerable mechanism is considered the vertical strip failure (partial collapse)

This page is left blank on purpose.

RESUMEN

El barrio histórico de La Barceloneta, en Barcelona, se caracteriza por sus estrechas y rectas calles que conducen al mar. Su ubicación privilegiada a lo largo de la playa de la Barceloneta lo hacen un vecindario muy popular. Inicialmente, casas de dos pisos fueron construidas durante el siglo XVIII para albergar a los residentes del barrio La Ribera que habían perdido sus hogares debido a la demolición ordenada por Felipe V para construir el Parc de la Ciutadella. Actualmente, sólo unas pocas viviendas del diseño original han sobrevivido y la mayoría corresponde a estructuras de cuatro, cinco y seis pisos.

Los edificios de albañilería no reforzada se encuentran entre las estructuras más vulnerables en regiones con actividad sísmica elevada, como la zona del Mediterráneo. Este estudio se centra en la evaluación del desempeño sísmico de la tipología presente en La Barceloneta, para estimar y evaluar el daño esperado. La intención es obtener resultados que sugieran si el vecindario es seguro o si futuras investigaciones debiesen ser desarrolladas.

Una investigación sobre el estado del arte fue realizada en el área de la vulnerabilidad sísmica a gran escala, en conjunto con el análisis no-lineal cinemático de estructuras de albañilería. El objetivo fue definir las mejores técnicas para llevar a cabo la evaluación sísmica de La Barceloneta.

El análisis utiliza la evaluación del método del índice de vulnerabilidad basado en el enfoque GNDT nivel II (GNDT, 1994) y entonces aplicado al contexto portugués. El análisis se basa en la evaluación de 14 parámetros que caracterizan al edificio en términos del tipo de estructura, nivel de conexión, calidad del sistema resistente, etc. Cada parámetro es definido en clases desde la A a la D, donde A significa alta calidad y D baja calidad. Estos parámetros son equivalentes a números que al final son multiplicados con el coeficiente de ponderación, que representa la importancia de la estructura. El resultado final es expresado en porcentaje del daño esperado en el caso de un terremoto.

El siguiente método corresponde al análisis no-lineal cinemático, el cual estudia la activación de mecanismos locales en construcciones de albañilería para determinar la capacidad del elemento. La evaluación del desempeño se lleva a cabo de acuerdo a códigos conocidos, como los son el Eurocódigo 8 (2004), el Código Sísmico Español (NCST-02, 2002), ATC (1996) y el NTC (2018). La geometría del modelo fue considerada de acuerdo a planos que representan la tipología de una casa en La Barceloneta. En total, 12 tipos de estructuras fueron identificadas, basadas en el número de pisos y en su ubicación dentro de la construcción. Para cada una de ellas se identificaron los posibles mecanismos locales. En el caso de edificios de esquina, 15 mecanismos fueron identificados, mientras que, en edificios interiores, sólo 8. La capacidad de los edificios de esquina fue inferior a la obtenida para edificios interiores. El mecanismo más vulnerable es considerado el de la falla de la banda vertical (colapso parcial).

Esta tesis brinda algunas recomendaciones sobre las técnicas de refuerzo más apropiadas, con la intención de asegurar el comportamiento de caja. Diferentes soluciones prácticas son sugeridas con el objetivo de aplicar los principios de preservación y que además sean simples y económicas.

Finalmente, esta tesis compara los dos métodos de análisis, discutiendo cómo los resultados comparan, contrastan y ponderan sus ventajas y desventajas. Se proveen conclusiones sobre el estado actual de La Barceloneta y cómo esto se ve reflejado en el estado de conservación del vecindario.

This page is left blank on purpose.

TABLE OF CONTENTS

LIST OF FIGURES

LIST OF TABLES

1. INTRODUCTION

1.1 Background

Culture Heritage buildings are constantly threatened by social changes, lack of maintenance, natural phenomena, material decay, etc... It represents a strong value for humankind and the Venice Chart (ICOMOS, 1964) reminds us every single day about the responsibility to protect it:

> *<<Imbued with a message from the past, the historic monuments of generations of people remain to the present day as living witnesses of their age-old traditions. People are becoming more and more conscious of the unity of human values and regard ancient monuments as a common heritage. The common responsibility to safeguard them for future generations is recognized. It is our duty to hand them on in the full richness of their authenticity.>>*

Conservation, as we perceive it today, is a complex activity. Since the nineteenth century, it has been developed in scope, strengthened in importance, and come of age. It has not always been this way; just a few decades ago, it was much simpler, and some decades before that, it did not even exist – it did not exist as we know it: as a particular activity, that requires special, well-trained skills, which are different from those of the artist, the carpenter or the sculptor.

Conservation began when it became clear that the views, approaches, and skills required to treat a painting were different from those required to treat the walls of a common peasant house.

However, the process itself is marked with many theoretical and practical mistakes, which are marked by loss of Cultural Heritage buildings, loss of values and, because of inappropriate intervention, etc.… (Salvador Munoz Vinaz, 2005)

In the nineteenth century, the ideas of the age of enlightenment gained momentum and wide recognition: science become the primary way to reveal and avail truths, and public access to culture and art become an acceptable idea. As a result, historical structures, artworks – and artists – acquired a special recognition, and science became an acceptable way to analyze reality (Salvador Munoz Vinaz, 2005).

In this context, the trend nowadays is to use scientific approaches in achieving the desired results in terms of evaluation, intervention, and protection. However, science has little to do with decisions based on taste, beliefs, and preferences but it has an important role to play in technical decisions, as it can collaborate in developing more efficient conservation techniques.

1.2 Objectives

The primary objective of the dissertation is to evaluate the seismic performance of the traditional unreinforced buildings located in La Barceloneta neighborhood in Barcelona, Spain. The evaluation will be conducted through the vulnerability index method and the non-linear kinematic analysis approach.

The primary objective requires the definition of many other secondary objectives that are going to be listed here below and treated in the state of the art and applied to the respective chapters.

Firstly, a comprehensive review regarding the approach methodologies for the structural assessment of the historical constructions hast to be performed. This will lead to the selection and implementation of the most appropriate methods for the present study.
Secondly, a search in the archives will improve our understanding regarding the historical developments and La Barceloneta morphology.

Thirdly, investigation on the typology, building material, and techniques, will be necessary to ensure that the building is representative of the typical construction of La Barceloneta neighborhood.

Fourthly, characterization of its structural layout will lead to; understanding of the structural walls and their implication in a seismic behavior, distribution of floors and their rigidity, the connection between horizontal diaphragms and vertical walls, and the mechanical properties of the materials.

Fifthly, an investigation on the seismic behavior of unreinforced masonry structures and the identification of local mechanisms will facilitate the understanding of the possible structural failures of La Barceloneta typology due to seismic events.

Finally, the identification of the seismic scenarios will determine the expected level of damage to the building for each scenario.

1.3 Work organization

The thesis report summarises the information laid down in seven chapters, as per the assessment methodology adopted for the study. Chapter two treats: the state of art in a context seismic evaluation on a large scale, the limit analysis, and the historical investigation. Chapters three, four, and five provides an overview of the case study’s application. Whereas the conclusions deriving from the case study are enlisted in chapter six. A synopsis for each of the chapters is laid down below.

Chapter one firstly gives a brief introduction of the study and its relevance and by considering the seismic context of the city. Secondly, an outline of primary and secondary objectives is provided to explain the expectations from the report

Chapter one starts with a brief introduction of the study and continues by explaining its relevance in line with the seismic context of the city. Then, an outline of primary and secondary objectives is provided to explain the expectations from the report

Chapter two comprises the state-of-the-art description in a seismic context. Two analysis techniques are detailed; the vulnerability index analysis method and the kinematic analysis method. Furthermore, a historical investigation on the evolution of the neighborhood, morphology, and building techniques is provided in order to increase the understanding regarding the building typology.

Chapter three explains the assessment of the unreinforced masonry buildings in La Barceloneta neighborhood through the vulnerability index method. The primary steps taken during the process are clearly identified and the methodology for each of the steps is provided.

Chapter fours are provided all the results from the nonlinear kinematic analysis, identification of local mechanisms based on Italian guidelines for the evaluation, and mitigation of seismic risk of cultural heritage. Identification of the type of soil and computation of the response spectrum by two current codes, Eurocode 8 (2004) and NCSE-02 (2002) is provided, followed by an assessment of their influence on seismic demand.

In Chapter four the following analysis and identification have been computed:

- Nonlinear kinematic analysis:
- Identification of local mechanism based on Italian guideline for the evaluation and mitigation of seismic risk of cultural heritage:
- Identification of the type of soil:
- Computation of response spectrum by two current codes, Eurocode 8 (2004) and NCSE-02 (2002)

The results streaming for each of the computations is provided, followed by an assessment of their influence on the seismic demand.

Finally, chapter five gives recommendations on strengthening proposals based on the best experiences in the Mediterranean region. They are preliminary suggestions, and validation through other techniques of seismic assessment is mandatory.

In chapter 7 recommendations on strengthening proposals-based on experiences in the Mediterranean region have been drafted. These proposals are preliminary, and validation complemented by other techniques of seismic assessment is mandatory.

2. STATE OF THE ART

In the 1960s, due to many wrong decisions in the treatment of cultural heritage buildings damaged after World War II, the Venice Charter was established, which should be considered as an ethical guideline, a sort of firm reference for the conservation of monuments. Together with many other documents, (Burra Charter, Nara Document on Authenticity) they are considered now the international doctrines. Anyway, the Venice Charter contained some of the embryonic issues, later developed, like Authenticity, Historic centers, Historical Urban Landscape, etc... (Jukka Jokilehto, 2010)

The 1960s were focused on monuments and archeological remains while the 1970s had a focus on the emphasis of urban heritage, historic towns, historic centers, conservation areas, etc… Certainly, this focus on the field culminating in 1975 which was marked as the European Architectural Heritage Year (1975). In 1976 UNESCO adopted the International Recommendation concerning the Safeguarding and Contemporary Role of Historic Areas which has remained a valid document until today. Another document adopted by UNESCO, with a focus on urban heritage, is the International Recommendation on Historic Urban landscapes of 2011 (Jukka Jokilehto, 2010).

In this context, the awareness regarding conservation of historic towns has been increased during the last 50 years and as a result, the number of disciplines helping in this process has increased. Throughout the human civilization historic towns have suffered a lot from natural disasters like earthquakes, fire, floods, etc... Losses caused to cultural heritage from human life are irreplaceable, and the reduction of these effects requires studies and interventions that increase safety in every aspect. Engineering which deals with historical structures is a relatively new discipline, but it is progressing very fast and while respecting conservation principles it is giving very good results in improving the structural stability of monuments.

2.1 Seismic Risk

Seismic risk is the potential or the probability of a loss because of the occurrence of an earthquake for a given period. According to (Smith W, 2005) seismic risk has different meanings for different stakeholders. For example, engineers are interested in the probability that a specific level of ground motion at a site of interest could be exceeded in a given period, a definition that is analogous to flood and wind risk (Sacks, 1978; Gupta, 1989), whereas insurance companies are more interested in the probability that a specific level of losses in a region or at a specific site could be exceeded in a given period. Generally, the seismic risk is defined as the combination of three main elements: (i)the *seismic hazard*; (ii) the *assets at risk* (i.e., the assets that are threatened by the earthquake in terms of value), and (iii) the *vulnerability* of the assets by the phenomena of the earthquake. Figure 2.1-1 depicts it conceptually.

While seismic hazard has relatively specific objectives related to the physical effects (faulting, shaking, liquefaction, land-sliding, tsunami, etc.) of the seismic event on the natural environment, no matter if defined deterministically or probabilistically, the elements of assets at risk and vulnerability need explanation. Assets at risk are used herein broad terms – it includes not only the material items that have financial value but also non-material items that have financial value (e.g., business interruption, reputation) and very specifically, those intangible non-material items of great value, such as disruption of everyday life, political union, education, mental health and so on. There are not a few instances of governments overthrown due to their inadequate response to a great earthquake (e.g., 1755 Lisbon, 1972 Managua). Vulnerability is the susceptibility of the assets to the hazard, so that vulnerability is defined here just as broadly as an asset.

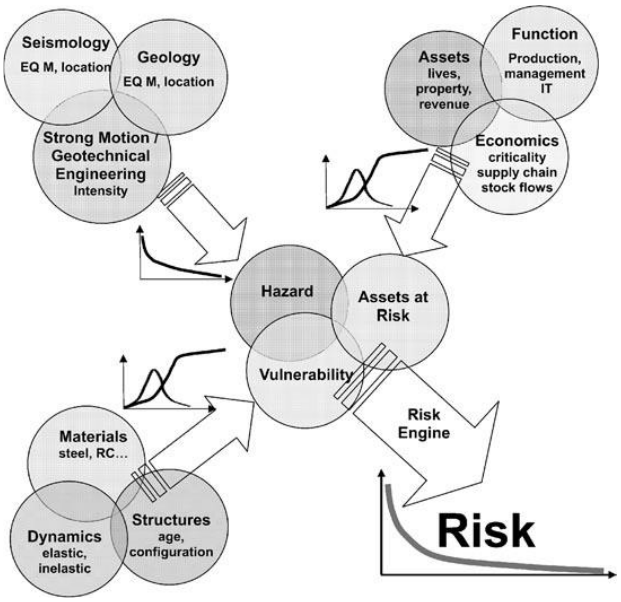

Figure 2.1-1 Elements of seismic risk (Risk Assessment, Modelling and Decision Support: Strategic Directions)

Anyhow the process of analyzing the risk must be materialized, for this reason, a mathematical operation is introduced.

Most of the authors, [Caicedo et al. (1994), Cardona (2001), Coburn and Spence (2002), McGuire (2004) and Barbat et al. (2010)] agree that absolute risk can be expressed as the result of the relationship between earthquake hazard, vulnerability, and exposure: *(UNDRO 1979)*.

$$R_{ie}|_T = (H_i, V_e)|_T * E|_T$$ Equation 2.1.1

Where:

- $R_{ie}|_T$ is the probability of exceedance of a certain level of loss of an exposed element e, because of the occurrence of a seismic event of certain intensity i.
- H_i *is the* seismic hazard defined as the probability that a certain ground motion parameter will be exceeded in a period of T years. (i.e., an earthquake of M8 or greater or MMI VIII or greater with a recurrence interval of 100 years)
- V_e is the vulnerability that is the intrinsic predisposition of a certain element e to suffer damage resulting from a seismic event of intensity i.
- $E|_T$ is the exposure of the assets at risk, reflecting the value of the one exposed (i.e., population, a building with a life of 50 years, etc...)

Thus, high seismic hazard does not necessarily mean high seismic risk if exposure is low, and vice versa.

Keeping this conceptual framework proposed by the group of UNDRO’s experts gathered in 1979 in a meeting proposed by UNDRO and UNESCO, the Institute of Seismic Engineering and Seismology (IZIIS) in Skopje, former Yugoslavia, proposed in 1985 to eliminate the exposure variable E, considering it implicit in vulnerability V, modifying significantly the original conception (Cardona 1985). In other words: you are not "vulnerable" if you are not "exposed". This formulation was initially proposed by Fournier d’Albe (1985), Milutinoviç and Petrovsky (1985b), and later, by Coburn and Spence (1992). This proposal in vulnerability and risk assessment widely accepted in the technical and scientific field was calculated using the following equation:

$$R_{ie}|_T = (A_i, V_e)|_T$$ Equation 2.1.2

In other words, this means that once the threat or danger A_i is known, understood as the probability of an event occurring with an intensity greater than or equal to i during a period of exposure T, and known the vulnerability V_e, understood as the intrinsic predisposition of an exposed element e to be affected or to be susceptible to damage upon the occurrence of an event with intensity i, the risk R_{ie} is expressed as the probability of a loss on the element e, as a result of the occurrence of an event with an intensity greater than or equal to i.

That is, risk, in general, can be understood as the probability of loss during a given time period t (Cardona 1985 / 86a)

2.1.1 Evaluation of the seismic hazard

Seismic Hazard can be expressed in two ways: (i) through a deterministic approach in which a specific earthquake scenario is identified, usually the most adverse and (ii) probabilistic approach in which all possible earthquake scenarios are identified and taken into consideration.

Deterministic approaches are considered simpler and more conservative while probabilistic earthquake analysis (PSHA) is complex and requires mathematical formulation to account for uncertainties related to earthquake size, location, time of occurrence related to various levels of ground shaking. The result of the relation between ground shaking and probability constitutes a hazard curve which expresses the probability of exceedance of an earthquake within a period of time (e.g. return period 500 years). All these probabilistic results are usually used to draw the hazard map of a town, region, or country.

The first inceptions of PSHA were done by (Cornell, 1968) and (McGuire, 1976). Since then several critical developments can be identified such as the derivation of new models to describe the recurrence of earthquakes, complex representation of earthquake sources, sophisticated ground motion prediction equations (GMPE), etc...

Probabilistic earthquake hazard analysis follows mainly two main approaches: (i) time-independent and (ii) time-depended. The first one incorporates geological and geodetic evidence to cover earthquakes up to thousands of years while the second one accounts for periodic trends in earthquake recurrence to predict the likelihood of earthquakes occurring in a source given the time elapsed since the previous event. As the time-depended approach requires detailed information and represents some difficulties, its application is still limited to only a few places (e.g. California and Japan)

2.1.2 Evaluation of the vulnerability

Vulnerability analysis in general is defined as the probability that a specific object will sustain a specific degree of structural damage for a given ground motion. It can be conducted on buildings, lifelines, etc… The deterministic or probabilistic approach is chosen based on the type of assets that are going to be evaluated. When we have of a group of buildings the used method is the probabilistic approach (observed vulnerability) which is based on the statistics of past earthquakes, while for single structural units (Sandi 1982) the deterministic approach (predicted vulnerability) is used referred as the assessment of expected performance based on performance and design specifications.

The vulnerability is usually represented in terms of Damage Probability Matrices (DPM) or Vulnerability (fragile) Curves. While the DPM describes a discrete relationship between the probability of damage occurrence and increasing ground motion severity, the fragility curves do it continuously as a function of the representative vulnerability index V_i and the ductile index. (Giovinazzi and Langomarsino 2004)

In the deterministic approach, the percentage of damage is assessed through performance points in conjunction with fragility curves. The performance point is derived by the intersection of the demand (spectral acceleration) and the capacity curve (spectral displacement) of the building.

On 2004 the European partnerships (RISK-UE, 2004; LESSLOSS, 2007) by constituting various workgroups which dealt with different aspects of vulnerability and earthquake risk mitigation came out with methodologies which are grouped into three essential approaches, the first, the second and the third, as per their level of detail, the scale of evaluation and data use.). The first level approach uses a considerable amount of qualitative information and is ideal for the development of seismic vulnerability assessment for large scale analysis. The Second level approach is based on mechanical models and relies on higher quality of information (geometrical and mechanical) with respect to building stock. The third and final level approach involves the use of numerical modeling techniques that require a complete and rigorous survey of individual buildings. The first and the second approach are considered a probabilistic method while the third as a deterministic one (Vincente et.al 2010)

Many researchers have been developing the systematization of these vulnerability assessment approaches that differ due to varying levels of dependency by the following factors: (i) nature and objective of the assessment; (ii) quality; (iii) availability of information; (iv) characteristics of the building stock inspected; (v) the scale of assessment (vi) methodology criteria (vii)degree of reliability of the expected results and (viii) use by the end-user of the information produced. As a result of these differences, there is a continuous issue regarding the coherency and consensus of the classification.
In this context, the most important methods and approaches developed are briefly explained below.
The first classification system, out of many others, was developed by (Corsanegno and Petrini,1990) who proposed the division of the methods into four groups according to their intended results: (i) direct; (ii) indirect; (iii) conventional and (iv) hybrid techniques. (see Figure 2.1-2).

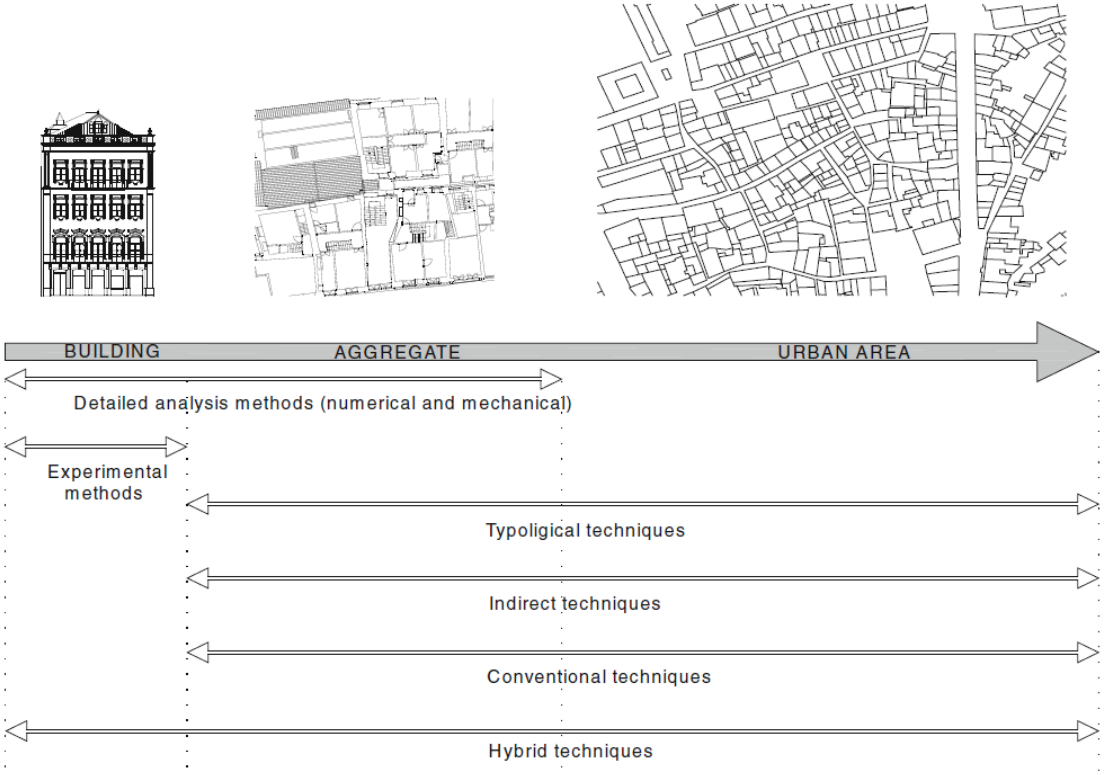

Figure 2.1-2 Analytical techniques used at different scales (Corsanego A, Petrini V. 1990)

In Direct techniques, the estimation of the damage caused to a structure by an earthquake is performed by two types of methods: (i) typological and (ii) mechanical (Vincente, 2011).
The typological method classifies the buildings in terms of materials, construction techniques, structural features, etc... The vulnerability is defined as the probability of a structure to suffer specific damage for a given seismic input.
Mechanical models predict the seismic effect on the structure based on appropriate mechanical models and they are classified into different groups based on their type of structure, i.e., analytical methods based on simple models and those more detailed analyses. The most well-known method for this method is the limit state method.

Indirect techniques involve the determination of a vulnerability index, followed by the establishment of the relationships between expected damage and hazard. One of many methods developed for the

seismic vulnerability is the GNDT (1980) which is still widely used for vulnerability assessment in large scale.

Conventional techniques are essentially heuristic because they introduce a vulnerability index which is independent by the prediction of the level of damage. They are used to compare different buildings of the same typology in a given region. Two types of approaches are used to qualify the physical characteristics of the structures: empirical and normative approach according to seismic design standards. ATC-13 (1985) is a well-known approach for this type (Section.2.3)

Hybrid techniques evaluate vulnerability through vulnerability functions based on observed vulnerability combined with expert judgments. For these techniques, vulnerability is based on the vulnerability classes developed in the European Microseismic Scale, EMS 98 (1998), (Grünthal 1998).

2.2 Masonry structures in a seismic context

Masonry is a specific construction material, which, requires structural configuration that relies on the geometry to withstand gravitational or seismic loads. Therefore, masonry buildings are simple and regular consisting of load-bearing walls. They are composed of units of walls, where the out-of-plane behavior of each unit is highly influenced by the type and strength of connections with the others. There are traditional (e.g., steel ties, wooden bands, buttresses) and innovative (e.g., mesh, composites) techniques that ensure a safe seismic behavior at the local level, by considering the typical biaxial stress state that could involve energy dissipation. If the global box behavior is not reached, the walls, mainly the peripheral ones, are more prone to out-of-plane overturning, which is one of the main reasons for damages or collapse induced by earthquakes on existing masonry structures. Main deficiencies that induce damage or collapse are the lack of proper connection between orthogonal walls, absence of connecting ties, low strength and deterioration of materials, and insufficiently rigid floor diaphragms. (Tomaževič, 1999).

(a) (b)

Figure 2.2-1 Past earthquakes, L’Aquila earthquake 2009 (The Guardian 2014), (b) Mesina earthquake 1908 (Eos, 2019)

In addition, the walls are also vulnerable to the earthquake-induced shear forces, the so-called in-plane behavior. The size and positioning of wall openings have a strong effect on the in-plane resistance as they contribute to the distribution and concentration of stresses when subjected to seismic loads. According to the results of earthquake damage analysis, three types of in-plane failure are identified; sliding shear, shear, and flexural (Figure 2.2-2) (Tomaževič, 1999)

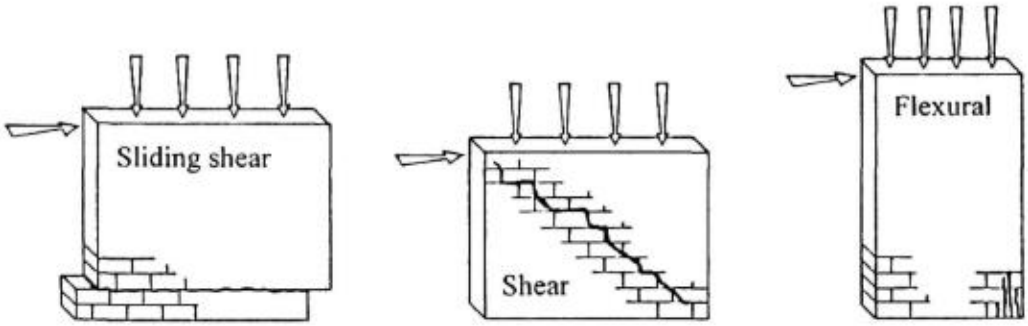

(a) (b) (c)

Figure 2.2-2 typical failure modes of masonry subjected to in plane forces (Tomaževič, 1999).

2.3 The development of seismic analysis guidelines for existing structures

The first attempts to define building vulnerability were made during the 1980s in the United States and Central and Eastern Europe, particularly in countries prone to seismicity such as: Bulgaria, Greece, Romania, and Italy. It is worth to mention that this attempt is focused on existing buildings, and the cultural heritage settlements are considered as part of them.

In 1982 the Federal Emergency Management Agency (FEMA) contracted the Applied Technology Council (ATC) to develop earthquake damage evaluation data for facilities in California. FEMA intended to use these data to estimate the economic impacts of a major Californian earthquake in the region, state, and nation.

Because there was no data available regarding the damage and loss caused by the earthquake damage, loos, or any literature inventory it was agreed that the best way for the economic impact to be measured was to build upon the experience and judgment of seasoned earthquake engineers. In 1985 ATC –13 report was published, providing damage probability matrices for 78 different buildings and facility classes located in California. This report contains background information and a detailed description of the methodology to be used to estimate the required earthquake damage/loss. Building stock was characterized based on material construction (e.g., W=wood) and lateral force resisting system (e.g., W1= single-family dwelling, S5= low-rise light metal steel buildings). Subclasifications of these categories haven’t changed very much, being used in two decades of work in the US, including HAZUS, and are model building types (MBT), which likely are going to be used for a longer period. The opinions of the experts are expressed according to beta distributions and presented in the form of Damage Probability Matrices. The resulting ground motion – loss vulnerability functions defined in ATC – 13 report streamed from empirical data collected by the experts’ observation due to the lack of statistical data. This report has stood the test of time very well.

2.4 Studies of urban assessment of seismic risk in historic centers

According to *Our World in Data,* from 1969 until now, 33% of human deaths during natural disasters are caused by earthquakes. Volcanos rank second with 30% and fire third with 14%.

Recent cases of the destruction of historical centers by earthquakes have demonstrated their vulnerability to natural hazard events. In front of this vulnerability, there is a need for efficient strategies to evaluate more in-depth their seismic risk. The comprehensive objective is to develop proper policies to enhance preparedness before any earthquake, manage the emergency, and ensure sustainable recovery after the earthquake. The management and safeguarding of urban assets and lifes require an interdisciplinary approach that combines different skills and tools. Due to the large scaling, the problem appears challenging because of the complexities of the analysis format. When it comes to individual buildings the experts have addressed the earthquake protection with great efforts but for urban risk mitigation, we must consider the coexistence of environment, citizens, open spaces, buildings, paths of the historical center. Besides that, the data collection procedure should be plausible to achieve an acceptable compromise between reliability and feasibility, ensuring time and cost sustainability. Usually, the object of the study is the clustered or the urban aggregates, which is typical for historic centers which are affected by their structural complexity, morphology, and geometry. The constituent materials may also pose further challenges because of the vernacular character that they can present related to the local culture. Under these conditions, the collected data of the building stock should be sufficient and reliable to conduct simplified analysis to obtain a reliable result within the acceptable error rate.

In 2014, Lagomarsino and Cattari (2014) established the PERPETUATE project funded by the European Commission. It was the first attempt to correlate the PLs (performance level) with DLs (damage level) where PLs is defined concerning three groups of Safety and Conservation requirements, namely: use and human life, building conservation, and artistic assets.

Mendes da Silva (2013) investigated the particularities of assets enclosed in aggregate. Due to unavoidable interaction between buildings when subjected to seismic shakes the problem complicates because of the inaccuracy. Later studies focused on the historic center of Faro and Coimbra investigated the interaction of aggregate buildings and encouraged the inclusion of aggregate effects when studying seismicity in Urban Cultural heritage assets.

In 2018, Aguado, Ferreira, and Lourenço (2018) presented a large-scale approach for the seismic vulnerability assessment of masonry buildings facade through the introduction of Vulnerability Index Methodology (VIM), which is specifically formulated for masonry facades. It allows the evaluation of the expected damage of the facade in case of earthquakes with different macroseismic intensities. The same methodology was used to study the vulnerability of Coimbria’s city aiming to assess the risk of the area, define the evacuation paths, identify inaccessible urban areas, define the number of the population affected and implement the emergency planning. Finally, the methodology proposes the potential impact of traditional seismic retrofitting to reduce the vulnerability of out of the plane failure of masonry facades.

Basaglia (2018) proposes a new approach based on the analysis of the problem from a performance-based perspective. The proposed model identifies the strategical and critical elements, to assess how their vulnerability, evaluated through VIM, affects the whole collapse probability of the urban system. This method used for the historic center of Concordia Sulla Secchia, in Italy was validated through the comparison of the results with on-site effects of the earthquake of 2012.

Applying a simplified model based on the VIM and the basic concepts of structural reliability, Cara (2018) proposed a method for seismic risk assessment and mitigation at the emergency limit condition of historical buildings. This approach allows the assessment of probable risk mitigation interventions on critical buildings to ensure the continuity of the functionality and evacuation of the urban system. The methodology is applied to the Antiga Esquerra de l´eixample a neighborhood in Barcelona, Spain.

Despotaki (2018) presented a simplified method for the large-scale assessment of UNESCO's World Heritage cultural sites in Europe. The method was used to evaluate the seismic risk of world cultural

heritage sites. It resulted that out of 351 UNESCO sites studied, 158 are located in higher seismically hazardous areas with PGA greater than 0.1g for a 10% probability of exceedance in 100 years on Soils V_{s30}= 360 m/s. The results of this study were used to reassign the soils' category and classify them in low, moderate, or high risk. The aim is to support relevant stakeholders on where to focus their funds – especially in those areas classified with high risk.

2.5 The Vulnerability index method

2.5.1 Building approach

The building approach is an assessment methodology adopted to evaluate traditionally constructed (masonry) structures, for their seismic performance in a simplified manner. This approach is based on the GNDT level II approach (GNDT 2003) to perform the vulnerability assessment as proposed by Vicente (2008) and was developed and calibrated to be applied in the Portuguese context (Ferreira 2010). This method is based on post-seismic observations, maps on damage, and data, a survey aiming to assess potential losses and post-seismic damage scenarios. The building approach considers the aspects and features of masonry structures, which define the structural damage in a building (Ferreira, 2010).

Further, the method has been adapted and tested for traditional and historic buildings of several Portuguese historic city centers, including Coimbra (Vicente, 2008), Seixal (Ferreira et al. 2013), Faro (Maio et al. 2016), Horta (Ferreira). et al. 2017b) and Leira (Elsa et al. 2019). In an international context, vulnerability assessment was also conducted for Mexico City (Salazar Flores, 2018) and the historic urban areas of Annaba City, Algeria (Athmani et al. 2018).
The building approach is determined by 14 parameters divided into 4 sets that jointly evaluate the seismic performance of the building. These parameters can be broadly organized into four groups, (Vicente 2008)

The first set of parameters evaluates the ‘Structural building system’ considering aspects such as resistance to horizontal actions or loads, and typology of the resisting system with a focus on quality, strength, and other factors influencing it. The second set of parameters evaluates irregularities and interactions, both inside and outside the building, in plan and elevation, as well as with its immediate environment. The third set evaluates the ‘Floor slabs and roof’ and the typology and strength of the horizontal diaphragms to resist seismic action. The fourth and the final set evaluates the ‘Conservation state and other elements, by means of classifying the condition, and quantifying actions due to other non-structural elements on the vulnerability.
Table 2.5-1 shows the different grouping of parameters in the building approach and the weight of each of them the final evaluation value. The total vulnerability index takes on an integer value in the range between 0 and 650 (Equation 2.5.1). It can be normalized in a global vulnerability index, I_v ranging between 0 and 100 or, 0 and 1.

Table 2.5-1 Vulnerability index associated parameters, classes, and post-calibration weights P_i (Ferreira et al. 2017)

Parameters	Class, C_{vi}				Weight	Relative weight
	A	B	C	D	P_i	
Group 1. Structural building system						
P1. Type of the resisting system	0	5	20	50	0.75	50/100
P2. Quality of the resisting system	0	5	20	50	0.75	
P3. Conventional strength	0	5	20	50	1.50	
P4. Maximum distance between walls	0	5	20	50	0.50	
P5. Number of floors	0	5	20	50	1.50	
P6. Location of soil condition	0	5	20	50	0.75	
Group 2. Irregularities and interaction	0	5	20	50		
P7. Aggregate position and interaction	0	5	20	50	1.50	20/100
P8. Plan configuration	0	5	20	50	0.75	
P9. Height regularity	0	5	20	50	0.75	
P10. Wall facade openings and alignments	0	5	20	50	0.50	
Group 3. Floor slabs and roofs	0	5	20	50		
P.11 Horizontal diaphragms	0	5	20	50	1.00	18/100
P.12 Roofing system	0	5	20	50	1.00	
Group. 4 Conservation status and other elements	0	5	20	50		
P13. Fragilities and conservation status	0	5	20	50	1.00	12/100
P.14 Non-structural elements	0	5	20	50	0. 50	

$$I_v^* = \sum_{i=1}^{14} c_{vi} P_i$$ Equation 2.5.1

where:
C_{vi} is the class of the parameter
P_i is the weight of the parameter

For example, the first three parameters are explained below while the complete list provided by Vincente et al (2008) is found in Anexx.111. Parameter 1 assesses the quality of the connections among walls, and between walls and horizontal diaphragms (floors and roofs). It evaluates the capacity of the structure to show box behavior in case of a seismic action (Table 2.5-2).

Table 2.5-2 Classification of the resisting system (parameter 1) (Vincente et al, 2008)

A	Structures built in accordance with earthquake-resistant construction reinforcement or consolidation of masonry buildings in accordance with the norms of reinforcement or strengthening referred to in European documents [European normative (Italian NTC, 2018), EC6, EC8 etc...]
B	The building has good connections with good earthquake-resistant equipment (e.g. ties), and interlocking between orthogonal walls, capable of transmitting vertical shear forces (case of stonework corners)
C	The building has no connections, defined in class B on any or only a few levels, but it has a good connection between its resistant orthogonal walls, guaranteed by the good apparatus, and overlap across the width of the walls.
D	The building does not have walls well joined. The total absence of ties and concrete confinement

The second parameter, P2, evaluates the quality of the masonry (Table 2.5-3). The evaluative experts need to get extensive knowledge regarding the type of stone or brick used for the structure (e.g. shape of stones or bricks, type of processing, etc.). The table shows the categorization of the building based on the quality of the masonry.

Table 2.5-3 Quality of the resisting system Vulnerability class definition for Parameter 3 (Vincente et al, 2008)

A	Good quality brick masonry (solid or perforated up to 45%) or well-cut stone masonry with homogeneous units and constant sizes along the entire length of the walls.
B	Brick with a perforated area less than 45% or well-cut (ashlar) stones with good quality mortar.
C	Low quality and irregular brickwork. Masonry with unworked stone units and heterogeneous dimensions. Irregular stone masonry without cross-connection, but well mortar and locked
D	Brick masonry of poor quality with the inlay of stone fragments. Masonry with very irregular stone units and a large number of voids or extremely poor-quality brick with the inlay of stone fragments. Poor condition of mortar.

The third parameter P3 evaluates the capacity of the building in shear by calculating the resistance of shear walls against horizontal seismic forces. The premise of this computation lies in the assumption that the floors are infinitely rigid, and the building does not have any eccentricity. Under this assumption, the horizontal action in both the x and y direction is computed independently, and the most vulnerable direction, i.e. the one with the minimum shear area, is taken into consideration for evaluating the conventional strength (Equation 2.1.2).

$$C_{conv} = \frac{\alpha_0 \cdot \tau_k}{q \bullet N}\left[1 + \frac{q \bullet N}{1.5 \bullet \alpha_0 \bullet \tau_k (1+\gamma)}\right] \qquad \text{Equation 2.5.2}$$

where:
q, is the average weight of the building per unit area is given by the following equation:

$$q = \frac{(A_x \cdot A_y) \bullet h \bullet p_m}{A_s} + p_s \qquad \text{Equation 2.5.3}$$

$A_x$and A_y, are the shear areas computed at the base in x and y directions
A_{min} is the minimum of A_x and A_y
A_{max} is the maximum of A_x and A_y
A_t is the total floor area covered by the building.
h is the Average height between stories
p_m is the specific weight of the masonry (in kN/m2).
p_s is the permanent load over the floor (in kN/m2).
τ_k is the characteristic value of the shear strength of the masonry unit
γ is the ratio of the minimum and maximum shear areas
α_0 is the ratio of the minimum shear area (A_{min}) and the total area covered (A_t)

The vulnerability class is assigned based on the parameter $\alpha = C_{conv}/C$ which is a ratio between the computed conventional strength of the masonry and the reference value, C=0,4. *The value of C corresponds to the* maximum seismic force or seismic action for a zone of moderate intensity.

Table 2.5-4 Mechanical properties of the masonry, Vulnerability class definition for Parameter 3 (Vincente et al, 2008)

Class	Criteria
A	Buildings with $\alpha \geq 1.0$
B	Buildings with $0.6 \leq \alpha \geq 1.0$
C	Buildings with $0.4 \leq \alpha \geq 0.6$
D	Buildings with $\alpha < 0.4$

2.5.2 Damage Scenarios and Mitigation

The vulnerability indexes calculated for each building constitute the first step in an assessment of a seismic hazard scenario. Since an earthquake can have different intensities, it is important to evaluate different scenarios to establish strategies to mitigate possible damages. The representation of the probable damages caused by a seismic event is given by the European Macro seismic Scale of 1998 (EMS-98, 1998). Through this reference of intensities and its correlation with each building vulnerability index, it is possible to establish loss scenarios comprised by:

- Probability of unusability of buildings
- Probability of collapse of buildings
- Probability of deaths and severely injured
- Probability of homelessness
- Costs of repair

However, this thesis will be calculated only the damage probability of La Barceloneta, which is considered as a reasonably well-defined structure that cannot be assessed through other methods (e.g. vulnerability index based on kinematic mechanisms (GemsrCH, 2011).

a) The Macroseismic Method

To establish the probable damage caused to a building by a specific seismic hazard it is necessary to calculate the mean damage grade (μ_D). According to Lagomarsino (2006), the assessment of a mean damage grade for a building can be done using Equation 2.5.4, and it is influenced by the macro seismic intensity defined by EMS - 98, the vulnerability index I_v, and a ductility factor Q, that corresponds to the building typology.

$$\mu_D = 2.5 + \left[3 \bullet tanh\left(\frac{I_{EMS-98} + 6.25 \bullet V - 13.1}{Q}\right)\right] \qquad \text{Equation 2.5.4}$$

where:

Q: ductility factor (2.3, for masonry buildings as suggested by Lagomarsino, 2006)
$V = 0.592 + 0.0057 \bullet I_V$ (conventional vulnerability index V)

The probability p_k of each damage grade $(D_k,\ (k = 1/5),$ in terms of both damage grade distributions and fragility curves for a certain mean damage μ_D is obtained by assuming the binomial distribution of the probability mass function (PMF), (Equation 2.5.5). (Lagomarsino, 2006)

$$PMF: p_k = \frac{5!}{k!\,(5-k)!}\left(\frac{\mu_D}{5}\right)^k \bullet \left(1-\frac{\mu_D}{5}\right)^{5-k} \qquad \text{Equation 2.5.5}$$

where ! indicates the factorial operator

b) Discrete damage grades

To visualize and simplify the mean damage grade,μ_D, caused by a seismic hazard to a building, the EMS-98 (1998) uses discrete damage grades (D_k, $k \in [0; 5]$) (Grünthal, 1998). The discrete damage grade represents the cost of returning a building to its previous condition before the earthquake occurred. The resulting Damage Factors (DF) are used to estimate the probabilities of many types of losses, from number of deaths to homelessness and even repair costs. The resulting correlations are summarized in
Table 2.5-5. A correlation between the continuous and the discrete values proposed by Bramerini et al. (1995) can be made by the application of Equation 2.5.6, an approximation suggested by Blyth et al. (2020) to the proposal made by Maio (2019). The resulting Damage Factors (DF) are used to estimate the probabilities of many types of losses, from number of deaths to homelessness and even repair costs. The resulting correlations are summarized in
Table 2.5-5.

$$\mu_D = 5 \bullet DF^{0.52} \qquad \text{Equation 2.5.6}$$

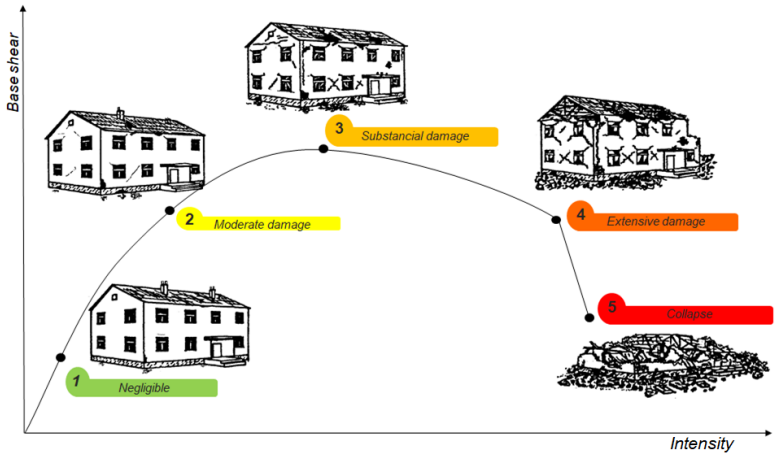

Figure 2.5-1 Discrete Damage Grades evolution (adapted from Azizi, 2017)

Table 2.5-5 Correlation between discrete damage grade and range of mean damage grade for the building approach adapted from Maio (2019) and Grünthal (1998)

Discrete damage grade Dk	**Description**	**Damage factor DF**	**Mean damage grade μD interval**
D0 – No damage	No observed damage.	0	[0.00, 0.73]
D1 – Slight damage	Hairline cracks in very few walls; Fall of small pieces of plaster only; Fall of loose stones from upper parts of the building in very few cases.	0.025	[0.73, 1.03]
D2 – Moderate damage	Cracks in many walls; Fall of fairly large pieces of plaster; Partial collapse of chimneys.	0.048	[1.03, 2.54]
D3 – Severe damage	Large and extensive cracks in most walls; Roof tiles detached; Chimneys fracture at the roof-line; Failure of individual non-structural elements.	0.272	[2.54, 4.14]
D3 – Severe damage	Serious failure of walls; Partial structural failure of roofs or floors.	0.697	[4.14, 5.00]
D5 - Destruction	Total or near-total collapse.	1	[5.00, 5.00]

c) Fragility curves

To visualize the probability of matching or exceeding the discrete damage degrees explained above, the fragility curves must be computed. (Equation 2.5.7). A beta cumulative density function is used to define the cumulative probability P_β based on the damage recorded in the database (Giovinazzi, 2005). The beta parameters are t, a, and b where t = 12, a = 0, and b = 5 (Blyth et al., 2020).

$$P(D) = 1 - P_\beta(k)$$ Equation 2.5.7

Finally, the discrete probability can be derived from the difference of cumulative probabilities which is described in Equation 2.5.8(Ferreira et al. 2013):

$$P(D_k = d) = P_D[D_K \geq d] - P_D[D_{k+1} \geq d]$$ Equation 2.5.8

2.6 Non-linear kinematic analysis of local collapse mechanisms

2.6.1 Background of the kinematic analysis

If a monolithic behavior is assured for the walls, they can be considered as rigid blocks, and their out-of-plane seismic response can be treated through two fundamental approaches: (i) rocking dynamics and (ii) kinematic analysis. To assess the response of the masonry structures under earthquakes, discrete and finite elements can be used, nevertheless, uncertainties are raised with the definition of the

constitutive laws of the materials, and therefore, these two elements are easily applied to masonry walls rather than monolithic behavior.

The basis for the subsequent research in the field of rocking blocks, studied in structural dynamics and earthquake engineering were established by Housner (1963) . He studied the dynamic behavior of a single block under seismic excitation. Aslam and Scalise were the next contributors who considered the motion of a free rocking block subjected to ground motions. They also analyzed the transition to the sliding phenomenon. Priestley et al. (1978) proposed to substitute the nonlinear dynamic system with an equivalent single degree of freedom suitable for slender structures and developed a practical methodology to compute displacements of the center of gravity of the structure due to rocking motion by using standard displacement and acceleration response spectra for an elastic SDOF oscillator. This approach was included in FEMA 356 document.

Makris and Konstantinidis [2001, 2003 (13, 14)] compared the dynamic behavior of regular and inverted pendulums and demonstrated that this methodology is oversimplified. They introduced the rocking spectrum as a distinct and valuable intensity measure of earthquakes in the case of rocking structures. However, for the assessment of existing structures, it is not fully feasible to apply this approach because rocking spectra have not been developed yet, within the ambit of Probabilistic Seism Hazard Analysis (PSHA). Therefore, rocking structures cannot be replaced by the “equivalent” SDOF oscillator. Nevertheless, if the system behaves as elastic up to the formation of a plastic hinge, the use of response spectra is justified and recommended. According to the Italian code NTC - 2018 the analysis is performed in terms of displacement capacity. The value of the displacement demand is taken from the response spectra corresponding to the secant period obtained from a capacity curve. However, for practical applications is strongly recommended a pure rocking analysis together with kinematic analysis, as well.

Out of plane bending response of parapet (free-standing) and simply supported walls (unloaded or lightly loaded), was studied by Doherty et al. (2002). Adoption of displacement-based philosophy was suggested for dynamic stability of rocking masonry elements, and even for displacement close to a quasi-static limit equilibrium condition. To sum up, a tri-linear simplified force-displacement relationship law was proposed with a finite initial stiffness is adopted and a substitute structure was defined. This procedure has been validated and through static and dynamic testing (Griffith et al. 2004). A step by step nonlinear dynamic analysis (Griffith et al. 2003) and a systematic comparison with the results given by the displacement-based simplified procedure showed that collapse can be estimated using a proper secant stiffness

Giuffre (1993) studied the local mechanisms in aggregate masonry buildings using the equilibrium limit analysis. The collapse mechanisms are arbitrarily identified and in order to build a kinematic chain, earthquake action is considered as horizontal force proportional, through a load multiplier, to dead and live load. Through the application of the theorem of virtual works, it was possible to obtain a static multiplier. A virtual infinitesimal varied configuration was considered correct if the actual collapse mechanism is selected, based on the unsafe theorem demonstrated by Heyman (1966) under the hypothesis of rigid blocks, no-tensile strength, infinite compressive strength, and absence of sliding between blocks. Similarly, D’Ayala and Speranza (2003) applied the overturning of the facades by taking into consideration the frictional behavior of mortar joints for different geometric configurations, masonry types and connections with orthogonal walls and horizontal diaphragms.

Usually, the static multiplier, which is directly linked to the peak acceleration of the seismic input (in g’s) is related only to the onset of rocking, and not to the overturning that occurs under dynamic actions. However, this is correct only if the part of the masonry structure involved in the mechanism is rigid (which is not always the case). D’Ayala (2005) proposed a displacement-based approach for the vulnerability assessment of traditional buildings. It consists of a set of possible collapse mechanisms (some of them

related to out-of-plane behavior), which evaluates the strength capacity by limit-equilibrium analysis and defines the capacity curve through estimation of the elastic period and rational value of ductility. While the displacement demand is obtained by inelastic spectra.

Lagomarsino and Resemini (2009) applied the equilibrium limit analysis not only for the out-of-plane behavior but also for the rocking of arch-piers systems (with or without tie rods). Considering geometric nonlinearity a pushover analysis was performed, to evaluate the static multiplier for varied kinematic configurations, as a function of displacement of a control point; in analogy with the capacity spectrum method (Freeman 1998; Fajfar 1999), For each bloc the nonlinear equivalent SDOF system is defined by lumping masses, at their barycenters and assuming as displacement shape the corresponding horizontal displacements of the virtual infinitesimal kinematic configuration. In the cases where rocking masonry is not resting on the ground, but it is located on the upper levels of the building, the filtering effect of the main build has to be taken into consideration for the seismic input motion. Verification of the nonstructural elements is an element in the following standards where: ASCE/SEI 41/06 (2007) gives only the seismic design force, by an empirical formula, while Eurocode 8 (EN 1998-1 2004) proposes a formula that also depends on the period of the nonstructural element, which is largely approximated. Taking into consideration the flexibility of the rocking element, it is
possible to develop a floor response spectrum, deriving from the dynamic response of the global structure. In the ’80s different authors proposed a rigorous analytical formulation for the verification of nuclear power plants. Taking this into account Curti (2007) proposed a simplified formulation for the seismic assessment of local mechanisms in ancient bell towers.

Lagomarsino and Resemini (2015) in their publication in 2014) reviewed their earlier proposal presenting a displacement-based procedure for rocking masonry. The procedure is based on the following steps: (1) definition of the rocking mechanism (by considering rigid blocks, constraints, internal and external elastic-plastic links, constructive features and masonry quality); (2) evaluation of the pushover curve, by the incremental equilibrium limit analysis performed on varied kinematic configurations; (3) definition of Performance Levels (PLs), in terms of displacement thresholds and related values of the equivalent viscous damping); (4) evaluation of the capacity curve, through the conversion to an equivalent SDOF system; (5) definition of the seismic demand, in terms of an overdamped elastic Acceleration-Displacement Response Spectrum (ADRS), modified from the seismic input at the ground level in case of local mechanisms placed at the higher levels of the structure; (6) evaluation of the values of the Intensity Measure (IM) that are compatible with the different PLs. The reliability of this proposal for the evaluation of the capacity spectrum is proved through static and dynamic experimental tests.

2.6.2 Objectives of the kinematic limit analysis

Earthquakes of past decades have shown that masonry buildings fail locally due to the lack of box behavior which allows the development of local mechanisms. These mechanisms became obvious during the 1997 earthquake in Umbria, Italy. Since then many papers dealing with kinematic analysis are published. Nowadays this analysis method is included in seismic codes where the most developed one is the Italian code (NTC – 2018). The objective of the kinematic analysis is to study the seismic behavior of masonry buildings based on the catalog of local failures developed by observations on past earthquakes. (Guidelines for evaluation and mitigation of seismic risk to cultural heritage, 2007)
The nonlinear kinematic analysis combined with N2 method which is based on the activation of the local mechanism will be applied to evaluate the safety of La Barceloneta houses and to obtain results related to the performance point and damage grade.

2.7 Explanation of the kinematic limit analysis

The limit analysis of the equilibrium according to the kinematic approach is based on the choice of significant collapse mechanisms and on the evaluation of the horizontal actions that activate this kinematic mechanism. From the comparison between the acceleration that activates the mechanism and that relating to the construction site, it is determined whether the verification is satisfied.

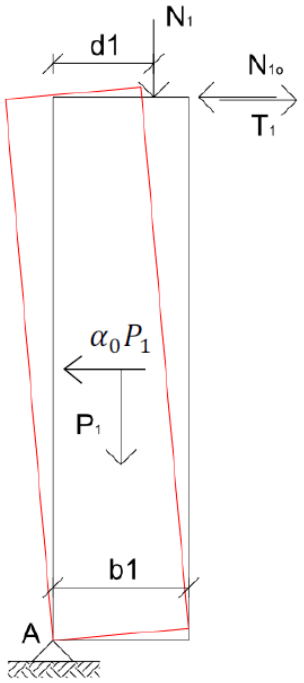

Figure 2.7-1 Overturning of the kinematic mechanism (Beninca et al., 2009)

The linear kinematic analysis of local collapse mechanisms develops according to the following phases:

- choice of the collapse mechanism that can be activated, based on the study of the crack pattern of the structure.
- definition of the portion of masonry subject to the instability mechanism (macro-element).
- transformation of the macro-element into a kinematic chain, through the identification of rigid bodies, defined by fracture plan hypothesized due to the low tensile strength of the masonry, capable of rotating or sliding between them (damage mechanism and collapse).
- calculation of the horizontal load multiplier (α_0) which involves activation of the mechanism.
- evaluation of the spectral acceleration at α_0* which causes the activation of the mechanism.
- calculation of the seismic acceleration relative to the site where the building is built.
- comparison between the 2 accelerations and safety assessment.

The first two phases are conducted by the designer based on the site evidence and the cracking state of the walls (Struture esistenti in muratura, 2015).
The most common mechanisms, with reference to Figure 2.7-2, are:

A	vertical overturning	M	failure with pillars
B1	overturning with one side wing	F	vertical arch
B2	overturning with two side wings	G	horizontal arch-top storey
C	corner failure	Gs	horizontal arch-top strip
D	partial overturning	H	in plane failure
E	vertical strip overturning		

For each significant mechanism, the microelement affected by the kinematic mechanism is hanged to determine the multiplier of the vertical loads which makes the structure labile, the method adopted is the principle of virtual works, which is applied by equaling the total work performed by external forces, applied to the system in correspondence with an act of virtual motion, to the work of internal forces.

$$\alpha_0 \left[\sum_{i=1}^{n} P_i \bullet \delta_{x,i} + \sum_{j=n+1}^{n+m} P_i \bullet \delta_{x,j} \right] - \sum_{i=1}^{n} P_i \bullet \delta_{x,i} - \sum_{h=1}^{0} P_i \bullet \delta_h = L_{fi}$$

Equation 2.7.1

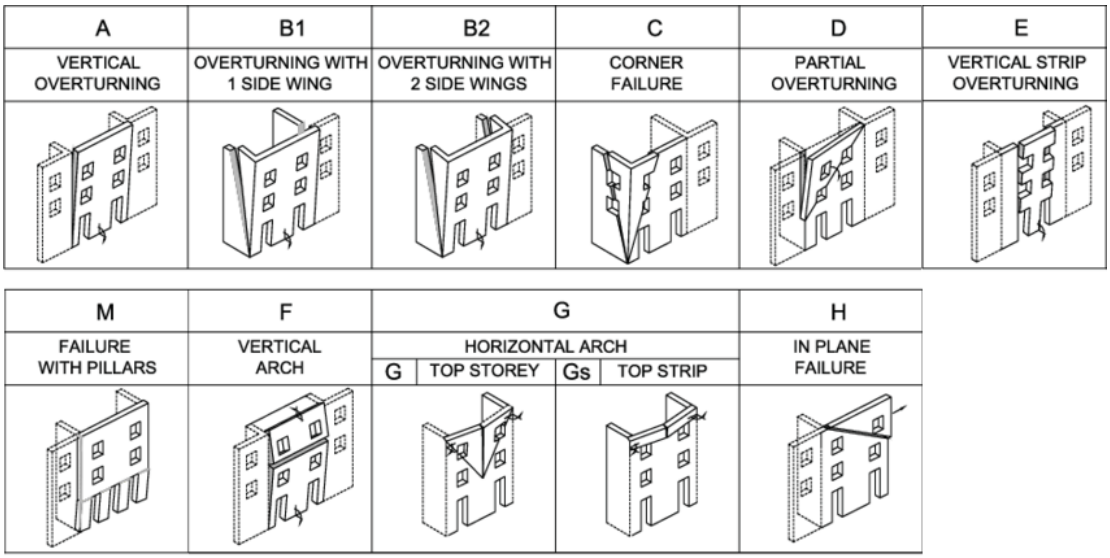

Figure 2.7-2 Mechanisms for overturning failures of (D’Ayala and Speranza 2003)

n is the total number of the forces applied on the blocks
m is the number of the influential loads not directly distributed on the blocks
o is the number of external forces applied to the blocks.
P_i is the generic weight force applied to the block.
P_j it is the generic weight force not directly weighing on the blocks, but influential to the ends of the seismic analysis as it is not effectively transmitted to other parts of the building.
$\delta_{x,i}$ is the virtual horizontal displacement of the point of application of the i-th weight P_i
$\delta_{x,j}$ is the virtual horizontal displacement of the point of application of the j-th weight P_j.
$\delta_{y,i}$ is the virtual vertical displacement of the point of application of the i-th weight P_i;
F_h is the absolute value of the generic external force applied to the block.
δ_h is the virtual displacement of the point of application of the h-th external force
L_{fi} is the work of any internal forces.

The displacements of the force application points are calculated by assigning a virtual rotation to the generic block.
The relationship cited turns into a balanced equation between stabilizing and overturning moments.
Once the collapse multiplier α_0 has been calculated, the behavior of the block is approximated to that of the system equivalent to SDOF and the mass participating in the kinematics is then assessed (Struture esistenti in muratura, 2015);

$$M* = \frac{\left[\sum_{i=1}^{n+m}(P_i \bullet \delta_{x,i})\right]^2}{g** \sum_{i=1}^{n-m} P_i \bullet \delta^2{}_{x,i}}$$ Equation 2.7.2

The spectral seismic acceleration α_0* that activates the mechanism is calculated as follows:

$$\alpha_0^* = \frac{\alpha_0 \sum_{i=1}^{n+m} P_i}{M* FC} = \frac{g \bullet \alpha_0}{e** FC}$$ Equation 2.7.3

where:

g: is the gravitational acceleration

FC: is the confidence factor

e^*: is the fraction of mass participation (Struture esistenti in muratura, 2015);

$$e^* = \frac{g \bullet M*}{\sum_{i=1}^{n+m} P_i}$$ Equation 2.7.4

In the cases that the compressive strength of the masonry is not taken into account for the evaluation of the multiplier, α_0, the confidence factor to be used will still be that relating to the level of knowledge LC1.

The acceleration α_0* must be compared with the one which is required for the site according to the Limit State of safeguarding Life $\alpha*$ as expressed in the following reports (Struture esistenti in muratura, 2015):

- if the verification involves portions of the structure in contact with the ground:

$$\alpha_0^* \geq \frac{a_g \bullet \langle P_{V_g} \rangle \bullet S}{q}$$ Equation 2.7.5

where:

a_g is a function of the probability of exceeding the chosen limit state and the reference life;

S horizontal spectral acceleration;

q is the structure factor, which can be assumed equal to 2.0;

- if the local mechanism affects a portion of the structure located at a certain altitude, it must be taken into account that the absolute acceleration to the altitude of the portion of the building affected by the kinematic mechanism is, in general, amplified compared to that on the ground (Struture esistenti in muratura, 2015);.

$$\alpha_0^* \geq \frac{S_e \bullet \langle T_1 \rangle \bullet \psi\gamma(Z) \bullet \gamma}{q}$$ Equation 2.7.6

T_1 is the fundamental period of the entire building; $T_1 = 0{,}005 \bullet H^{0{,}75}$, where H is the height of the building (Struture esistenti in muratura, 2015);

$S_e(T_1)$ is the elastic spectrum at SLV, corresponding to the value T_1. The response spectrum refers to the probability of exceeding 10% in the reference period V_R;

$\Psi(Z)$ is the first mode of vibration, equal to Z/H where H is the overall height of the structure and Z is the height of the barycentre of gravity of the constraint lines between the blocks involved in the mechanism and the rest of the structure;

γ is the modal participation coefficient; $\gamma = 3N/(2N+1)$ (Struture esistenti in muratura, 2015);

q Is the factor of the structure.

The analysis of the collapse mechanisms can also be performed with the non-linear kinematic method that determines the evolution of the horizontal load multiplier, α, not only in the initial configuration but also in various system configurations, indicating the evolution of the mechanism and describing it by the displacement d_k of a control point.
For the calculation of the collapse multiplier of different kinematics, each configuration is defined by the Virtual Works Principle, as explained above which is valid also for the non-linear kinematic analysis. The calculations are conducted until the multiplayer α concerning the displacement $d_{k,0}$ becomes 0.
The analysis can be carried out graphically, identifying the geometry of the system in the various configurations up to the collapse, or analytically-numerically, considering a sequence of finite virtual rotations and progressively updating the geometry of the system. The aim of the analysis is however to define the trend of α, as a function of the displacement d_k of the control point.
By defining the trend of the collapse multiplier, α, with the displacement of the control point, d_k, we define the capacity curve of the equivalent oscillator, as the relationship between the acceleration $a^*(g)$ and the displacement d* (Struture esistenti in muratura, 2015);

$$d* = d_c \bullet \frac{\left[\sum_{i=1}^{n+m}(P_i \bullet \delta_{x,i}^2)\right]}{d_{x,c} \bullet \sum_{i=1}^{n-m} P_i \bullet \delta_{x,i}} \qquad \text{Equation 2.7.7}$$

The safety check at the limit state to safeguard life consists in the comparison between the ultimate displacement capacity, d^*_u, of the local mechanism and the displacement demand obtained by the displacement spectrum at the secant period T_s (Struture esistenti in muratura, 2015);

$$T_s = 2\pi \sqrt{\frac{d_s^*}{a_s^*}} \qquad \text{Equation 2.7.8}$$

where:

$$d_s^* = 0{,}4 \bullet d_u^* \bullet \sqrt{\frac{d_s^*}{a_s^*}} \qquad \text{Equation 2.7.9}$$

a_s^* spectral acceleration corresponding to d_s^*.
The verification of the safeguard life against the limit state for the safeguard is considered satisfied if $du* \geq SDe(Ts)$ where S_{De} is the response spectrum in displacement for the cases in which the verification is regarding an isolated element or a part of the building supported on the ground.

The above procedure will give the inelastic portion of the curve, which is valid if we consider the body as completely rigid before the mechanism form. But in reality, there is an elastic behavior of the masonry before being inelastic (formation of the mechanism). This elastic curve can be calculated following the procedure described in the Italian code NTC 2018, Circolare 2019 section C.8.7.1.2.1.2.

$$a_e = \frac{4\pi^2}{T_0^2} \bullet d \qquad \text{Equation 2.7.10}$$

where:

$$T_0 = k \bullet \lambda \bullet L \sqrt{\frac{E}{E \bullet g}} \qquad \text{Equation 2.7.11}$$

k is a coefficient of the value 6.2 for cantilevered elements and 2.2 for mechanisms undergoing vertical bending;

L is the length of the element.
λ is the slenderness of the element (ratio between length H and thickness t).
W is the specific weight of the masonry.
E is the modulus of elasticity of the masonry.

The elastic and inelastic curves are combined to get the bilinear capacity curve of the nonlinear SDOF equivalent system. As the yield point is considered the moment when the activation of the mechanism appears, right at this moment, the point of the inelastic curve with value α_0^* should horizontally move until it meets the elastic curve. Following Circolare 2019 section C7.3.4.2, the inelastic curve should be truncated when $F=0.85F_{max,}$ in our case considering the relation is expressed in ADSR diagram the inelastic curve should be truncated when $a_{s=}0.85a_y$. The final curve is considered as the bilinear capacity curve of the nonlinear SDOF equivalent system.

Method A: equal energy (N2) method

The bilinear curve is composed of two lines:

1. elastic
2. plastic, which has as initial value the force that activates the mechanism.

The elastic period of the system is given by the formula below. (NTC 2018)

$$T^* = 2 \bullet \pi \bullet \sqrt{\frac{m^*}{k^*}}$$ Equation 2.7.12

where:
k^* is the stiffness of the elastic curve of the bilinear curve
$m^* = \sum m_i \bullet \Phi_i$ is the mass of the equivalent bilinear system

The capacity curve of the equivalent bilinear system thus determined represents the structure's ability to withstand seismic stresses regardless of the seismic event, to which no reference is ever made, but based on the intrinsic resistance characteristics of the system. It is, in broad terms, a simplified constitutive link of the structure. On the capacity curve, it is possible to follow, the progress of the damaged state, as the deformation induced by the seismic stress increases. Therefore, the limit states of the structure are identified based on the performance and operativeness of the building.

Analytically, the maximum displacement can be determined by referring to the following conditions, and as graphically explained from Figure 2.7-3:

If $T^* \geq T_C$, the system is considered flexible (Circolare 2019)

$$d_{max}^* = d_{e,max} = S_{de}(T^*)$$ Equation 2.7.13

where $S_{de}(T^*)$ is the displacement demand for the period T^*, obtained from a response spectrum defined later in this section. (NTC 2018)

If $T^* < T_C$, the system is considered rigid (Circolare 2019)

$$d_{max} = \frac{d_{emax}^*}{q^*} \bullet \left[1 + (q^* - 1) \bullet \frac{T_c}{T^*}\right] \geq d_{emax}^*$$ Equation 2.7.14

where $q^* = S_{De}(T) \bullet m^*/F_y^*$ is the relation between the elastic response force and yield force of the equivalent system.
If $q^* \leq 1$ then:

$$d_{max}^* = d_{e,max} = S_{de}(T^*)$$ Equation 2.7.15

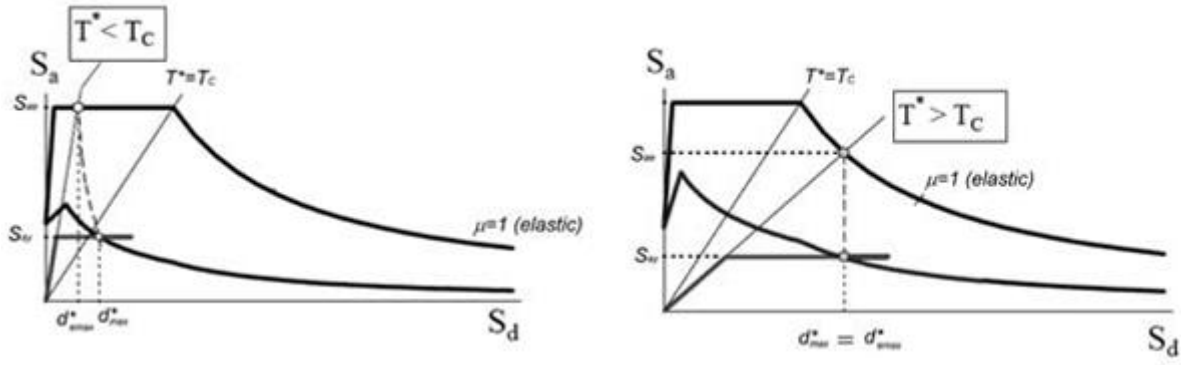

(a) (b)

Figure 2.7-3 Graphic definition of an SDOF system seismic response (a) intersection in the elastic range where $T^* \geq T_C$, (b) intersection in the inelastic range $T^* \leq T_C$ (Struture esistenti in muratura, 2015)

Method B: capacity spectrum method

In Method B, the performance point is obtained under an iterative process. It is necessary to present the demand spectrum in the spectral ordinates (ADRS) format, or the $a - d$ plane, with the spectral acceleration S_a, represented in functions of the spectral displacements S_{De}, obtained by Equation 2.5.11 from the NTC-2018 (NTC,2018) to obtain the performance point.

$$S_{De}(T) = \ Se(T)\left(\frac{T}{2\pi}\right)^2$$ Equation 2.7.16

The first assumption for the performance point is that the maximum displacement d^*_{max} is equal to the displacement of the elastic structure with period T^*. The equation below was used for the first assumption during the analysis performed in this thesis.

$$d_{max}^{*(0)} = d_e = S_{De}\ (T*)$$ Equation 2.7.17

For the case when the bilinear curve of the equivalent system F^*-d^* is conducted through kinematic calculations, to find the performance point the corrected damping factor is introduced.

$$\eta = \sqrt{\frac{10}{\xi_{eq}^{(1)} + 5}}$$ Equation 2.7.18

The associated equivalent damping, $\xi_{eq}^{(1)}$, is expressed as a percentage.

$$\xi_{eq}^{(1)} = k\frac{63.7(F_y^{*(0)}d_{max}^{*(0)} - F_{max}^{*(0)}d_y^{*(0)}}{F_{max}^{*(0)}d_{max}^{*(0)}} + 5 \qquad \text{Equation 2.7.19}$$

Where k, is a coefficient that considers the dissipative capacity of the material and its hysteresis characteristics whose values are given in Circolare Section C7.3.4.2 (NTC, 2019).
Thanks to this coefficient, it can be calculated the corrected response spectra. The intersection of the response spectrum and equivalent capacity curve in the ADSR ordinate will obtain the updated performance point as shown in Figure 2.7-4, characterized by the displacement $d_{max}^{*(1)}$ close to the previous displacement $d_{max}^{*(0)}$,found through method A. The iterative procedure of spectral reduction is repeated several times until the solution converges within the tolerances of 0.001m.

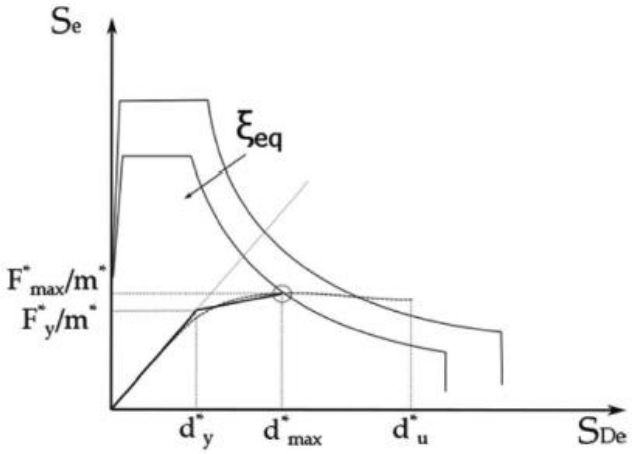

Figure 2.7-4 Detection of the performance point (NTC 2019)

Response spectra

The response spectrum for the location of La Barceloneta in Barcelona can be obtained from the seismic code of Spain, NCSE – 02. Besides NCSE-02, also Eurocode 8 provides the instructions to calculate the response spectrum of the mentioned location.

Chapter 2 of NCSE-02 provides information on how to obtain the response spectrum for the Spanish territory. Both codes give values for the typical shear wave velocities and the equivalent soil types which are defined in the map of soil types in Barcelona (Cid. J 1998). The seismic acceleration is first calculated through Equation 2.7.20 and then used to plot the response spectrum given by Equation 2.7.21, Equation 2.7.22 and Equation 2.7.23

$$a_c = S \bullet \rho \bullet a_b \qquad \text{Equation 2.7.20}$$

where a_b is the basic seismic acceleration from Annex 1 of NCSE-02 for Barcelona;
ρ is the nondimensional risk coefficient based on the importance of the structure, 1 for normal structures of and 1.3 for important structures;
S is the terrain amplification coefficient, from Section 2.2 of NCSE-02.

The normalized elastic response spectrum for horizontal accelerations corresponding to a simple linear oscillator with a reference damping of 5% concerning the critical one is defined by the equations:

$T < T_A \qquad \alpha(T) < (1 + 1.5 \bullet T/T_A)$ Equation 2.7.21

$T_A \leq T \leq T_A \qquad \alpha(T) = 2.5$ Equation 2.7.22

$T < T_B \qquad \alpha(T) = K \bullet C/T$ Equation 2.7.23

Where $\alpha(T)$ is the normalized value of the elastic response spectrum;
T is the natural period of the oscillator [s];
K is the coefficient of contribution based on the type of earthquakes expected and varies by region. (Values are given in Annex 1 of the NCSE-02);
T_A, T_B are characteristic periods of the response spectrum, of the values:

$T_A = K \bullet C/10$ Equation 2.7.24

$T_A = K \bullet C/2.5$ Equation 2.7.25

where C is the terrain coefficient dependent on the type of soil, from section 2.4 of NCSE-02.

Finally, through the introduction of the calculated seismic acceleration a_c, and damping correction factor $\eta = \sqrt{10/(5 + \xi)} \geq 0{,}55$, where ξ is the viscous damping ratio of the structure, is possible to calculate the elastic response spectrum $S_e(T)$ according to Equation 2.7.26.

$S_e(T) = \alpha(T) \bullet a_c \bullet \eta$ Equation 2.7.26

In contrast to NCSE, Eurocode 8 gives a slightly different elastic response spectrum given by the following equations:

$0 < T < T_B \qquad S_e(T) = a_g \bullet S \bullet \left[1 + \frac{T}{T_B}(2.5\eta - 1\right]$ Equation 2.7.27

$T_B \leq T \leq T_C \qquad S_e(T) = a_g \bullet S \bullet \eta \bullet 2.5$ Equation 2.7.28

$T_C \leq T \leq T_D \qquad S_e(T) = a_g \bullet S \bullet \eta \bullet 2.5 \left[\frac{T_c}{T}\right]$ Equation 2.7.29

$T_D \leq T \leq 4s \qquad S_e(T) = a_g \bullet S \bullet \eta \bullet 2.5 \left[\frac{T_c T_D}{T^2}\right]$ Equation 2.7.30

where $S_e(T)$ is the elastic response spectrum;
a_g is the design ground acceleration on type C ground (EC8), corresponding to type III ground of the seismic code of Spain (NCSE-02). It is recommended to consider as low seismicity cases those in which the design ground acceleration, a_g, is not greater than the product $ag.S = 0.08g$ (EC8, Note 3.2.1(4)).
T_B, T_C, T_D, are characteristic periods of the response spectrum, according to Table AN/2 of the Spanish National Annex. (“Anejo Nacional AN/UNE-EN 1998-1,” 1998; CEN, 1998).
S is the terrain amplification coefficient, for $a_g < 0{,}1g$ the S=C, from table AN/2 of Spanish National Annex (AN/UNE-EN 1998-1).
T is the period of the oscillator

- **Vulnerability assessment using the Capacity Spectrum Method**

According to Lagomarsino and Penna if the capacity spectrum is computed then performance levels of the building can be obtained. The first step is to identify the yield point and the ultimate displacement. In the following step, the capacity curve is divided into 5 parts where each one of them determines the expected damage grade for the structural element. Finally, the position of the performance point calculated through Method A & B to provide a better understanding of the behavior of the building during an earthquake. Classification of damage states according to spectral displacement is provided in Table 2.7-1

Table 2.7-1 Performance levels and criteria (Lagomarsino and Penna, 2007)

Damage State k	**Spectral displacement** SD_k
0- No damage	-
1- Slight damage	$Sd_1 = 0.7D_y$
2- Moderate damage	$Sd_2 < 1D_y$
3- Extensive damage	$Sd_3 = D_y + 0.25(D_u - D_y)$
4- Very heavy damage	$Sd_4 = D_u$
5- Complete	$Sd > D_u$

2.8 Catalonia

2.8.1 Seismicity of Catalonia

Catalonia is located in a region of moderate seismicity, that is to say, the seismic activity is lower compared to other regions close to the plate tectonic boundaries (e.g. Alicante), where the intensity is higher. This means that destructive earthquakes are uncommon but, can happen. According to Spanish seismic code NSCE-02, the basic ground acceleration PGA for Barcelona is 0.04, which combined with the soil amplification parameter the values increases to 0.12g. As can be seen in Figure 2.8 1(a), the intensity values on the MKS scale range from V to VIII for an earthquake with return period of 500 years (ICGC, 2001).

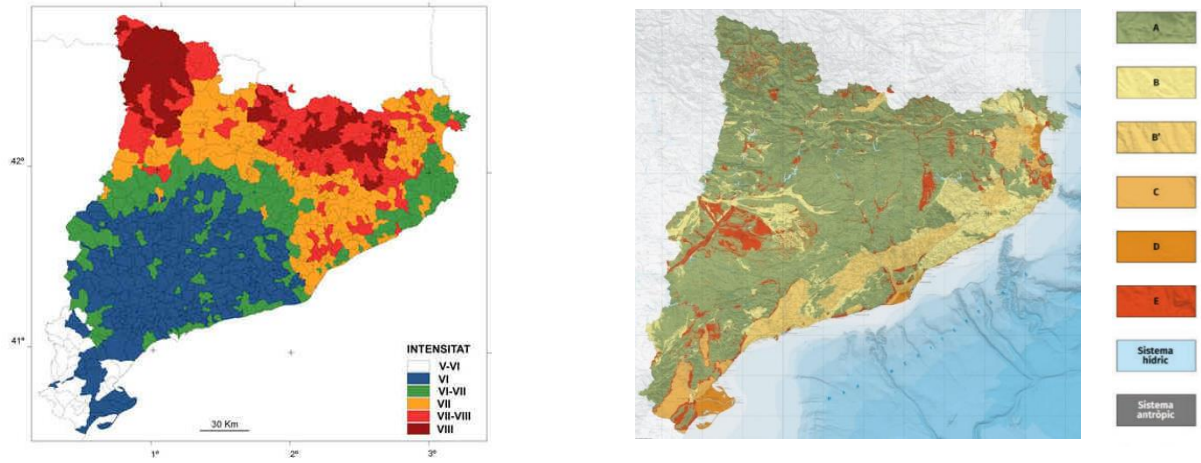

(a) (b)

Figure 2.8-1 (a) Intensity of earthquakes with a return period of 500 years, (b) Mesozonation map Catalonia (ICGC, 2018)

With reference to Figure 2.8-1 (b), soils are categorized in 5 classes: (A) solid rocks covered with soft deposits less than 5 m, (B) sedimentary rock or rigid clays, with a thickness of less than 100m, (B’) sedimentary rock or rigid clays, with a thickness exceeding 100m (C) dense deposits of sand or very rigid clays ranging from 20-100m and covering a rock substrate, (D) soils formed by deposits of fine sand and dense slabs or rough clays to medium rigid ones of a thickness that oscillates between 20 and 100, (E) lands formed by deposits of fine sand and dense slabs or soft clays of medium to thickness ranging between 5 and 20 m and that cover a well-consolidated rock substrate (class A) (ICGC, 2018). In terms of the range of speeds of the shear wave propagation, soils in Catalonia are classified into four groups (Figure 2.8-2) (ICGC, 2018).

Lithological classification	Shear speed V_s (m/s)	SPT (N_{30})	Resistance to non-drained cutting C_u (KPa)
Roca dura (HR)	> 800	-	-
Roca tova i sòl dur (SR)	360 – 800	> 50	> 250
Sòl tou (SS)	180 - 360	15 - 50	70 - 250
Sòl molt tou (VSS)	< 180	< 15	< 70

Figure 2.8-2 Geomechanical classification from the shear wave propagation velocity values, correlated with SPT values and non-drained **(**Cu**)** resistance values. (ICGC, 2013)

2.8.2 Historic earthquakes

During the 14th and 15th centuries in Catalonia, there was an increase beyond normal of the seismic activity which caused damages in Barcelona. On February 2nd, 1428, an earthquake in the Pyrenees with a local magnitude of 6.5 and an epicentral distance of 90 km damaged slightly some churches in Barcelona. Certainly, the mainshock was preceded by one or more foreshocks and many aftershocks. In 1448 another earthquake with a magnitude of 5.5 hit Catalonia and caused some structural cracks on the walls of Montjuic castle. Over the centuries there have been many other earthquakes but due to lack of evidence not much is known regarding their impact on existing structures of that period. During the 20th a few earthquakes had been felt in the city with a maximum intensity of IV degrees in the MSK intensity scale.

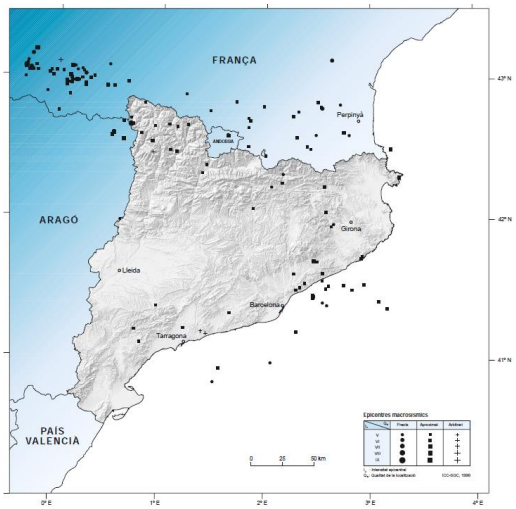

Figure 2.8-3 Epicentres of earthquakes strongly felt that occurred during the XX century (Atlés Sismic de Catalunia)

2.9 La Barceloneta

2.9.1 Location

La Barceloneta is a neighborhood located in the city of Barcelona, Spain. Its triangular shape is bordered by beaches and maritime areas, with the Port Vell and La Ribera district, France Station, and the city’s new Olympic Port.

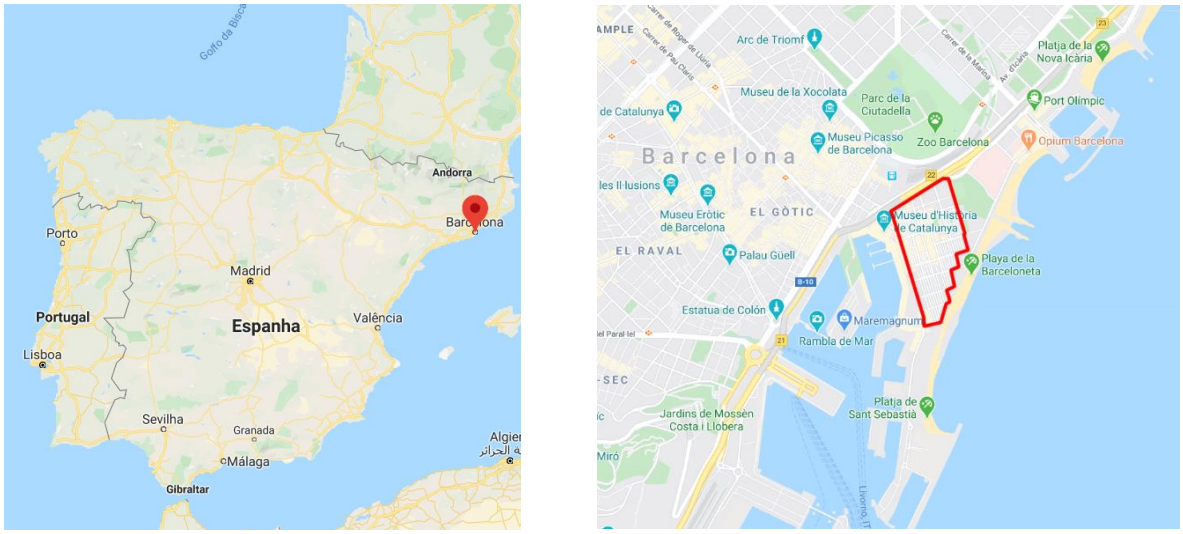

(a) (b)

Figure 2.9-1 Location map, (a) location of Barcelona (Google Maps), (b) location of La Barceloneta (Google Maps)

2.9.2 Barcelona during the 18th century

2.9.3 History of La Barceloneta

La Barceloneta is a sailor neighborhood of the District of Ciutat Vella of Barcelona designed by engineer Juan Martín Cermeño in 1753 (Figure 2.9-2) to accommodate the residents of the neighborhood La Ribera who lost their homes because of the demolition ordered by Felipe V to build the Parc de la Ciutadella.

This was the first urban initiative that was carried out to reduce the population density inside the walled area. The works began in February 1753 and after a year and a half, eight streets, the church, and the plaza had already been built. The urban structure of the neighborhood designed with the principles of Baroque urban planning is a good example of the type of urbanism that was implemented during the Age of Enlightenment, with straight streets and blocks of regular houses. This system initially used in Asia continued to be present in Hellenic societal and city planning but was not pervasive before the 5th century BC. It slowly became the primary urban system because of the work of Hippodamus of Miletus who designed many towns in ancient Greek. Forgotten during the middle ages it was revived by the scholars of the Age of Enlightenment (often known as Age of Reason). The type of dwelling was originally single-family, and the floors had access on both streets providing excellent ventilation.

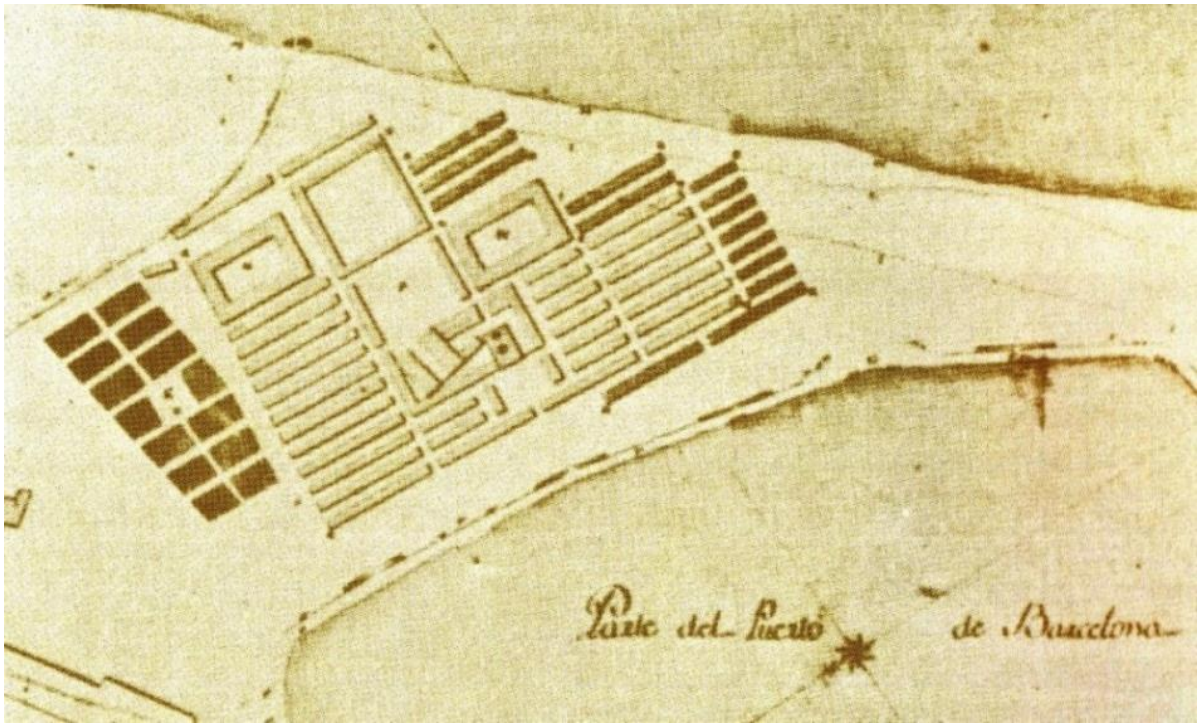

Figure 2.9-2 La Barceloneta, site plan proposal, 1753 (Caminar Barcelona blogspot)

During the 19th century, rapid industrial development with large factories that have disappeared today influenced population growth. Factories such as Maquinista Terrestre and Marítima, are currently being converted to sports pavilions or educational institutions. Because of population growth, need for dwellings, and speculation the two-story house is almost disappeared now. Today we find a bigger neighborhood and buildings with heights much higher than those that were originally built, apart from sharing the original houses in halves and quarters of floors.

2.9.4 Morphology and site evolution

The project, due to the military engineer Juan Martín Cermeño, was carried out on real-estate land located next to the port. It is an orthogonal structure based on long blocks and regular buildings. Each block was divided into square plots of 8.4 meters each, where a 7-meter-high single-family house - corresponding to a ground floor and a first floor - with 141 square meters of surface stood. Initially, the neighborhood had to form a square of about ten hectares delimited by the broadside of the pier and the current streets Geneva, Giné Partagàs, and Almirante Cervera. The works began in February 1753 and after a year and a half, eight streets, the church, and the plaza had already been built. In 1759, the neighborhood had about 1,570 inhabitants, a figure that changed in 1787 with an increase to 2,392 inhabitants. Figure 2.9-3 shows the initial state of the neighborhood (Scripta Nova, UB).

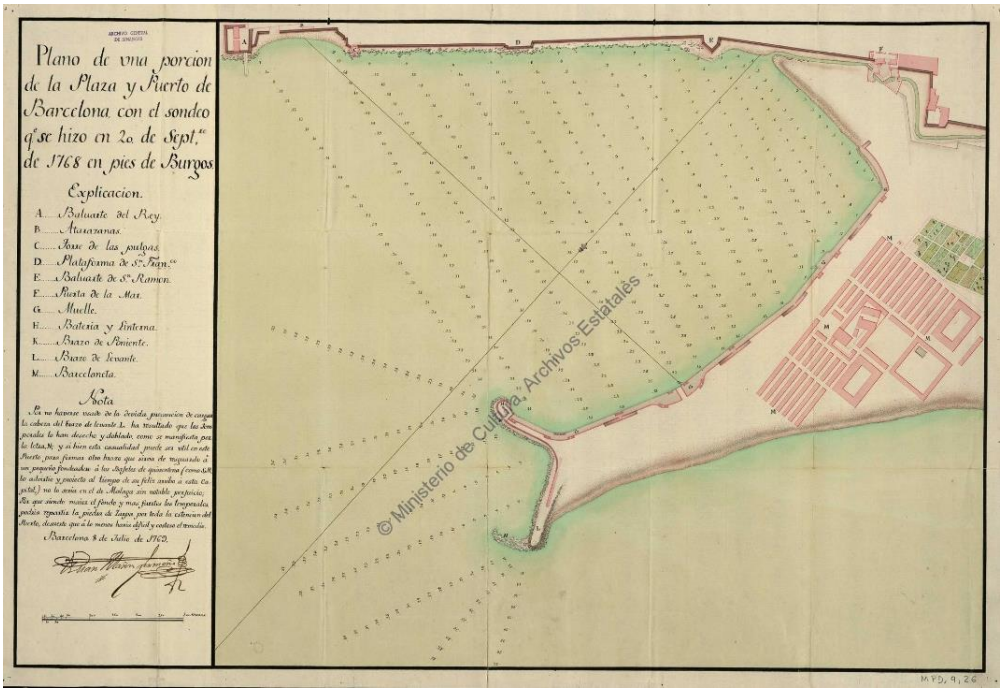

Figure 2.9-3 La Barceloneta, site plan, 1768 (Ministero de Cultura, Archivio de Simancas)

At the beginning of the 19th century, Rafael de Amat y de Cortada, baron of Maldà, pointed out in his extensive personal diary - the *Calix de Sastre*, written between 1769 and 1819 - that Barceloneta housed some seven hundred houses, all of them with the same height, width, and decoration, and described the streets of the suburb as straight, cobbled, wide and clean. Figure 2.9-4 shows the expansion of the neighborhood while in Figure 2.9-8 is showing the evolution of the house in verticality which began in the early 19th century (Scripta Nova, UB).

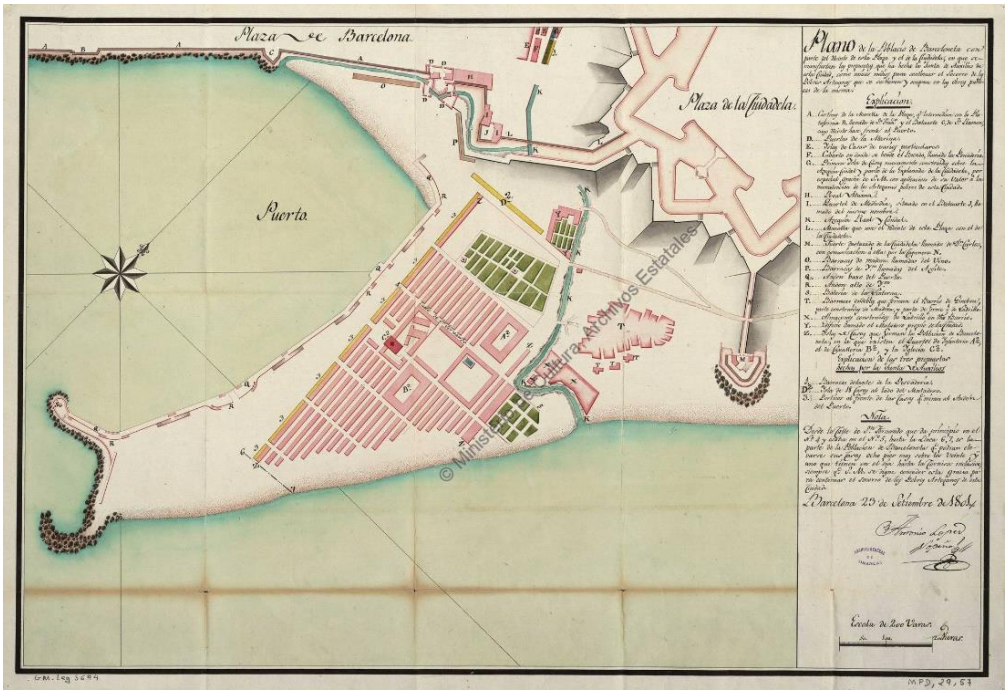

Figure 2.9-4 La Barceloneta, site plan, 1805 (Ministero de Cultura, Archivio de Simancas)

The orientation of the houses is NW-SE and they have access to both streets. This type of structure allows for transverse ventilation which is considered as the best way of ventilation for buildings. The ground floor was used as a living space while the first floor as space for sleeping. Natural light in the house is considered optimal as the surface area of the openings per surface area of the floor is of a good ratio.

Figure 2.9-5 La Barceloneta, original design, and hypothetical 3d reconstruction. (bcn.cat/ciutatvella)

As can be seen from the evolution site plans and facade timeline, La Barceloneta neighborhood has been steadily expanding in horizontality and verticality (Figure 2.9-7). Originally built as two - story houses of a Baroque style they have been expanding in verticality by keeping the same style (Figure 2.9-8); openings, story height , cornices, etc... From the original design just a few buildings have survived today. , while the others have been modified in four, five, and six-story buildings (Figure 2.9-5, Figure 2.9-6, Figure 2.9-8).

Figure 2.9-6 La Barceloneta, 2019 (Erasmus, 2020)

Figure 2.9-7 La Barceloneta site evolution (bcn.cat/ciutatvella)

Figure 2.9-8 La Barceloneta evolution of the house. (bcn.cat/ciutatvella)

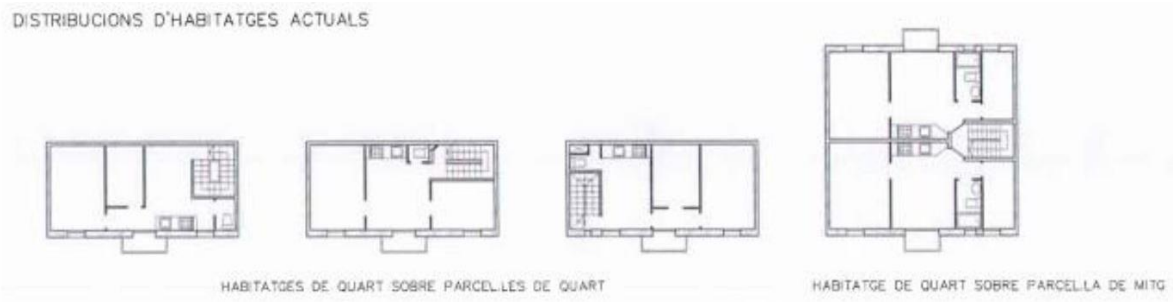

Figure 2.9-9 Plans of La Barceloneta house (Scripta Nova, UB)

2.9.1 Categorization of buildings

La Barceloneta is a neighborhood composed of aggregate buildings of the same typology. Due to changes made over time now we have a variety of buildings ranging from two to six-story and sometimes seven stories. Through Google Maps all the buildings in the neighborhood were identified based on the number of floors and positioning with the other surroundings, (Table 2.9-1). Due to the alterations, it was decided to consider one building as two buildings because there are many cases when half of the building is five or six stories while the other half three, four, or five stories (Figure 2.9-10). A map based on the number of floors was compiled. These buildings are categorized as structures which are at the corner of the block or attached buildings amongst a row (see Figure 4.2-3) and (Table 4.2-1). A total of twelve types of buildings were identified and for each of them calculations on the vulnerability index (Section 3), and the kinematic local mechanisms (Section 4) were performed

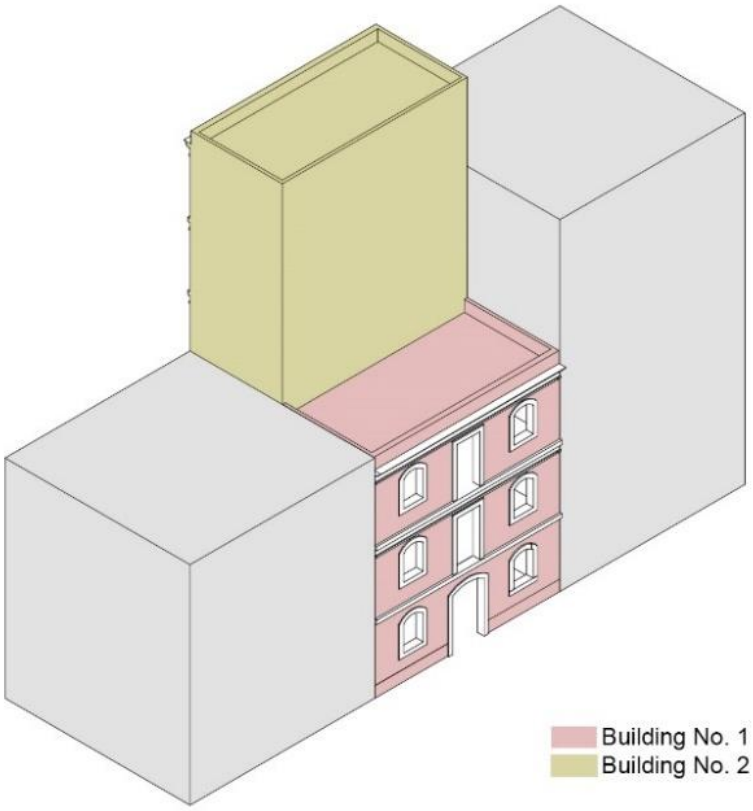

Figure 2.9-10 Alterations in La Barceloneta neighborhood

Table 2.9-1 La Barceloneta figures in terms of percentage and number of buildings in the neighborhood

Aggregate position: Corner building (CB)						
No. of floors	2 stories	3 stories	4 stories	5 stories	6 stories	Total no. CB
No. of buildings	10	20	30	48	88	196
Percentage	5.1%	10.2%	15.3%	24.5%	44.9%	
Aggregate position: Attached building amongst a row (AB)						
No. of floors	2 stories	3 stories	4 stories	5 stories	6 stories	Total no. AB
No. of buildings	18	122	162	204	432	938
Percentage	1.9%	13%	17.3%	21.7%	46.1%	
Total						
No. of floors	2 stories	3 stories	4 stories	5 stories	6 stories	Total no. CB+AB
No. of buildings	28	142	192	252	520	1134
Percentage	2.5%	12.5%	16.9%	22.2%	45.9%	

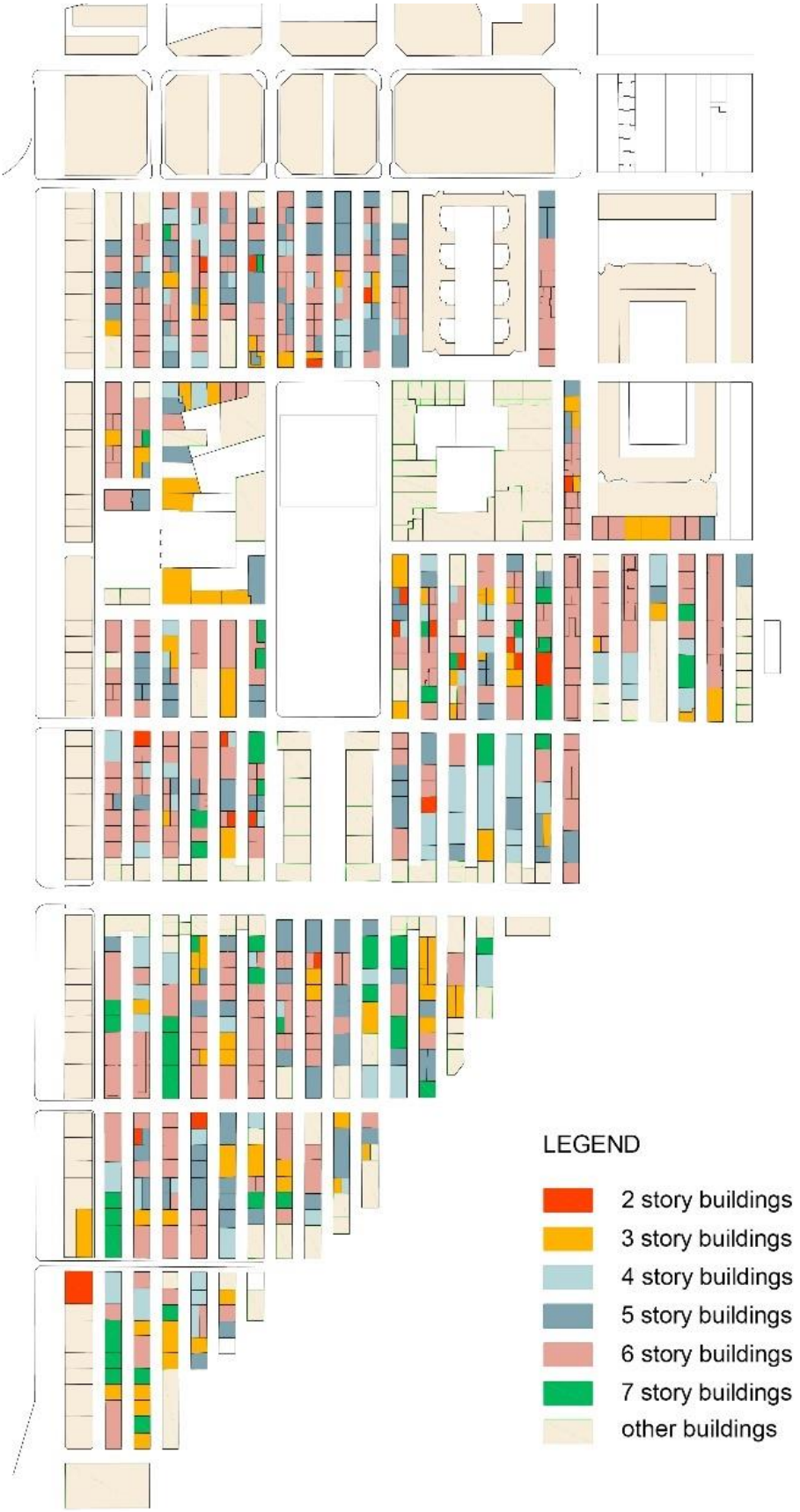

Figure 2.9-11 La Barceloneta, building heights in stories map.

2.9.2 Structural description

La Barceloneta is an unreinforced masonry house typology characterized by a regular structural plan, with load-bearing walls uniformly distributed in both directions. It was built during the 18th century (Ministero de Cultura, Archivio de Simancas) without any earthquake - resistance measures (e.g. ties, ring beams). Initially build as two - story houses with basements (Figure 2.9-12, Figure 2.9-13 (a), (b)) now many of them have three, four, five, and six stories. The basement is built of stone walls and vaulted with solid bricks masonry, while the walls above the ground are built with fired clay bricks, and most likely bonded with lime mortar, as they are structures of the 18th century. However, this may be true for two or three - story buildings, but for those with four, five, and six-story, it is difficult to give an accurate opinion, because of the Portland cement that was introduced in the 19th century (Courland R, 2011). Most likely they are hybrid structures in terms of building mortar; lime mortar in the walls of the lower floors and cement mortar in the upper floors. The walls of the main facades are 30 cm thick while the other walls, the side, and the inner ones are 15 cm. The corners of the buildings are built of well-carved stones as high as 5 bricks and well interlocked with the brick masonry (Figure 4.2-10, (b)). In these structures, none of the earthquake resistance measures, developed based on experience, has been applied.

(c) (d)

Figure 2.9-12 The original 2-story house, (a) the house, (b) corner of the house

The masonry jack arch slab is the predominant flooring technique used in La Barceloneta's house. Wooden beams were used to support the brickwork arches of the ground floor ceiling (Figure 2.9-15), while for the ceilings of the upper floors which were built during the XIX century, due to developments in construction technology and the introduction of new techniques, iron I-beams were used instead of wooden beams (Figure 2.9-16), (Niker, 2010).
According to Figure 2.9-5, the roofs were built with a king-post truss structure but it is just an assumption. Today only a two - story building covered by a roof and retaining s the original features in appearance is identified (Figure 2.9.12).

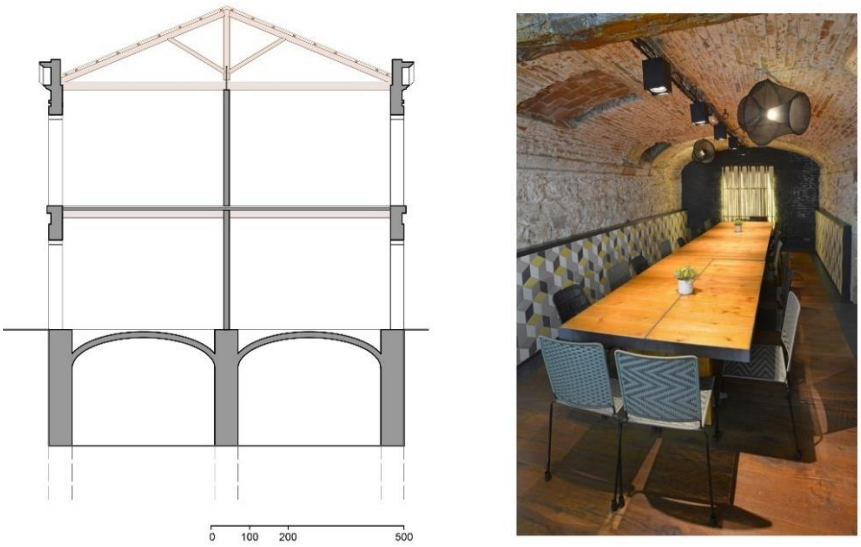

(e) (f

Figure 2.9-13 Hypothetical section of the 2-story house, (a) section of La Barceloneta, (b) image of the basement

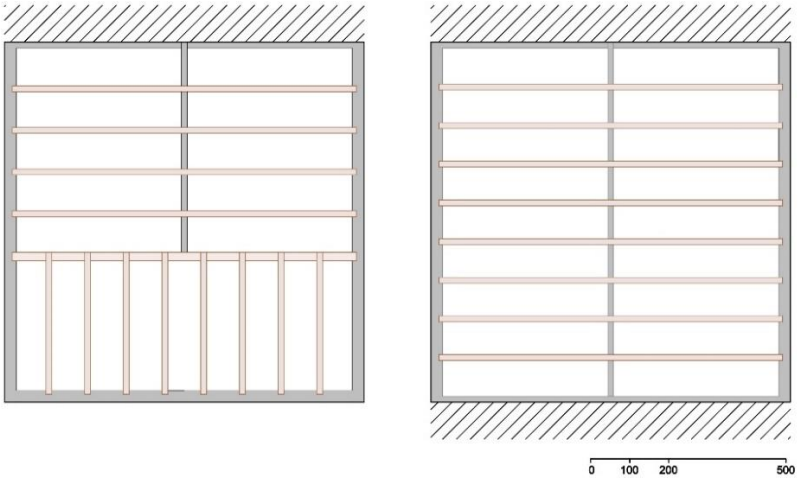

(a) (b)

Figure 2.9-14 Plan view of slabs, (a) corner building, (b) attached building amongst a row.

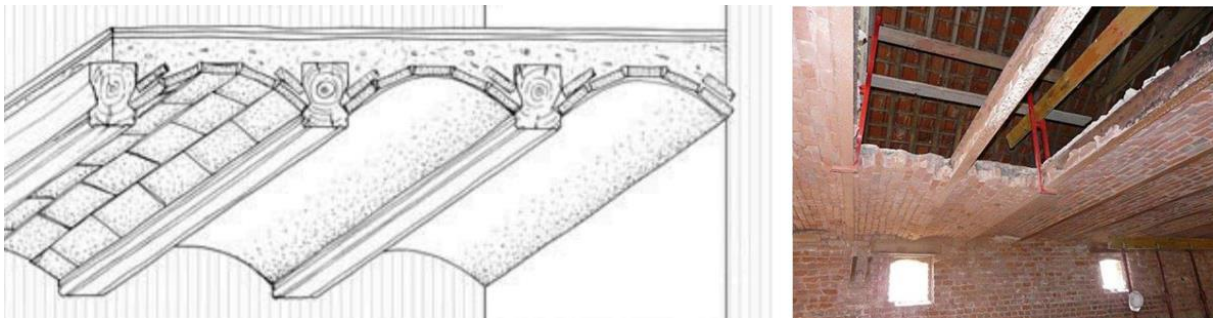

(a) (b)

Figure 2.9-15 Jack arch slab supported by timber beams, (a) 3D drawing of the slab, (b) image of the slab

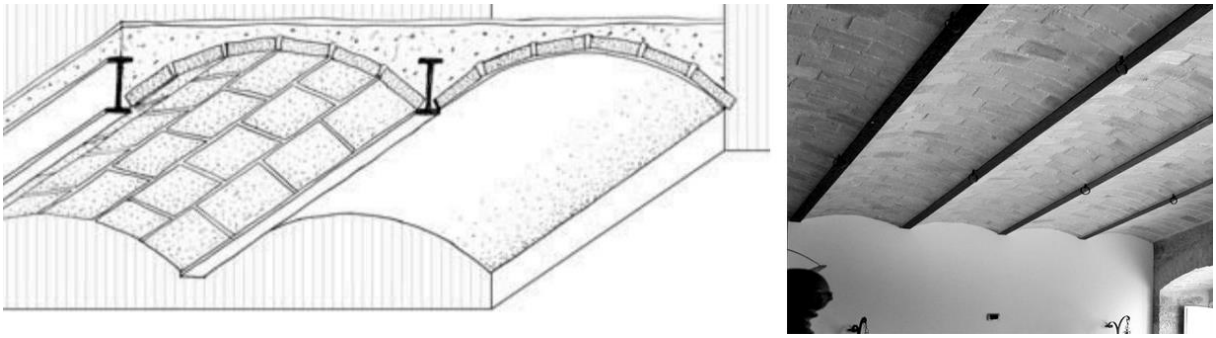

Figure 2.9-16 Jack arch slab supported by iron I-beams, (a) 3D drawing of the slab, (b) image of the slab

2.9.3 Present condition

In 2008 Heritage English published the Method Statement for the risk assessment of the seven types of heritage assets that exist in UK. It aims to identify England’s heritage assets that are at risk of loss through neglect, decay, new developments development, or are vulnerable to becoming so. Also, this methodology has been used successfully in other countries (Scotland, Albania). Buildings and structural monuments are assessed based on their condition and, where applicable, occupancy (or use). According to this method, the condition of buildings and structures ranges from very bad to poor, fair, and good. (English Heritage, 2008)

Condition is graded as follows:

- **very bad** means a building or structure where there has been structural failure or where there are clear signs of structural instability; (where applicable) there has been loss of significant areas of the roof covering, leading to major deterioration of the interior; or where there has been a major fire or other disaster affecting most of the building.
- **poor** means a building or structure with deteriorating masonry and/or a leaking roof and/or defective rainwater goods, usually accompanied by rot outbreaks within and general deterioration of most elements of the building fabric, including external joinery; or where there has been a fire or other disaster which has affected part of the building.
- **fair** means a building or structure which is structurally sound but in need of minor repair or showing signs of a lack of general maintenance.
- **good** means structurally sound, weather-tight, and with no significant repairs needed

In general, La Barceloneta exhibits a fair condition. The exterior walls of the buildings have always been plastered, so it is expected they are in good condition, and protected from external atmospheric agents. Lack of maintenance is presents, and the deterioration of the plaster is obvious in some buildings. The roofs and gutters are in good condition and under permanent maintenance. As for the internal conditions, it is difficult to have evidence, but they are expected to be in good condition given the fact that they are occupied buildings. These structures are located near the sea, so it is suggested to carry out a detailed inspection to see the condition of the foundations. Besides, it is strongly recommended to check the structures on the possibility of developing instability due to bad execution during the works and alterations in case of potential earthquakes.
Following Method Statement, it is possible to have a preliminary idea regarding the Risk Category which in this case is LOW RISK (Figure 2.9-17). However, this categorization is not associated to natural

disasters; earthquakes, landslide, floods, etc.... It is a categorization that deals with natural decay and deterioration because of a lack of maintenance and occupancy.

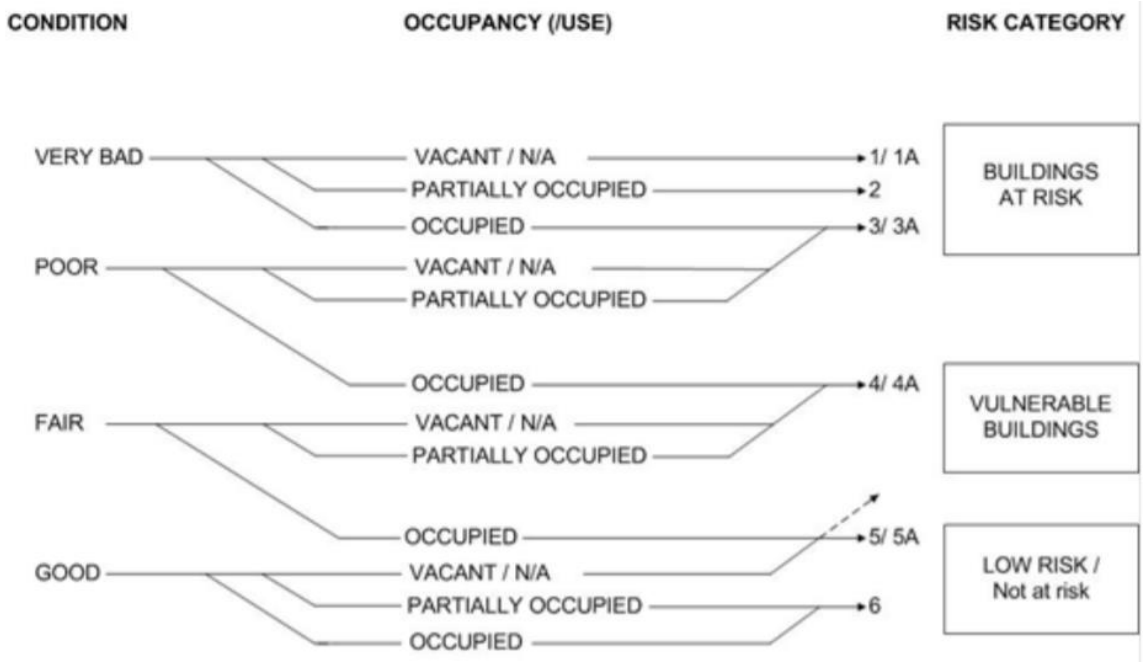

Figure 2.9-17 Condition and occupancy interaction and generation of the degree of risk for buildings (English Heritage, 2008)

Anyhow, if a detailed study classifies the neighborhood as in POOR condition then, the risk category assigned will be VULNERABLE BUILDINGS. This categorization is done considering the features presented in Figure 2.9.17

Figure 2.9-18 Presence of lack of maintenance (Google Maps).

3. VULNERABILITY INDEX ANALYSIS

3.1 Assumptions

Although La Barceloneta is composed of around 1150 buildings, the vulnerability assessment was conducted to only 12 buildings, the ones identified as the most representative ones. Following the methodology (Section 2.5), it was possible to calculate the 14 parameters that are divided into four sets. For all the sets the assumptions were conducted based on the description in section 2.9.2. This chapter is going to be explained only the calculations performed for the 6-story corner building. In addition, this chapter is also going to be presented also the results for the 6-story attached building amongst a row.

Group 1

With respect to Table 2.5-2, parameter P1 fits under class C, because of the lack of connections, defined in class B. However, it has a good connection between its resisting orthogonal walls Vicente (2008).
For the quality of the resisting system was used Table 2.5-3. To be conservative, for parameter P2 was chosen the class B, where masonry is built up of bricks with a perforated area less than 45% or well-cut (ashlar) stones with good quality mortar Vicente (2008).
P3 is related to the conventional strength that was calculated based on Equation 2.5.2 with reference to Circolare 2019 (NTC,2018). Shear strength and specific weight were chosen 40kPa and 18kN/m^3, respectively Vicente (2008).
Parameter P4 is a result of the rations between (section 2.5) height, length, width, number of floors, and thickness of walls. The final results are not satisfactory as the relation between the walls and the thicknesses are characterized by the following values Vicente (2008).

Slenderness criteria

$$\left(\frac{h_0}{s}\right)_{max} = 28.3$$

Distance criteria

$$\left(\frac{L}{s}\right)_{max} = 28.3$$

These values are higher than any value of the geometric relations of the classes A, B, C, and D (section 2.5). Therefore, for parameter 4, class D was chosen.

Parameter P5 is related to the number of stories. Taller masonry buildings tend to be more vulnerable to earthquakes than lower buildings. The class of the parameter was selected based on Table 3.1-1 (Salazar, 2018).

Table 3.1-1 Vulnerability class definition for Parameter 5

Class	Number of floors
A	1-storey
B	2 or 3 storeys
C	4 or 5 storeys
D	6 or more storeys

In the Table 3.1-2 is going to be presented the value for the 6 - story building as it is the most vulnerable one.

P6 is a combination of the type of soil and the foundations’ conditions of the buildings. According to Ferreira. et.al 2020, buildings in flat cities with soil type B or C are categorized as class B. In addition, it should be considered also the condition of the foundations which in this case is considered as fair.

Table 3.1-2 Vulnerability index associated parameters, Group 1 classes, and weights P_i (Ferreira et al. 2017)

Parameters	Class, C_{vi}				Weight	Relative
	A	B	C	D	P_i	weight
Group 1. Structural building system						
P1. Type of the resisting system			20		0.75	15
P2. Quality of the resisting system		5			0.75	3.75
P3. Conventional strength				50	1.50	75
P4. Maximum distance between walls				50	0.50	25
P5. Number of floors				50	1.50	75
P6. Location of soil condition		5			0.75	3.75

Group 2

P7 evaluates the influence of the position of the buildings with the other surrounding/connected buildings. Corner buildings without floor misalignments are included in class C (Salazar. Flores, 2018).
P8 is related to the geometry criteria which is calculated as a ratio of width and length of the building. In this case $\beta_1 = a/L = 1$ (Salazar Flores, 2018). therefore, for parameter P8, class A has to be considered, but in this case, was chosen class B instead of A.
P9 is related to the variation of the area in relation to the height of the building, and its influence on the seismic behavior of the building. The variation is expressed as a ration and in this case, is less than 10% as the structures are very regular. Therefore, for parameter P9, class A should be chosen.
Parameter P10 assesses the opening for their mechanical influence on the vertical and horizontal rupture of the walls, and further their in-plan or out of plan behavior that could be a response to seismic actions (Salazar, 2018). La Barceloneta is characterized by a very regular layout of openings, therefore, class A should be chosen. However, in order to be conservative, class B was considered as a final class.

Table 3.1-3 Vulnerability index associated parameters, Group 2 classes, and weights P_i (Ferreira et al. 2017)

Parameters	Class, C_{vi}				Weight	Relative
	A	B	C	D	P_i	weight
Group 2. Irregularities and interaction						
P7. Aggregate position and interaction			20		1.50	15
P8. Plan configuration		5			0.75	3.75
P9. Height regularity	0				0.75	0
P10. Wall facade openings and alignments		5			0.50	2.5

Group 3

Parameter P11 is related to the rigidity and connection of the slab with the masonry. According to Vicente (2008), for semi rigid slabs and without any connection to the walls (e.g. tie), class C is chosen.
Paramete P12 is related to the typology of the roof, and for flat slabs without any type of strengthening (e.g.tie), class B is chosen (Vicente (2008).

Table 3.1-4 Vulnerability index associated parameters, Group 3 classes, and weights P_i (Ferreira et al. 2017)

Parameters	Class, C_{vi}				Weight	Relative weight
	A	B	C	D	P_i	
Group 3. Floor slabs and roofs						
P.11 Horizontal diaphragms			20		1.00	20
P.12 Roofing system		5			1.00	5

Group 4

P13 takes into account the fragilities and conservation status of the buildings and is one of the most significant parameters of the building approach, as it highly impacts in the final evaluation of parameters 2,3 and 11. For this case it was decided to be conservative so, class C was chosen.
The same class was applied also for the parameter P14.

Parameters	Class, C_{vi}				Weight	Relative weight
	A	B	C	D	P_i	
Group. 4 Conservation status and other elements						
P13. Fragilities and conservation status			20		1.00	20
P.14 Non-structural elements			20		0. 50	10

3.2 Results

The methodology was applied in the evaluation of twelve types of buildings. This method is considered as a hybrid technique in respect to Figure 2.1-2. The vulnerability index formulation is based on the GNDT II level approach (GNDT 1994) for the seismic evaluation of cultural heritage buildings. Each parameter is characterized by the vulnerability class whether A, B, C or D and the weight coefficient. The conclude, vulnerability index is calculated as the sum of 14 parameters. The obtained vulnerability indexes are presented in Table 3.2-1.

Table 3.2-1 Table of vulnerability index

6-story, i_v		5-story, i_v		4-story, i_v		3-story, i_v		2-story, i_v	
CB	AB	CB	AB	CB	AB	CB	AB	CB	AB
0,46	0,41	0,37	0,31	0,37	0,31	0,25	0,21	0,25	0,19

0-1 normalized vulnerability index i_v
CB- Corner building
AB- Attached building amongst a row

Table 3.2-2 Vulnerability index values for the EMS-98 V_i

6-story, i_v		5-story, i_v		4-story, i_v		3-story, i_v		2-story, i_v	
CB	AB	CB	AB	CB	AB	CB	AB	CB	AB
0,84	0,80	0,80	0,77	0,80	0,77	0,73	0,71	0,73	0,70

With reference to Table 3.2-2 the values of vulnerability index according to EMS-9 (1998) are in the ranges of Figure 3.2-1. The reason for having this high value is because of the conservative classes applied for the assesment of the vulnerability index.

Typologies		Building type	Vulnerability classes				
			$V_{I\,min}$	V_I^-	V_I^*	V_I^+	V_{Imax}
Masonry	M1	Rubble stone	0.62	0.81	0.873	0.98	1.02
	M2	Adobe (earth bricks)	0.62	0.687	0.84	0.98	1.02
	M3	Simple stone	0.46	0.65	0.74	0.83	1.02
	M4	Massive stone	0.3	0.49	0.616	0.793	0.86
	M5	Unreinforced M (old bricks)	0.46	0.65	0.74	0.83	1.02
	M6	Unreinforced M with r.c. floors	0.3	0.49	0.616	0.79	0.86
	M7	Reinforced or confined masonry	0.14	0.33	0.451	0.633	0.7
Reinforced Concrete	RC1	Frame in r.c. (without ERD)	0.3	0.49	0.644	0.8	1.02
	RC2	Frame in r.c. (moderate ERD)	0.14	0.33	0.484	0.64	0.86
	RC3	Frame in r.c. (high ERD)	-0.02	0.17	0.324	0.48	0.7
	RC4	Shear walls (without ERD)	0.3	0.367	0.544	0.67	0.86
	RC5	Shear walls (moderate ERD)	0.14	0.21	0.384	0.51	0.7
	RC6	Shear walls (high ERD)	-0.02	0.047	0.224	0.35	0.54
Steel	S	Steel structures	-0.02	0.17	0.324	0.48	0.7
Timber	W	Timber structures	0.14	0.207	0.447	0.64	0.86

ERD – “Earthquake Resistance Design”

Figure 3.2-1 Vulnerability index values for the EMS-98 building typologies

The second part consists on the calculation of a mean damage μ_D, for each type of building according to the European Macroseismic scale EMS-98, (Figure 3.2-2) with the implication of vulnerability index V and ductility factor Q (Lagomarsino, 2006).

According to Kasem et, al (2019) each intensity scale I_{EMS-98} can be associated with a peak ground acceleration (PGA) (Table 3.2-3). The reference ground accelerations for the region obtained from Spanish Code NCSE-02 (2002) and EC-8 (2004) are 0.51 and 0.57g, respectively. With reference to Figure 2.8-1 and Table 3.2-3, an intensity VI-VII is the earthquake of return period 500 years for La Barceloneta. Therefore, the expected damage for a 6-story corner building for an earthquake of intensity 7 would be $\mu_D = 1{,}67$

Table 3.2-3 The correlation between the seismic intensities (PGA) and EMS-98 scale

PGA(g)	0.017	0.031	0.057	0.1	0.2-0.3	0.35-0.6	0.65-1.15	1.2
I_{EMS-98}	V	VI	VII	VIII	IX-X	X-XI	XI	XII

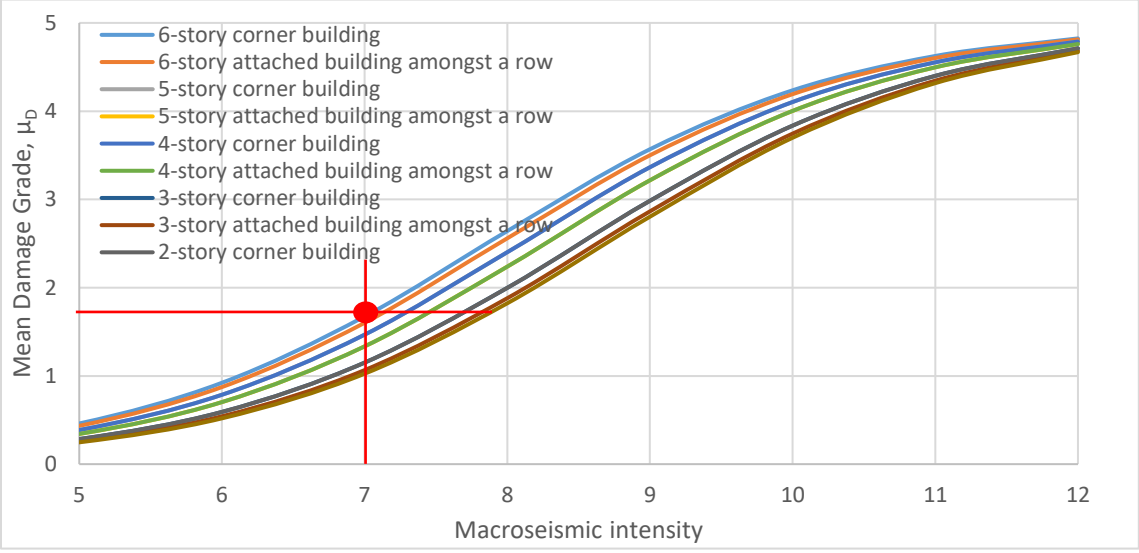

Figure 3.2-2 Macroseismic method, expected damage graph.

Both fragility models were created (Figure 3.2-3, Figure 3.2-4) according to European macroseismic scale EMS-98 (1998), where the first shows the probability of any given damage level occurring for a specific intensity of earthquake, while the second probability of reaching or exceeding each damage level (Grunthal, 1998).

For an earthquake of intensity 7, the 6-story corner building would most probably be affected by damage level $D_k = 2$ (moderate damage), with probability 34% (Figure 3.2-3). With respect to the fragility curves $D_k = 3$, and $D_k = 4$ is 24% and 2%, respectively.
Definitely, according to the result, the structure will be affected by damage level $D_k = 1$ (99%). To conclude, it can be said that the 6-story corner building most probably will experience damage level $D_k = 2$ (moderate damage) and no collapse is predicted. The same conclusion stands also for the six-story attached building, but in this case, the figures are a little bit more optimistic as the ``confinement`` provided by the other buildings reduces its seismic vulnerability. However, the results provided by the vulnerability index have to be checked with also with other methods: kinematic approach and if possible numerical models.

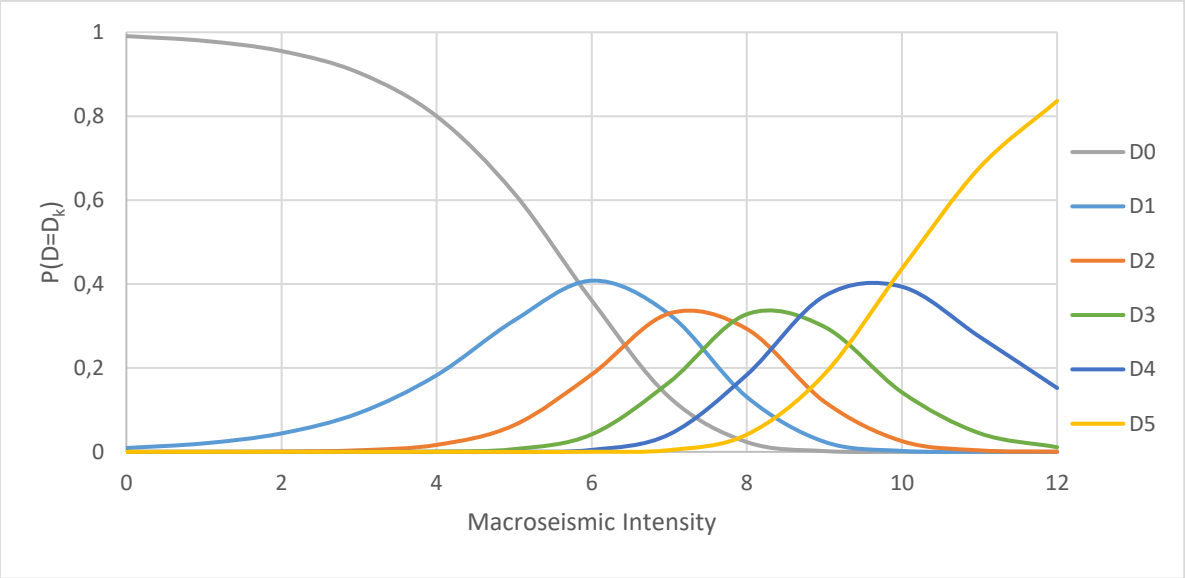

Figure 3.2-3 La Barceloneta, 6-story corner building; probability of each damage level

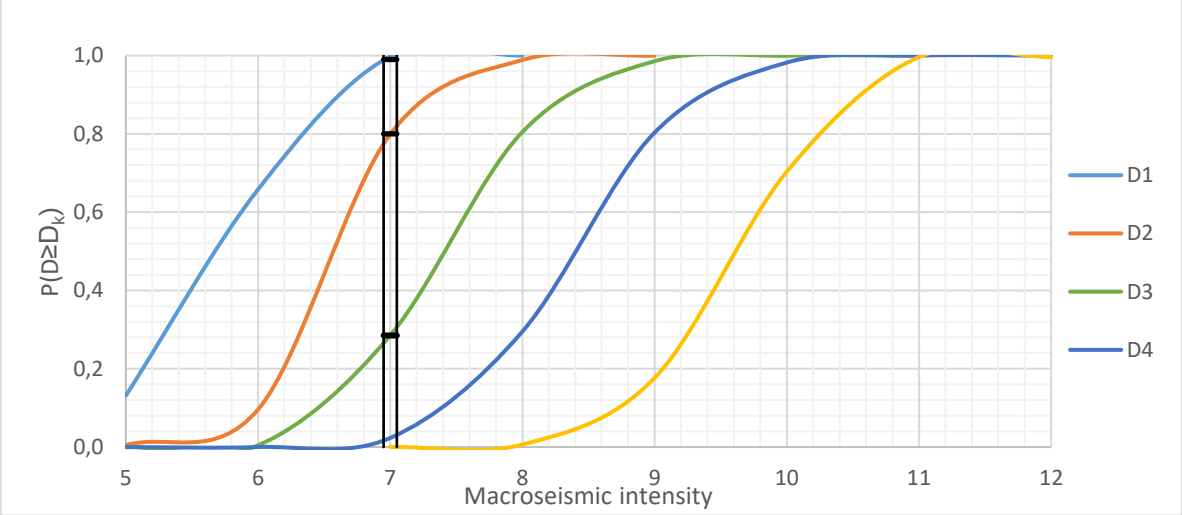

Figure 3.2-4 La Barceloneta, 6-story corner building; probability of reaching or exceeding each damage level

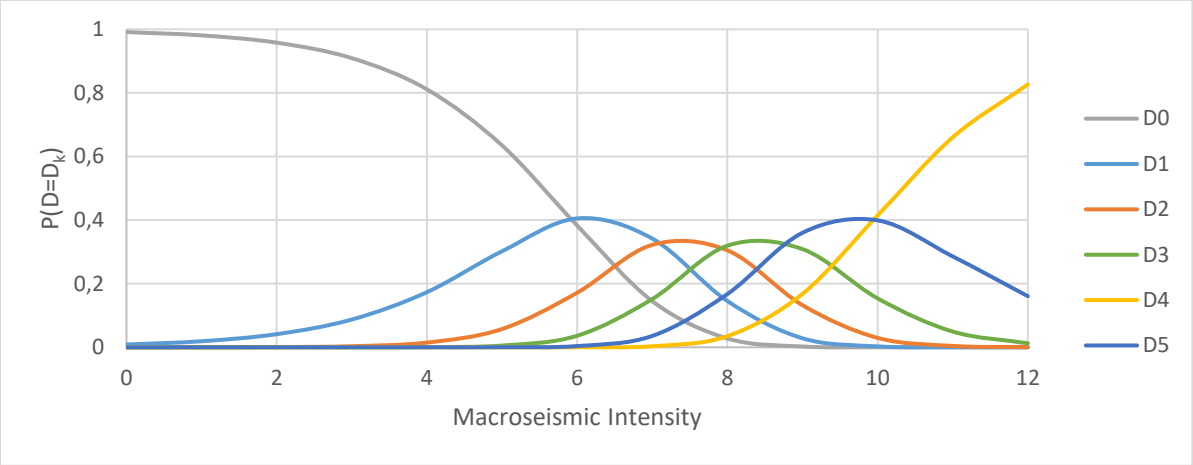

Figure 3.2-5 Figure 3.2-6 La Barceloneta, 6-story attached building; probability of each damage level

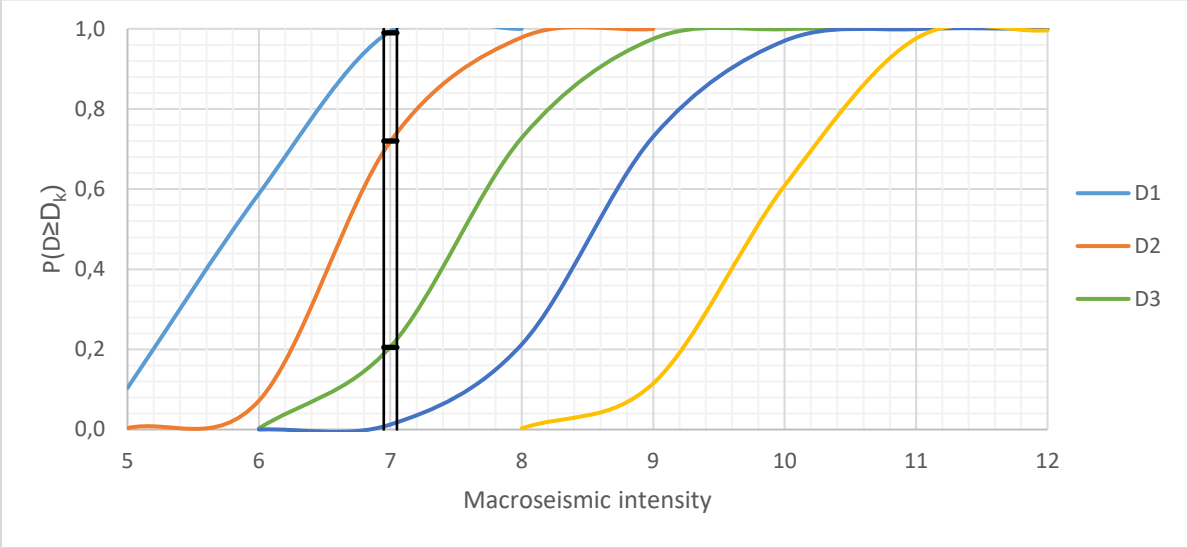

Figure 3.2-7 La Barceloneta, 6-story attached building; probability of reaching or exceeding each damage level

4. KINEMATIC LIMIT ANALYSIS

4.1 Response spectra for La Barceloneta house

The main aim of the dissertation is to conduct nonlinear kinematic analysis for La Barceloneta house, and to compare the results that were obtained with Eurocode 8 and Spanish seismic code NCSE-02. For this reason, some parameters which are based on the characteristics of the soil that are going to be used for the construction of the response spectrum must be defined. These parameters are presented in table 4.1.1. The Eurocode guideline for Barcelona recommends using only Type 1 spectrum (far-field earthquake) and to neglect Type 2. The soil characteristics were obtained from Cid. 2001, the seismic zonation of Barcelona that considers the local effects. Seismic acceleration a_c was calculated for a_b=0,04 and ρ=1 where a_b is the basic acceleration given by Spanish seismic code annex 2.1 while, ρ is the coefficient that influences the acceptable probability for the earthquake to happen. In this case, the return period is chosen to be 475 years as the buildings are considered of normal importance. There are two types of objects, ordinary and of special importance. Ordinary buildings have an important factor

equalling 1 and those of special importance have an important factor equalling 1.3. Under this case the important factor is considered 1, therefore the whole neighborhood is treated as ordinary (importance class II) according to EC8 AND NCSE – 02. The elastic response spectra are displayed in Figure 4.1-1.

Table 4.1-1 Parameters for the response spectra (EC 8, NCSE-02)

Parameter	**La Barceloneta**	
	NCSE-02	**EC 8**
S	1,28	1,40
C	1,60	-
K	1	1
a_b	0,04	-
ρ	1	-
$a_{g,R}$	-	0,05
γ_1	-	1

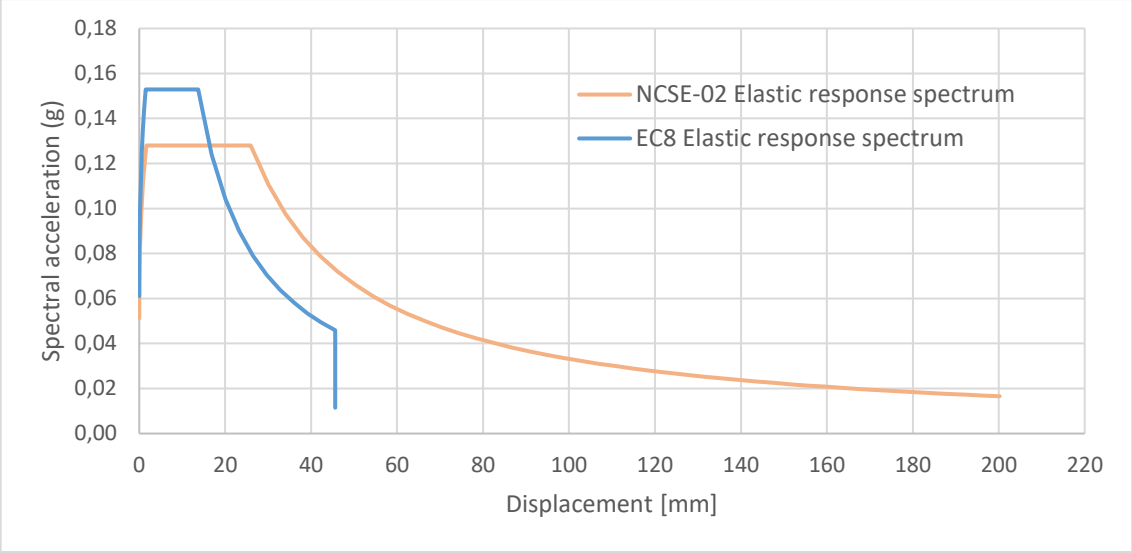

Figure 4.1-1 Elastic response spectra, EC8 and NCSE-02

4.2 Analysis of La Barceloneta

4.2.1 Assumptions

Floor supporting beams with the 100 mm load-bearing length into the masonry wall will collapse when subjected to 100 mm out of plane displacement of the load-bearing wall [Figure 4.2-1 (c)].
If the embedded length of the beam is 200 mm, in case of 100 mm displacement of the wall, the beam would still have 100 mm of effective supporting length which would not lead to the collapse of floor beams.
If the embedded length of the beam is assumed to be 120 mm, in the event of seismic activity, a 100 mm out of plane displacement would leave the beam with only 20 mm of support length, that would lead to stress concentration which can propagate the failure of the supporting wall [Figure 4.2-1 (b)].
All these cases are developed based on the assumption that the friction between the beam and masonry wall is negligible.

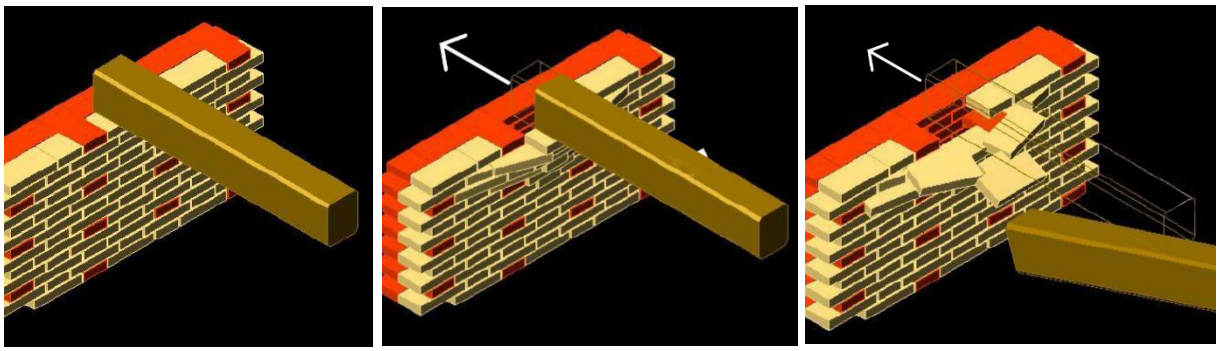

(a) (b) (c)

Figure 4.2-1 Possible failure of simply supported beams (Manuale delle murature storice, 2011).

If the structure has not undergone strengthening by means of introduction of ties, bond beam, or ring beams, then it is assumed that the only way for the structure to withstand the overturning exerted by seismic activity is governed by the friction of the contact surface, and this will lead to the development of local failures, shown below. As mentioned above in the state of the art, D’Ayala and Speranza (2002) applied the overturning of the facades through the introduction of friction coefficient μ, for the frictional behavior of mortar joints for different geometric configurations, masonry types, and connections with orthogonal walls and horizontal diaphragms.
The resistive action caused by friction between the beams and the walls is the result of both, the vertical stabilizing loads transferred from the floors to the façade, and the self-weight of the walls. The friction on the lower floors is higher compare to the upper floors.
However, all these considerations are neglected, and the calculations are conducted through a simplified model, where the cracks in the orthogonal walls are developed based on empirical models, and the transfer load from the slab is considered as fixed.

- **Masonry**

The facade is built up of bricks and the thickness is 30cm while orthogonal walls are assumed 15 cm thick. Considering the corners of corner buildings are built up of stones it was decided to investigate both cases, good connection, and bad connection of the facade with the orthogonal walls (Figure 4.2-2 (a)). The same practice was followed also for the attached buildings amongst a row, as we don’t have information on the quality of the connection between the facade and the orthogonal walls. The render covers everything, so it is difficult to obtain information visually (Figure 4.2-2(b)). For the cracks which are developed in the orthogonal walls was assumed a very conservative angle of 15º (Figure 4.2-2 (c)) (D’Ayala and Speranza, 2003)

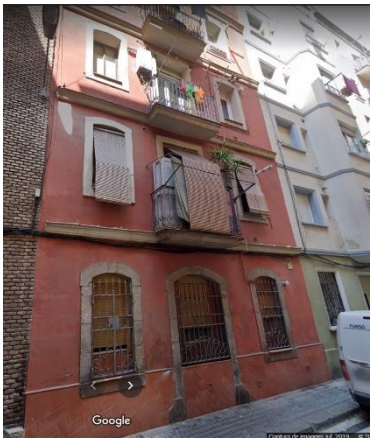

(a) (b) (c)

Figure 4.2-2 Quality of the connection of the corner: (a) corner building (Google Maps), (b) attached building amongst a row (Google Maps), (c) crack development angle (Milani. G, 2016)

- **Slabs**

Two types of slabs are identified; those built up with brickwork arches supported by timber beams and those with brick arches supported iron by I-beams. For simplification reasons a load of 2 kN/m^2 was assumed and the type of slab was neglected. No confinement or seismic strengthening connection between slab and walls was considered (e.g. steel ties).

Soil Type

The soil type is Type III for the NCSE-02 (Cid, Seismic Zonation of Barcelona) and the corresponding soil for the EC 8 is Type C characterized by a slight difference in terms of velocity from the values of Spanish code. Thus, the NCSE-02 spectrum was obtained for soil parameters Type III, while the EC response spectrum was obtained following the Type C soil parameters.

- **Material Properties**

Following Table 8.5.1 of Circolare 2019 for solid brick masonry, the specific weight of the masonry was considered γ=18,00 kN/m^3, the compression strength as 4 MPa, and Young’s modulus 1.7 GPa. The fundamental period of the structure was calculated according to the formula $T1 = 0{,}05 \bullet H^{0,75}$, as suggested in the Italian code NTC 2018. Based on these assumptions it was possible to calculate the identified overturning mechanisms and cylindrical overturning (horizontal-arch failure)

4.2.2 Results

Table 4.2-1 Categorization of La Barceloneta house by aggregate position and number of stories and identification of the number of out of plane local mechanisms

Aggregate position: Corner building		Aggregate position: Attached building amongst a row	
No. of floors	No. of Local Mechanisms	No. of floors	No. of Local Mechanisms
2 stories	13	2 stories	6
3 stories	13	3 stories	6
4 stories	15	4 stories	8
5 stories	15	5 stories	8
6 stories	15	6 stories	8

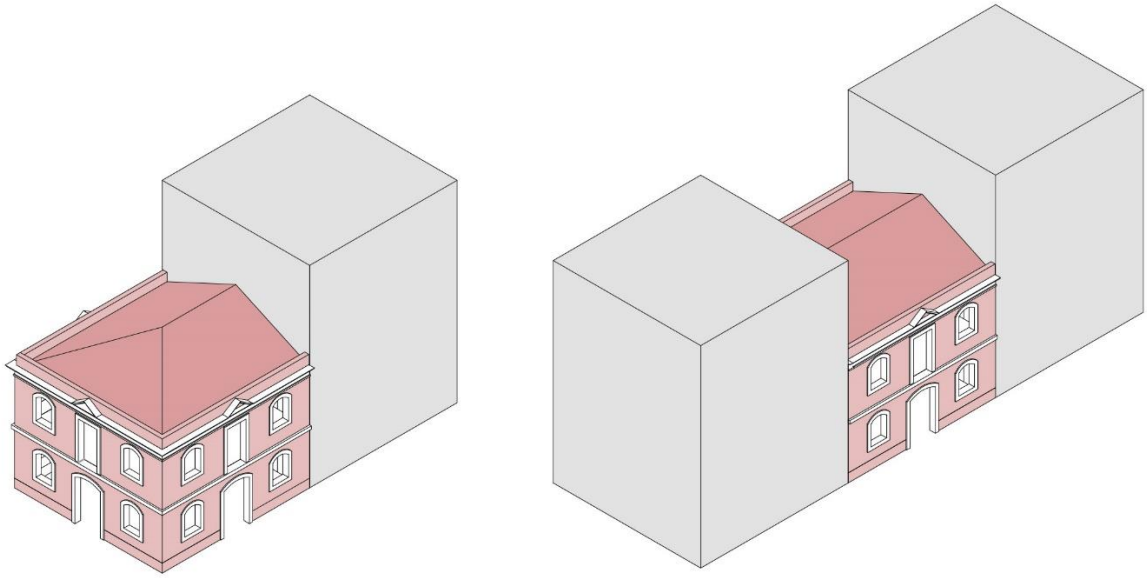

Figure 4.2-3 Aggregate position, representation through the two-story building. (a) the corner building, (b) attached building amongst a row

The calculations for the performance point were conducted with both Methods A and method B (Section 2.7) using both Eurocode 8 and Spanish seismic code (NCSE-02). To explain the steps for the calculation of performance point through method B (capacity spectrum), the reduction of the response spectrum is shown graphically in (Figure 4.2-21) for the overturning of the front facade of the six-story corner building (Figure 4.2-19 (a)) Since the Eurocode elastic response spectrum intersects with the capacity curve in the elastic part, it was not necessary to reduce it, as the performance point was located at the intersection. When intersection happens in the elastic part of the curve then the performance point obtained through Method A overlaps with the one of Method B. Whereas, for the NCSE-02 code a few iterations were conducted to achieve the reduced response spectrum within the tolerance of 0.001m (Section 2.7).

In addition to the graph for the overturning of the six-story front facade with the implication of orthogonal walls in the following pages are going to be presented also the results for all the mechanisms.

Out of twelve categories of La Barceloneta house here below will be presented only the results for the six-story corner buildings and attached buildings amongst a row. The results for the other categories which are considered as less vulnerable will be included in Annex 1

The results obtained from Eurocode 8 and Spanish seismic code are quite different. To analyze the performance point obtained with Method A it is necessary to divide the elastic response spectrums into parts based on the angle (or location) of the elastic curve (Figure 4.2-4).

- If the elastic curve is in between line no.1 and line no.2 than the displacement obtained by Eurocode 8 is lower than the displacement obtained by NCSE-02.
- If the elastic curve is in between line no.2 and line no.3 than the displacement obtained by Eurocode 8 is higher than the displacement obtained by NCSE-02.
- If the Elastic curve is in between no.3 and no.4 than we might have two cases which depend by the value of a_{yield}.

  For: $a_{yield} > 0{,}128$ $d_{EC8} > d_{NCSE-02}$
  $a_{yield} < 0{,}128$ both cases are possible
- If the elastic curve is located after line no. 4 then the displacement obtained by Eurocode 8 is lower than the displacement obtained by NCSE-02.
-

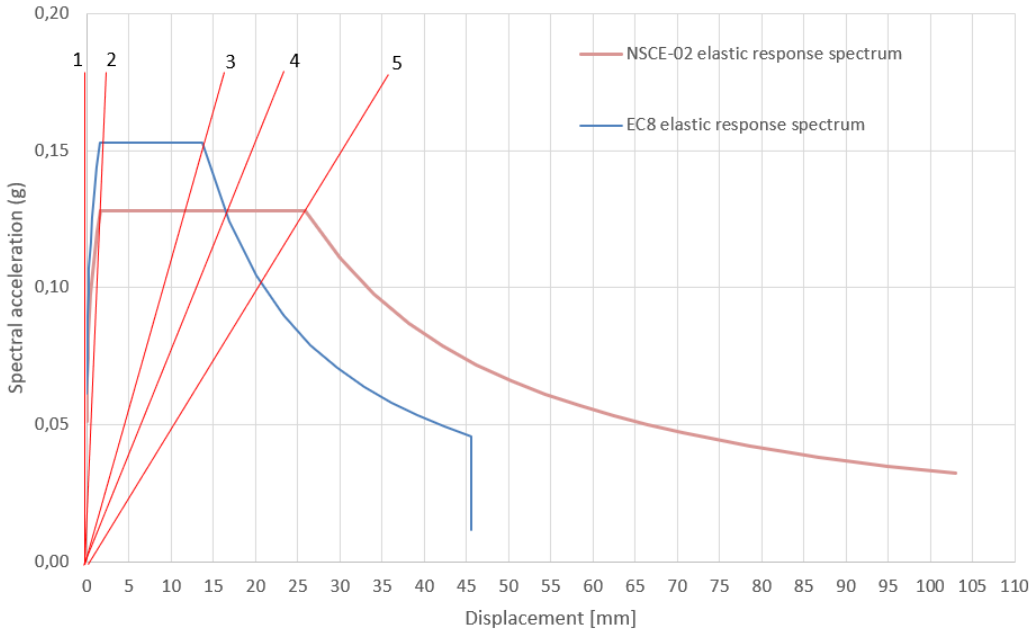

Figure 4.2-4 The relationship between the elastic curve and the elastic response spectrums

Attached building amongst a row

The local mechanisms identified are listed below:

- Overturning of the main facade with two side wings (Figure 4.2-5 (a))
- Overturning of the top story (horizontal arch-top strip) (Figure 4.2-5 (b))
- Overturning of the last story with two side wings (Figure 4.2-5 (c))
- Vertical strip overturning in the front facade (Figure 4.2-6 (a))

- Overturning of the orthogonal wall with two side wings (Figure 4.2-6 (b))
- Overturning of the orthogonal wall (Figure 4.2-6 (c))
- Overturning of the facade (Figure 4.2-7 (a))
- Failure of the corner (Figure 4.2-7 (b))

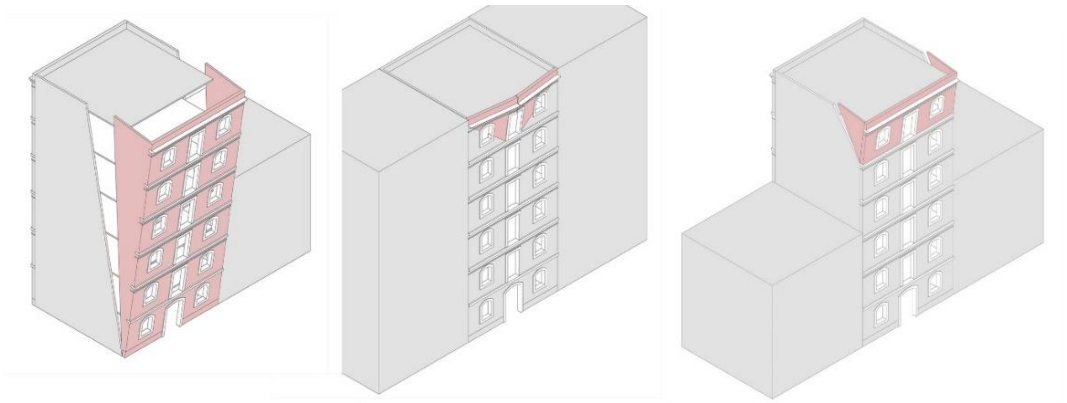

(a) (b) (c)

Figure 4.2-5 Local mechanisms: (a) Overturning of the main facade with two side wings, (b) Overturning of the top story (horizontal arch-top strip), (c) Overturning of the last floor with two side wings

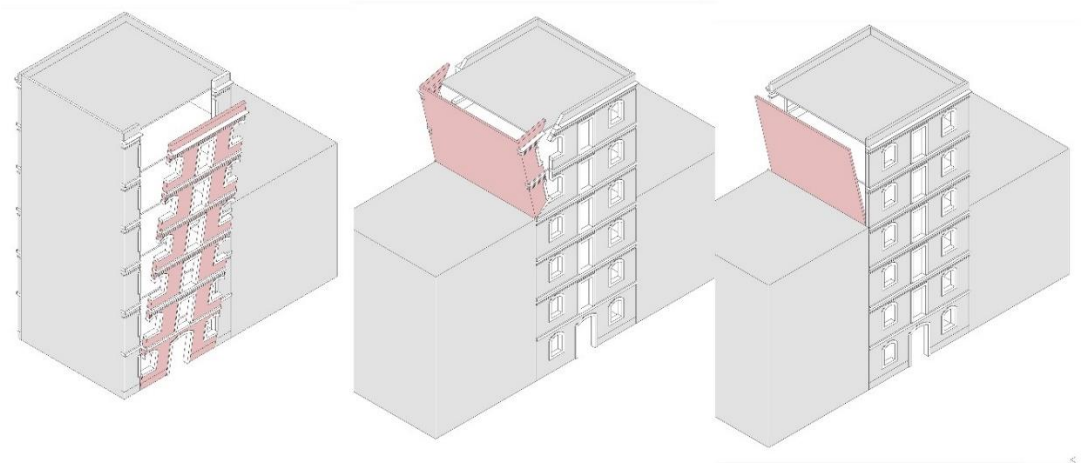

(a) (b) (c)

Figure 4.2-6 Local mechanisms: (a) Vertical strip overturning in the front facade, (b) Overturning of the orthogonal wall with two side wings, (c) Overturning of the orthogonal wall

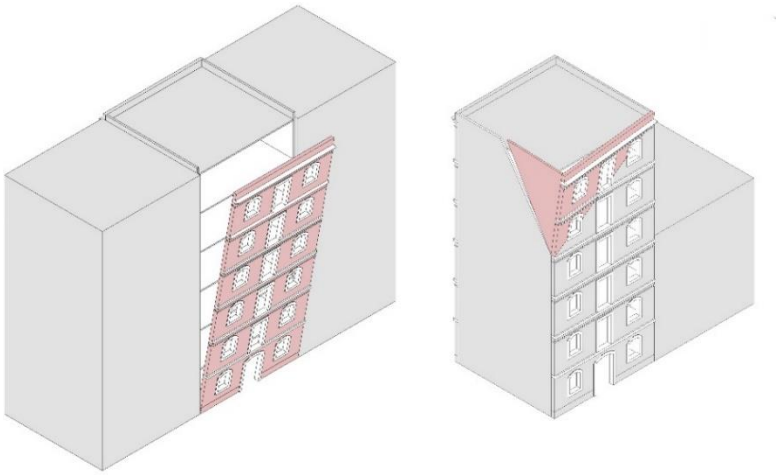

(a) (b)

Figure 4.2-7 Local mechanisms: (a) Overturning of the facade, (b) Failure of the corner

Figure 4.2-11 illustrates the position of the performance points for the overturning of the main facade. This mechanism is characterized by the overturning of the whole facade with the implication of sidewalls, when the edge connection is active so that the crack can happen in the side walls (Figure 4.2-5 (a)). It has an and activation acceleration $\alpha_0 = 0.147g$. In both cases, the performance point from EC8 and NCSE-02 is in the elastic region between 0 and Sd_1. Considering that both performance points are close to Sd_1, especially the one obtained from NCSE-02 analysis which lies in damage level 1, it can be said that damage level 1 should be expected.

As verifying the overturning of the top story mechanism (Figure 4.2-5 (b)) presents some challenges, to be confident in our judgment, the other mechanism involving the side walls was also verified (Figure 4.2-5 (c)). Both mechanisms are very rigid, and a minor degree of deformation can occur before the structure passes into the plastic state. The first mechanism is the particular case in which the activation of the kinematic mechanism is due to the crushing of the masonry at the plastic hinges, due to the tensional state induced by the seismic actions (Figure 4.2-8). The mechanism can only occur in the presence of a lateral contrast structure, similarly to La Barceloneta typology. (ReLuis, 2013)

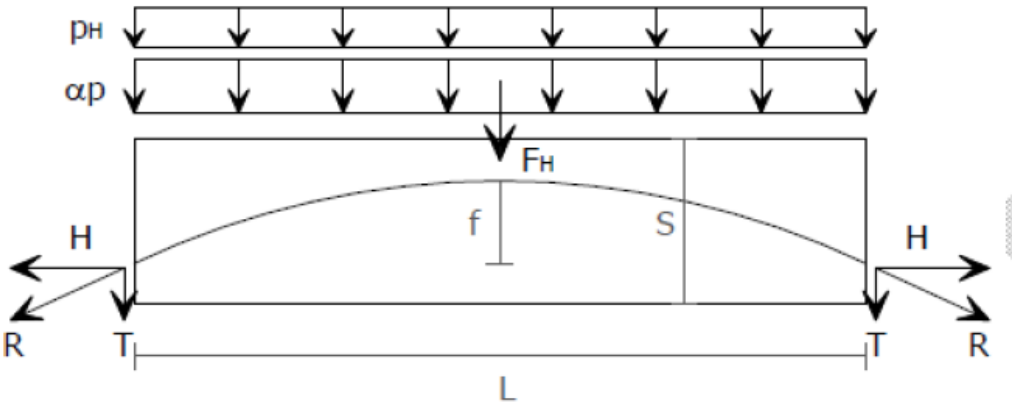

Figure 4.2-8 Mechanism scheme

For this second mechanism, the performance points obtained from EC 8 analysis and NCSE-02 analysis are in the elastic region between 0 and Sd_1, therefore it can be said that no damage is expected (Figure 4.2-12)

The second mechanism is less stiff, but it has a lower activation acceleration mechanism compare to the first one (0,148g vs 0,222g). The performance point obtained from EC 8 analysis is in the elastic range between Sd_1 and Sd_2, while for NCSE-02 the performance point is in the plastic range and lies in damage level 3. Method A and Method B achieved similar results also because the yield point is very close to the constant part of the EC 8 spectrum (Figure 4.2-13)

The vertical strip (Figure 4.2-6 (a)) mechanism is considered when facades are characterized by openings with regular dimensions, aligned throughout the height and rough opening is smaller than the side pier. Moreover, the edge connection has to be active so that the vertical crack can occur within the facade itself. It is assumed that this mechanism can involve any number of stories up to the whole facade, but in this thesis is studied only the whole facade (Figure 2.1-1) (D’Ayala and Speranza, 2003).

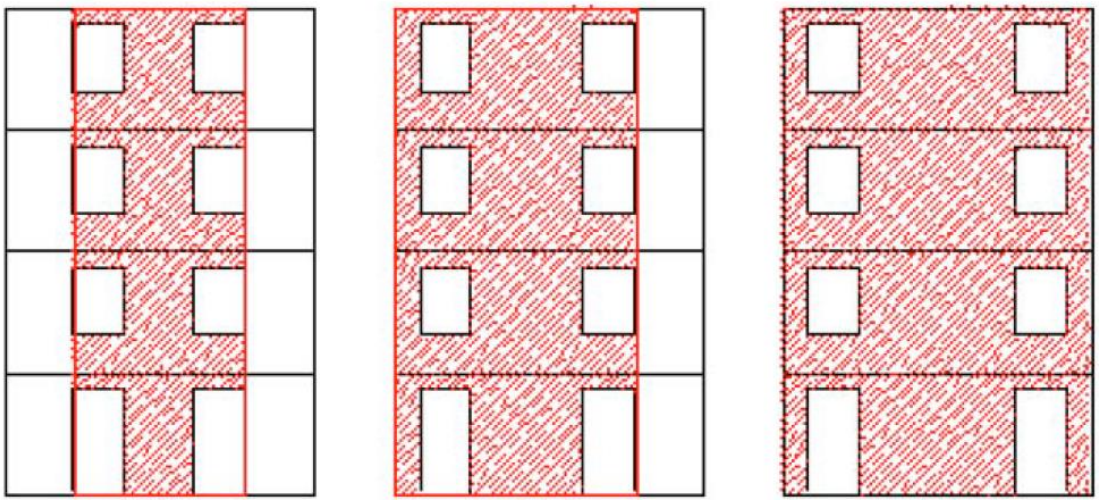

(a) (b) (c)

Figure 4.2-9 vertical strip overturning, portions of the facade involved in the collapse concerning the pier width (a) width of the side pier is greater than the width of the window, (b) width of left pier smaller than the width of the window (c) width of the side pier smaller than the width of the window. (D’Ayala and Speranza, 2003)

This mechanism has the lowest activation acceleration compared to other mechanisms ($\alpha_0 = 0.006g$). The performance points obtained with Method A from EC 8 and NCSE-02 are in the plastic region after Sd_4. For EC 8, Method A and Method B achieved the same results as the performance point is located in the steady part of the spectrum (Figure 4.2-14).

Calculations were conducted also for the overturning of the facade mechanism (Figure 4.2-7 (a)). Although the results were not satisfactory ($\alpha_0 = 0.006g$) on our judgement this is a pessimistic mechanism because the edge connection of the corner buildings is of decent quality and correctly executed (Figure 4.2-10).

Figure 4.2-10 Quality of the edge connection

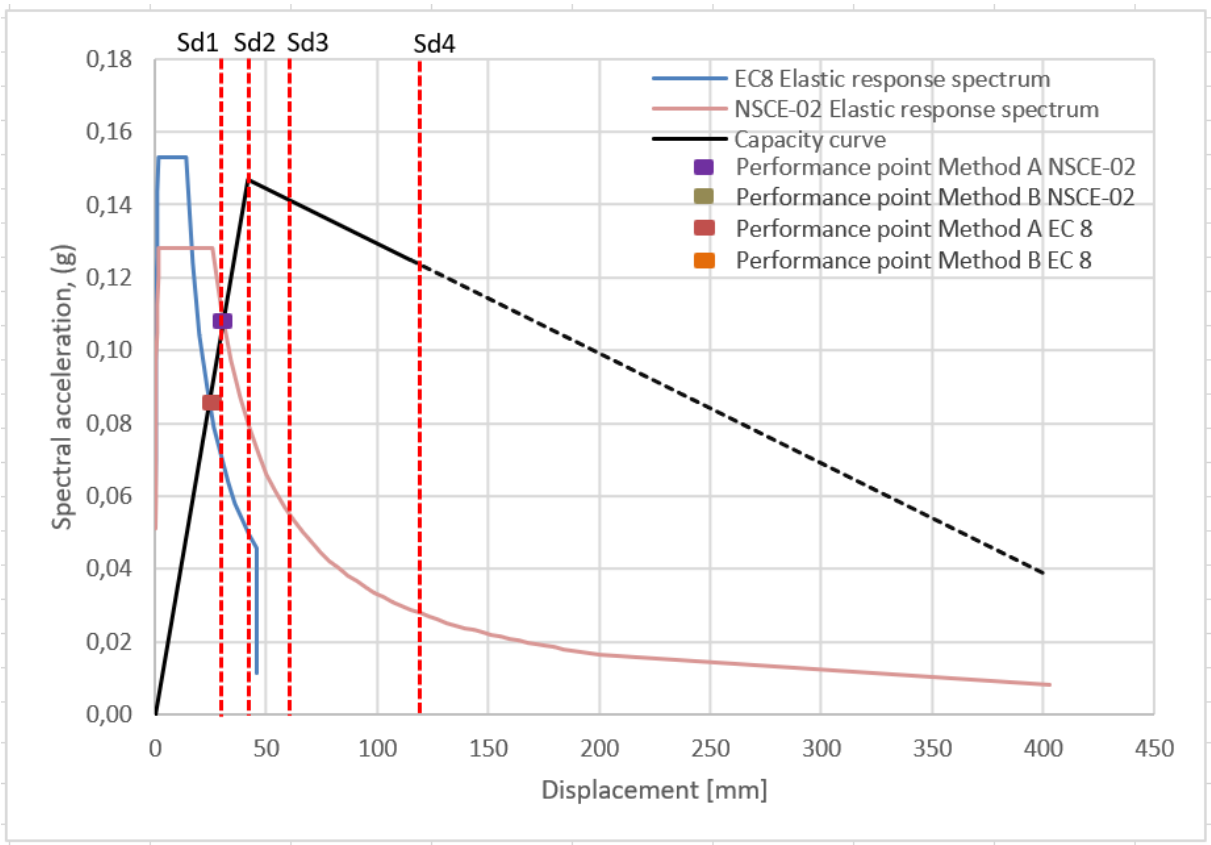

Figure 4.2-11 Performance point for of the main facade with two side wings (Figure 4.2-5 (a))

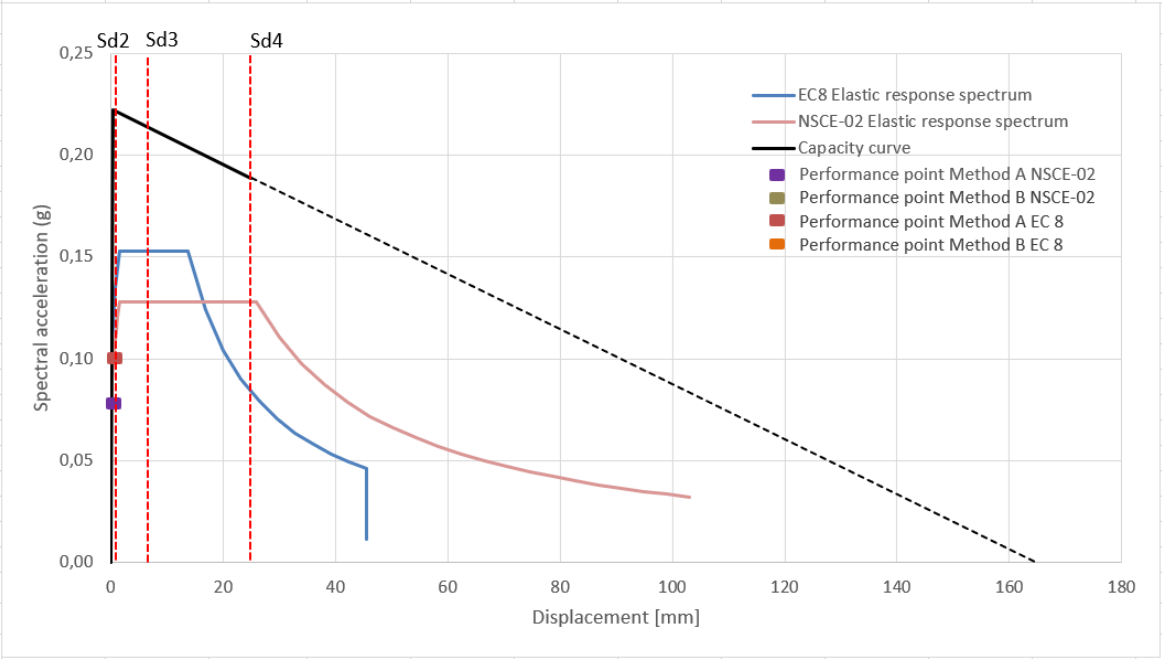

Figure 4.2-12 Overturning of the top story (horizontal arch-top strip) (Figure 4.2-5 (b))

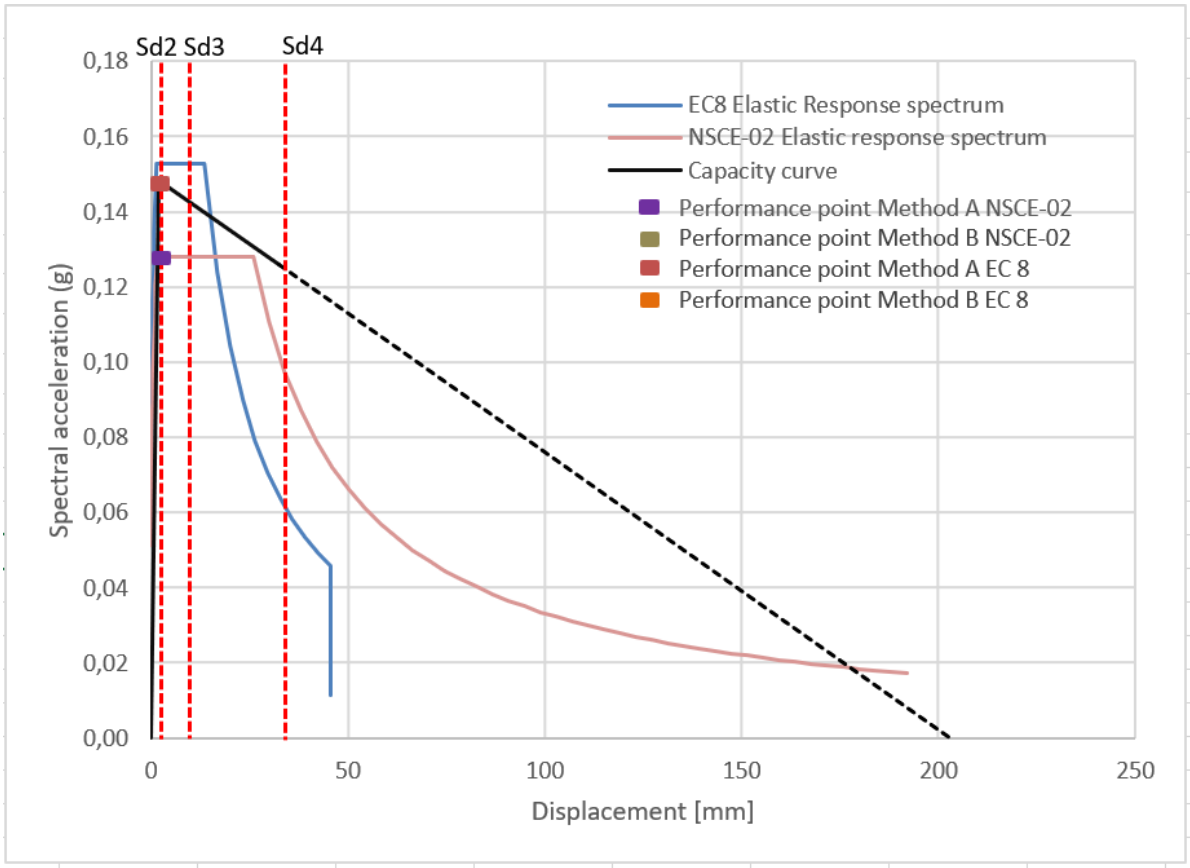

Figure 4.2-13 Overturning of the last story with two side wings (Figure 4.2-5 (c))

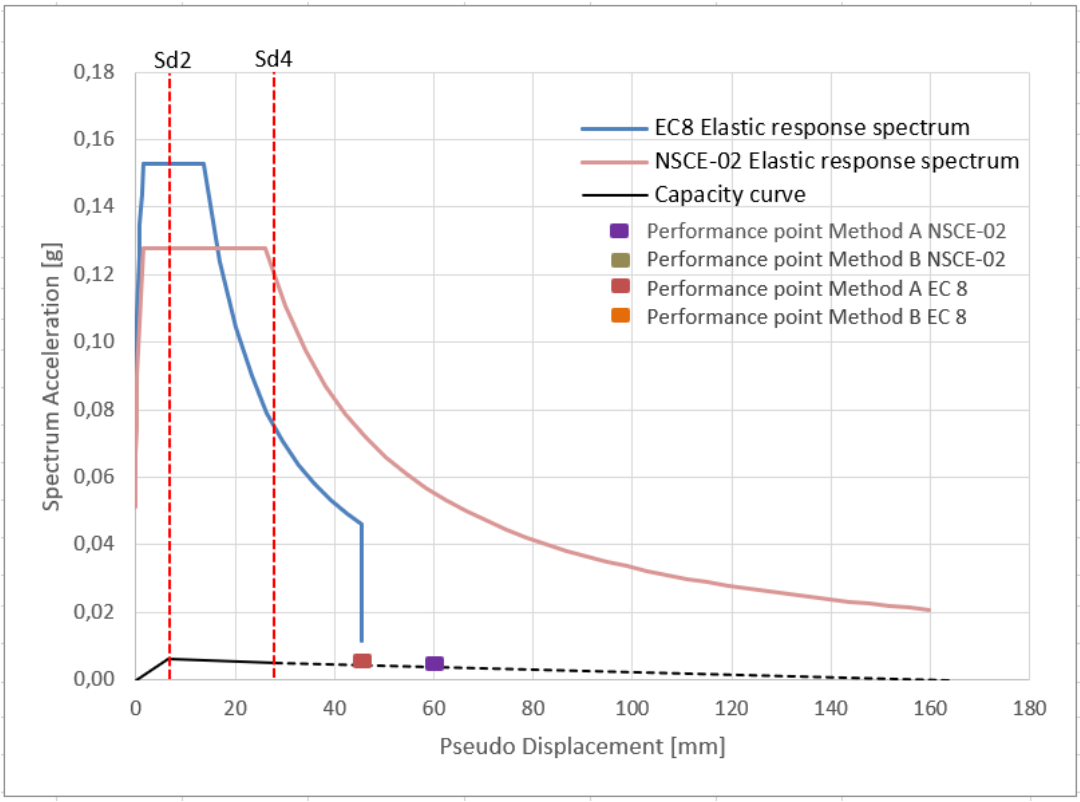

Figure 4.2-14 Vertical strip overturning in the front facade (Figure 4.2-5 (a))

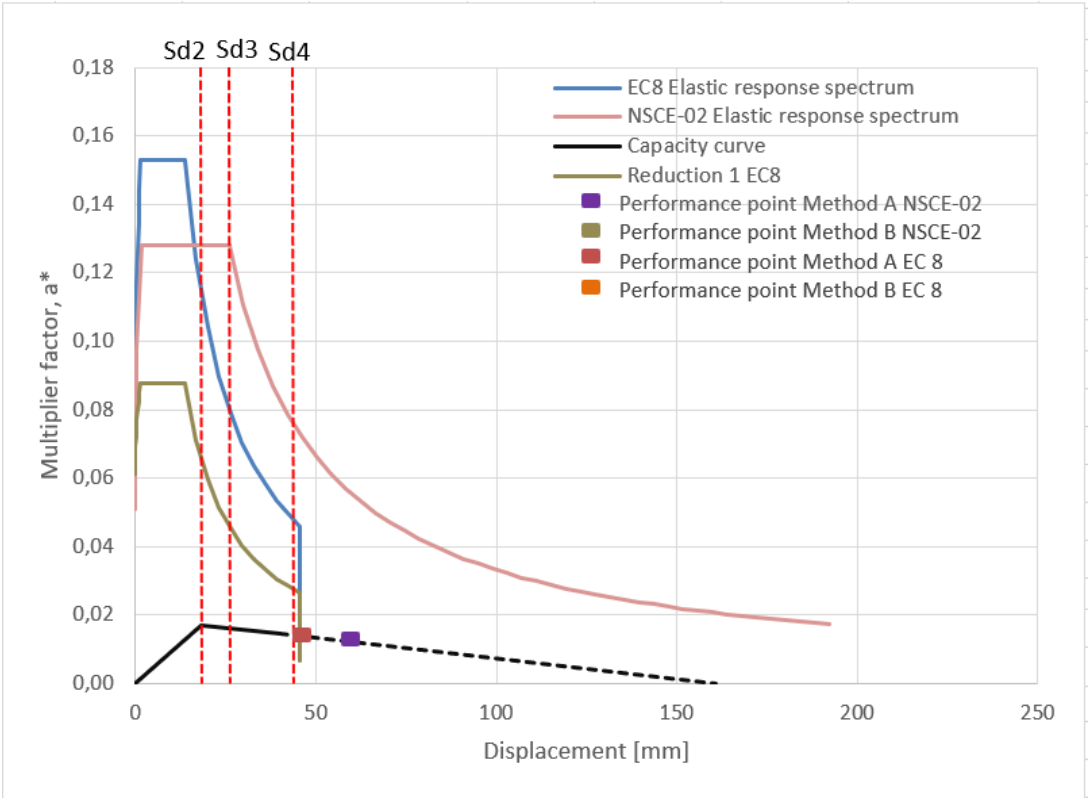

Figure 4.2-15 Overturning of the facade (Figure 4.2-7 (a))

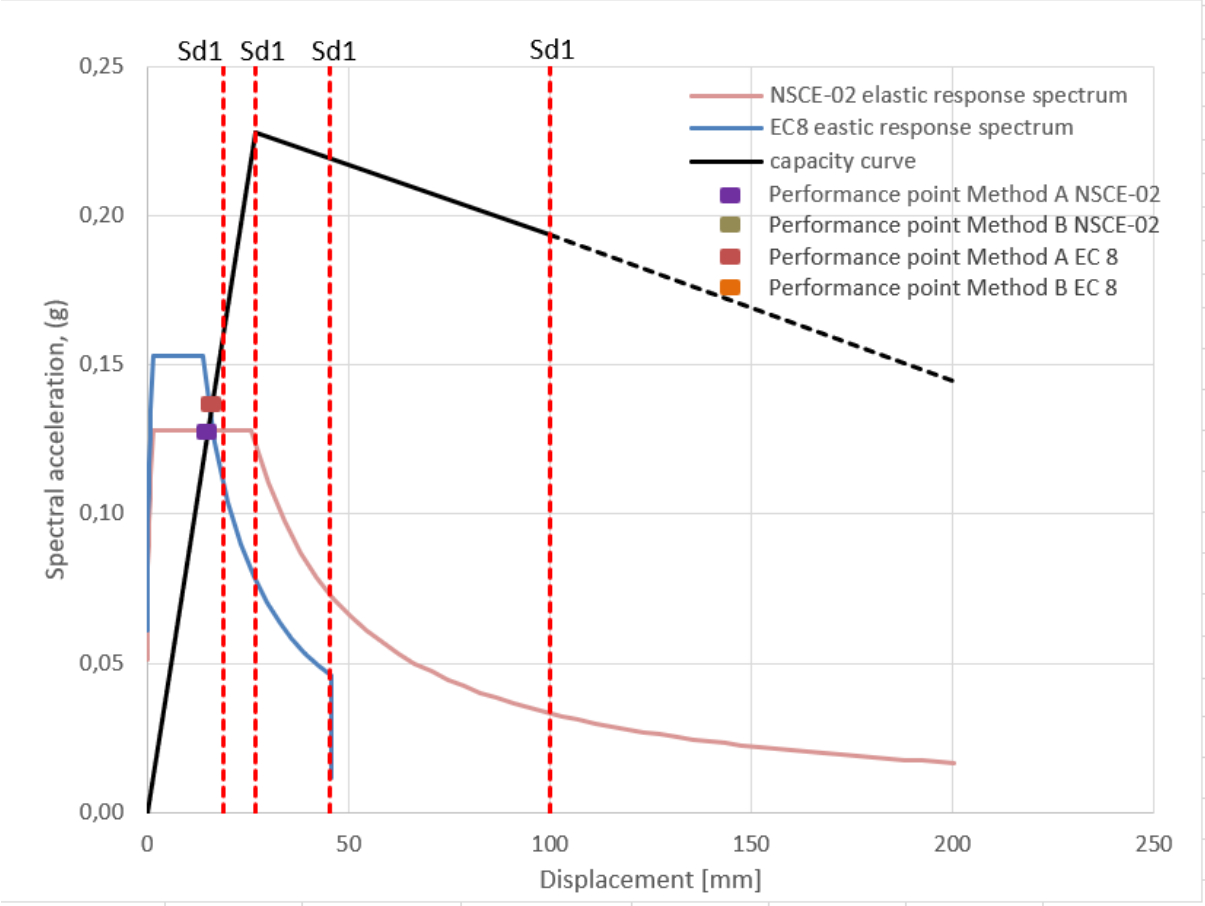

Figure 4.2-16 Overturning of the orthogonal wall with two side wings (Figure 4.2-6 (b))

Table 4.2-2 Activation acceleration for all calculated overturning mechanisms for 6-story building attached amongst a row

Macroelement	**Overturning activation acceleration** α_0
Overturning of the main facade with two side wings	0.147
Overturning of the top story (horizontal arch-top strip)	0.222
Overturning of the last story with two side wings	0,148
Vertical strip overturning in the front facade	0.0051
Overturning of the orthogonal wall with two side wings	0,23
Overturning of the orthogonal wall with the influence of the internal wall	0.16
Overturning of the facade	0.017

Mechanisms for the corner building

- Overturning of the facade with two side wings (Figure 4.2-17 (a))
- Overturning of the top story (horizontal arch-top strip) (Figure 4.2-17 (b))
- Overturning of the last story with two side wings (Figure 4.2-17 (c)

- Vertical strip overturning in the side facade (Figure 4.2-18 (a))
- Partial overturning, triangular shape
- Overturning of the side facade (Figure 4.2-18 (b))
- Failure of the corner (Figure 4.2-18 (c)
- Overturning of the front facade with two side wings (Figure 4.2-19 (a))
- Overturning of the top story (horizontal arch-top strip) (Figure 4.2-19 (b))
- Overturning of the last story with two side wings (Figure 4.2-19 (c))
- Vertical strip overturning in the front facade (Figure 4.2-20 (a))
- Partial overturning, triangular shape (Figure 4.2-20 (b))
- Overturning of the front facade
- Failure of the corner (Figure 4.2-20 (c))

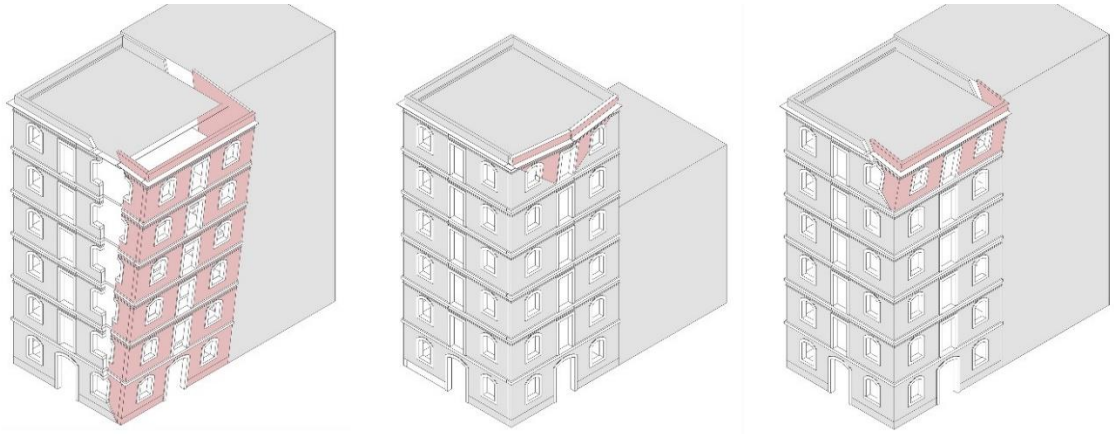

(a) (b) (c)

Figure 4.2-17 Local mechanisms: (a) Overturning of the facade with two side wings, (b) Overturning of the top story (horizontal arch-top strip), (c) Overturning of the last floor with two side wings

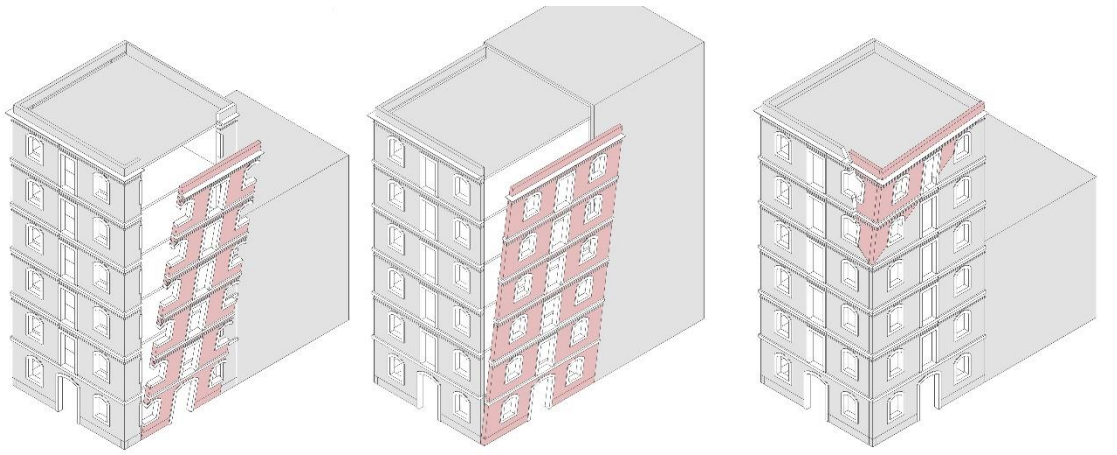

(a) (b) (c)

Figure 4.2-18 Local mechanisms: (a) Vertical strip overturning in the front facade, (b) Overturning of the side facade, (c) Failure of the corner

Mechanisms for corner building, the front facade

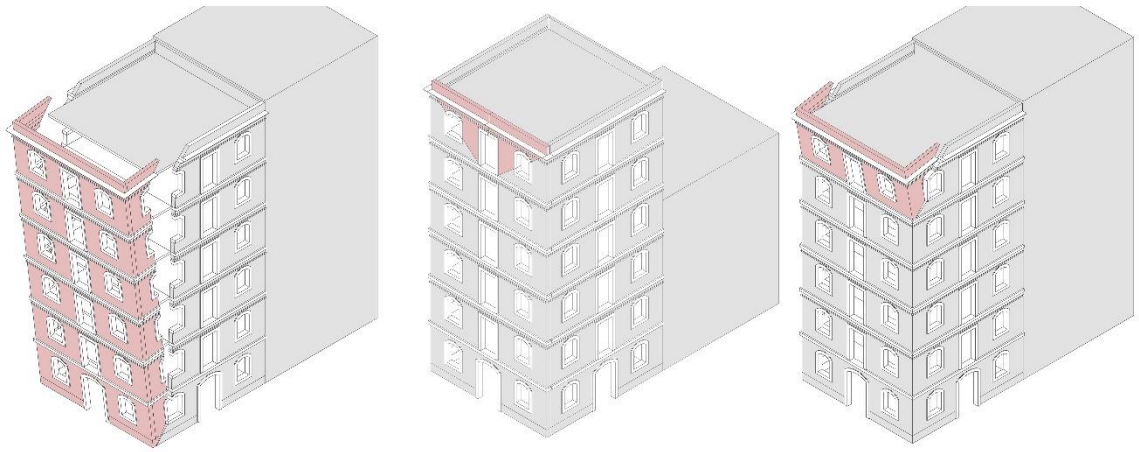

(a) (b) (c)

Figure 4.2-19 Local mechanisms: (a) Overturning of the front facade with two side wings, (b) Overturning of the top story (horizontal arch-top strip), (c) Overturning of the last floor with two side wings

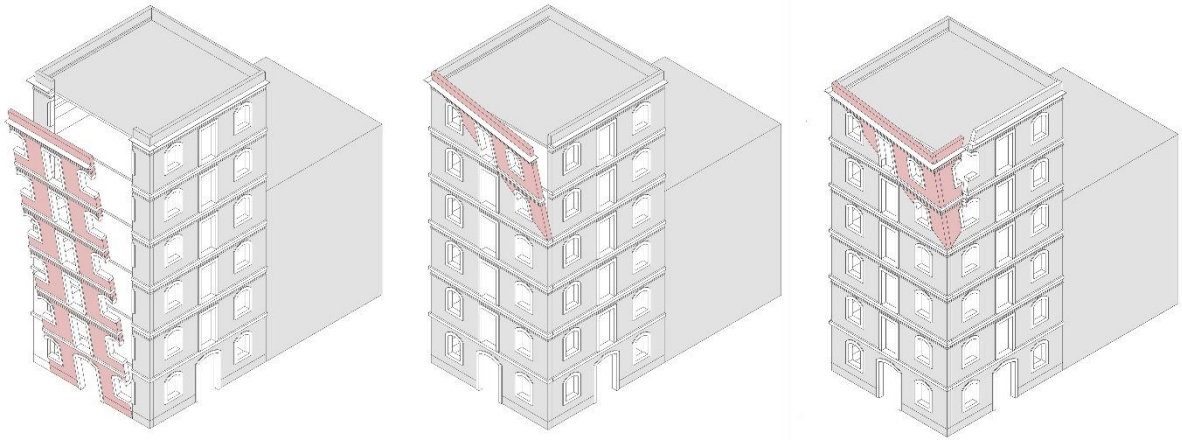

(a) (b) (c)

Figure 4.2-20 Local mechanisms: (a) Vertical strip overturning in the front facade, (b) Partial overturning, triangular shape, (c) Failure of the corner

Table 4.2-3 Activation acceleration for all calculated overturning mechanisms for 6-story corner building amongst a row

Macroelement	**Overturning activation acceleration** α_0
Overturning of the main facade with two side wings	0.142
Overturning of the top story (horizontal arch-top strip)	0.222
Overturning of the last story with two side wings	0.148
Vertical strip overturning in the front facade	0.0051
Overturning of the orthogonal wall with the influence of the internal wall	0.16
Overturning of the facade	0.017
Overturning of the main front facade with two side wings	0.052
Overturning of the last story with two side wings	0.148
Vertical strip overturning in the front facade	0.0051

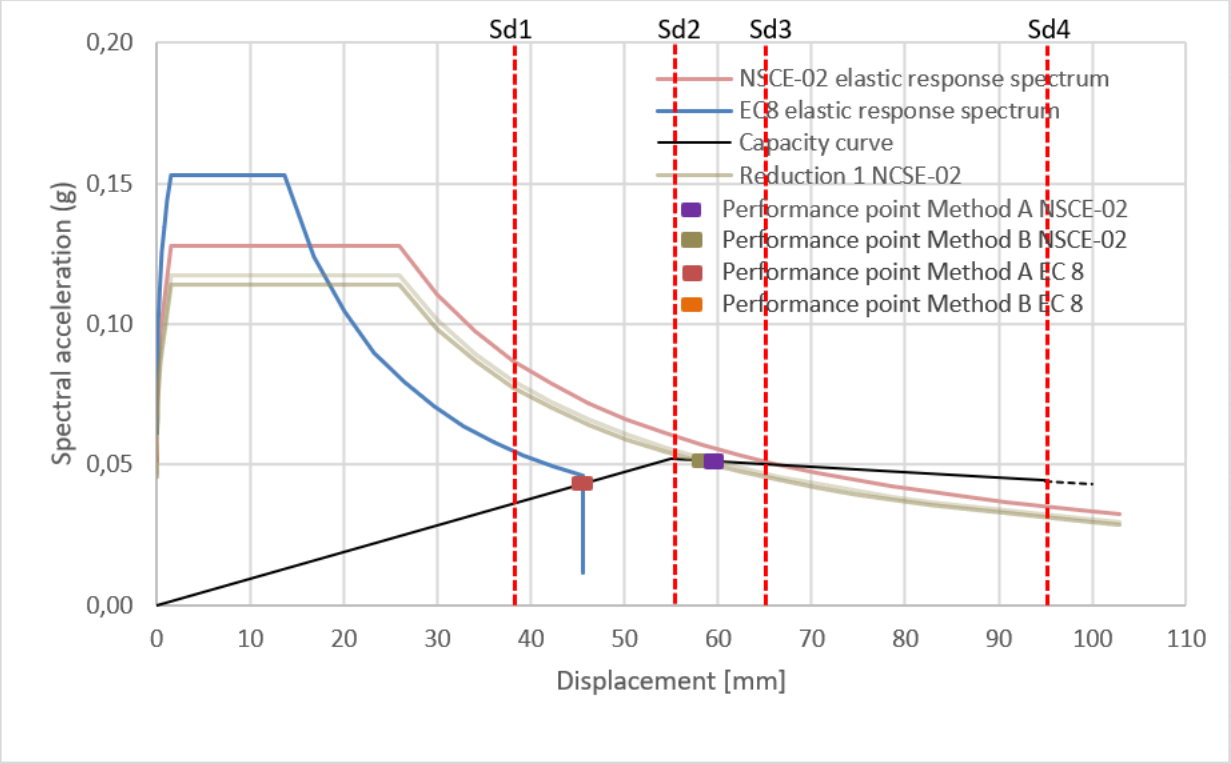

Figure 4.2-21 Overturning of the front facade with two side wings (Figure 4.2-19 (a))

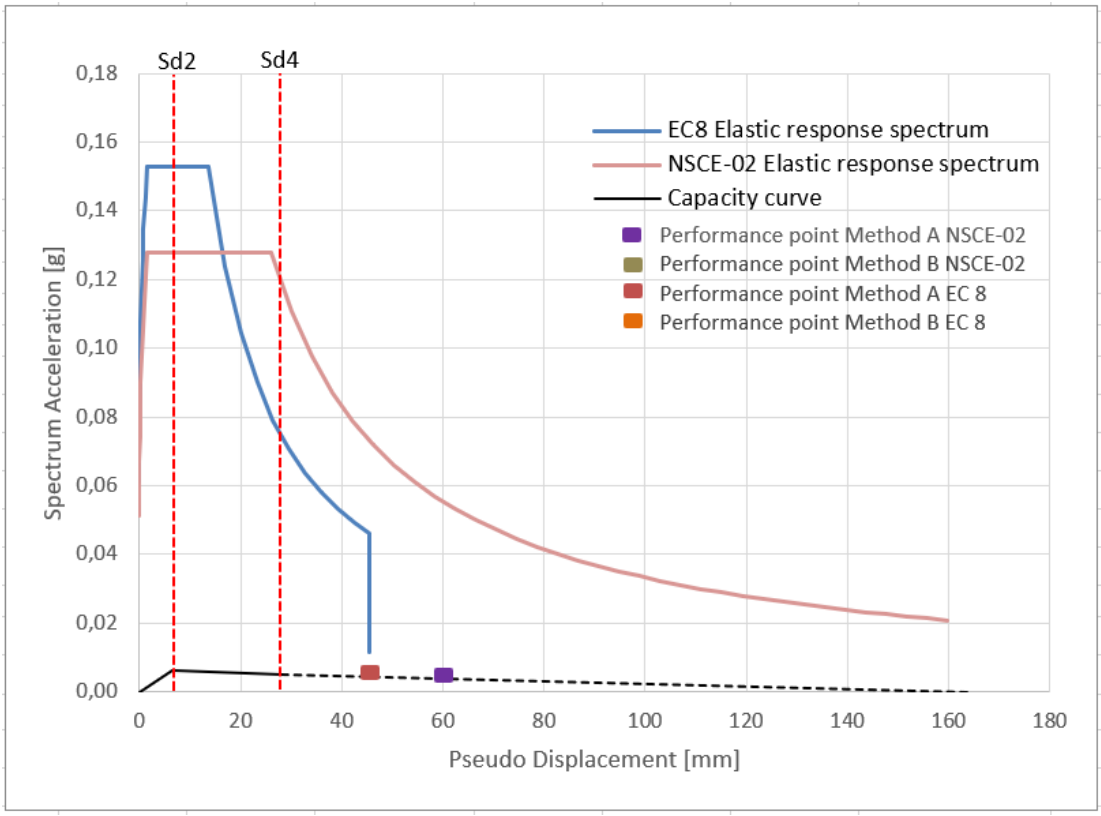

Figure 4.2-22 Vertical strip overturning in the front facade and side facade (Figure 4.2-18, Figure 4.2-20)

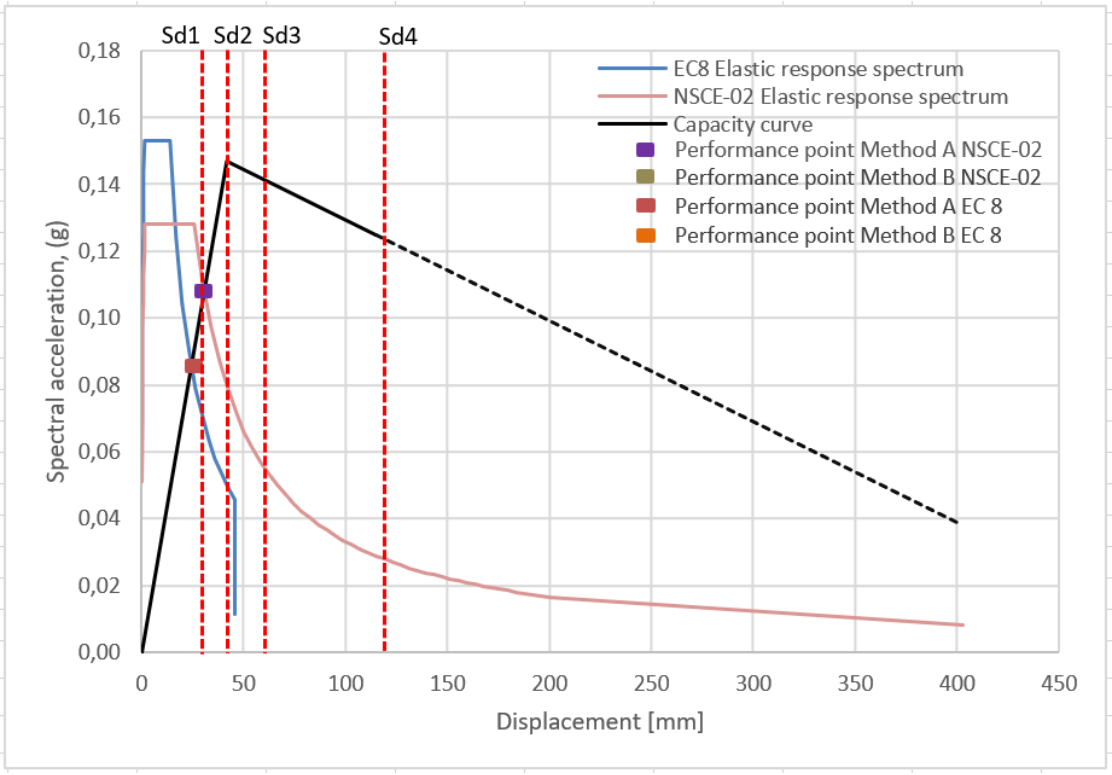

Figure 4.2-23 Overturning of the facade with two side wings (Figure 4.2-20 (a))

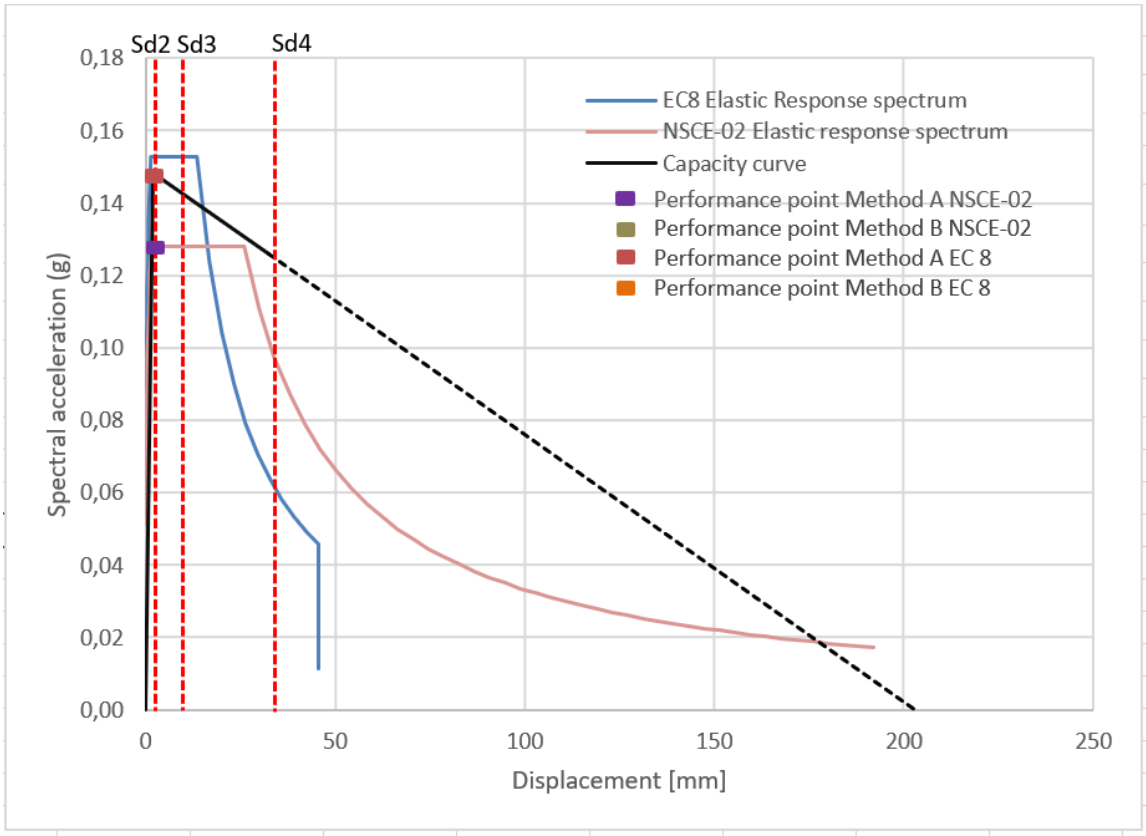

Figure 4.2-24 Overturning of the top story (horizontal arch-top strip),(Figure 4.2-17, Figure 4.2-19)

4.3 Evaluation of the method and possible improvements

In applying the kinematic method to define the damage state in case of an earthquake several steps were taken. During the first step, all the local mechanisms created during an earthquake were defined. Also, material characteristics such as loads, specific weight, compression strength, young modulus were assigned. In the second step, the proper discretization and simple calculations were used in achieving reliable results regarding the capacity of the building. In the third step, Method A and B were applied to calculate the performance point. And in the last step, to define the damage state the location of the performance point and conditions defined by Lagomarsino and Penna (2007) were used.

The choice of mechanisms requires a deep understanding of the behavior of the masonry in case of a seismic event. However, if the engineer is not that experience the best choice would be to calculate all the possible mechanisms and then to discuss the results. The identification itself of the mechanism requires advanced knowledge of historical constructions, building techniques, the interaction between buildings in case of aggregate structures, etc... Due to time constraints and complexity of the neighborhood, this thesis could only address the overturning failures, and only the macroelements recognized as most vulnerable. In-plane failure and interaction between aggregate buildings were not possible. Definitely, this study cannot be called complete without these studies.

In addition, it should be mention that friction within the masonry and masonry with horizontal diaphragms was neglected and the real capacity of these mechanisms should be updated taking into consideration friction.

In most of the cases, the performance point was in the elastic part of the curve and the performance point for both, Method A and Method B was in the same place. On the other hand, for the cases when the performance point was in the inelastic region, with reference to Equation 2.17.19, for the *($F_{max}^{*(0)}$; $d_{max}^{*(0)}$)* was chosen ultimate displacement. ATC (1996) states that it is possible to choose as the first assumption ‘‘any other point is chosen on the basis of engineering judgment’’, therefore, some other points instead of ultimate displacement were chosen for the ($F_{max}^{*(0)}$; $d_{max}^{*(0)}$). Unfortunately, the results were not so promising as the iterations diverged, for no obvious reason. For the mechanism in figure 4.2.6 (a), chart figure 4.2.15 because the performance point with Method A was after the ultimate displacement, it was impossible to obtain the performance point with Method. Although the introduction of the correct damping factor $\eta = 0{,}57$ reduced the NCSE-02 response spectrum, still it didn’t intersect with the capacity curve. The explanation for this lies in the fact that the capacity of this mechanism is very low.

Certainly, one must keep in mind that in this approach the body of the mechanism is assumed as a rigid body (good quality of masonry, with homogenous constructive characteristics and structural behavior), which is a gross oversimplification. However, although it is a simplified technique

In the case of an almost rigid structure where the elastic region was very small, the damage thresholds Sd_1 and Sd_2 are very close together. The differences between them are fractures of a millimeter, meaning that the structure could pas from damage 0 to 2 with just a tiny increase in displacement. According to Lourenco and Mendes (2009) who conducted shaking table test for the Gaioleiro buildings in Lisboa (similar to La Barceloneta), the last floors and the base are most probably the most vulnerable parts of the building; (a) cracking around the corners of the window, (b) out of the plane collapse of the last floor’s piers. The vibration modes with higher frequencies have a significant contribution to the behavior. In respect to that; in-plane failure, friction within the masonry, and slabs with walls have to be investigated.

To conclude, despite the strong capabilities and the reliability of the nonlinear kinematic analysis it should be noted that the selection of the adequate mechanisms is a complex task and it requires a careful in situ inspection. The experience of a seasoned engineer with excellent structural capabilities is mandatory, otherwise, the selection of erroneous mechanisms might result in totally incorrect structural assessment and remedial measures.

5. POSSIBLE INTERVENTIONS

La Barceloneta is characterized by a vulnerability index that lies in the intervals 0.18-0.50, where $i_v = 0.5$ stands for the six-story corner buildings while $i_v = 0.18$ for the two-story attached buildings amongst a row, on a scale from 0-1. For Mediterranean countries, this is a high value and it must be reduced somehow. Out of 1150 buildings, almost half of them (50%) are six-story buildings. If referring to kinematic analysis one of the identified mechanism has a very low activation acceleration $\propto_0 = 0.006g$ (Figure 4.2-6(a), Figure 4.2-18(a)). Certainly, this is not a realistic value, as it doesn’t take into account the friction within the masonry, and between slabs and vertical walls but it is an indication that this is the most vulnerable mechanism. Strengthening of cultural heritage buildings involves many aspects, such as not only the correlation of the expected seismic loads with the resistance of the structural system but also the application of the principles of preservation and the application of simple and economical solutions.

According to Tomaževič (1999), measures for repair and strengthening of masonry buildings are classified into:

a. measures for strengthening of masonry walls
b. measures for tying the walls, and for anchoring and stiffening of floors.

In this thesis, the strengthening proposal will be focused on the second point, as the shear capacity of the structure has not been verified. It is well recognized that the floors should be well connected to the walls, to prevent out of plane failure mechanisms. Structural continuity of vertical and horizontal elements should be provided through the introduction of newer ductile elements. Therefore, the capacity of the building to dissipate energy will lead to the improvement of seismic response. Moreover, this intervention will ensure box behavior without adding rigidity to the structure.
Based on the vulnerability index and kinematic calculations, the riskiest buildings are those with four, five, and six stories.
Two solutions can be considered; anchoring of the .beams on the exterior face with a simple iron bar, with double steel anchors (Figure 4.3-1), or bond beam all around the perimetral walls, Figure 4.3-4. (Tomaževič, 1999).

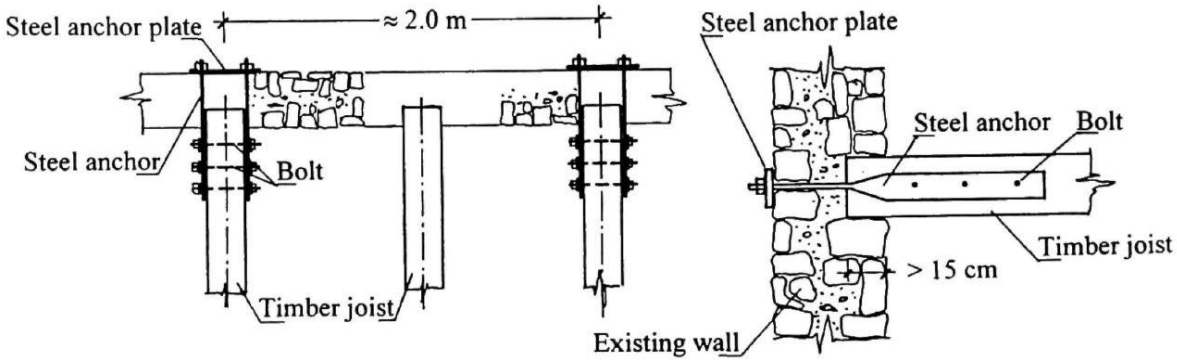

Figure 4.3-1 Detail of anchoring of a wooden floor into a stone-masonry wall (Tomaževič, 1999).

In a similar way to the example in Figure 2.1-1, anchoring details have been developed also for the brick masonry(Figure 4.3-2). Implementation of these anchors will require calculations regarding the diameter of the tie and anchor plates to avoid yield or rupture of the connector rod, rupture at the join between connector rod and joist plate, failure of fixing at joist plate, etc...(Figure 4.3-2).

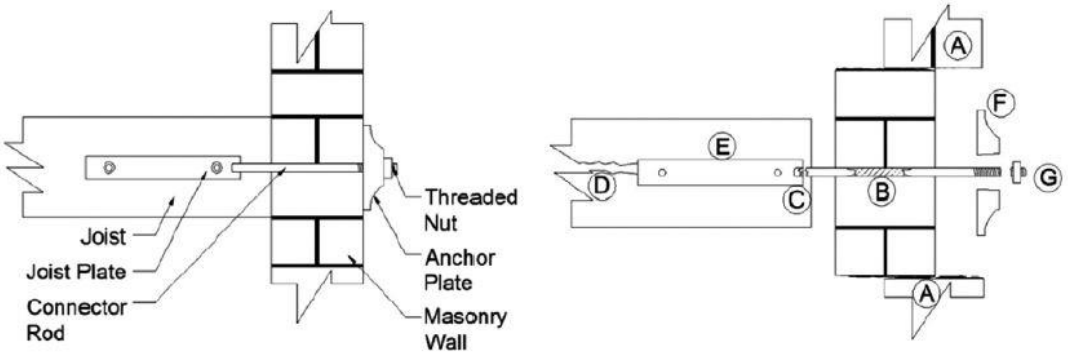

(a) (b)

Figure 4.3-2 wall diaphragm anchor plate connections, (a) connection detail, (b) location of failure modes (Campbell. J et. al, 2012)

Jack arch slabs supported by iron beams represent some difficulties as the I-beam is completely covered by bricks, therefore it can’t be implanted in the same manner. Most probably the I-beams are wrought iron so if welding is applied instead of bolts according to BS EN440 (1995) standards maybe it is a solution. Besides that, the epoxy resins used in the automobile industry would be a reasonable solution, instead of welding. In contrast to timber beams, the insertion of anchors to I-beams has to be a little different because of the issues mention above, they should lie on top and underneath the beam. The figure illustrates the position of the anchors concerning the I-beams (Figure 4.3-3)

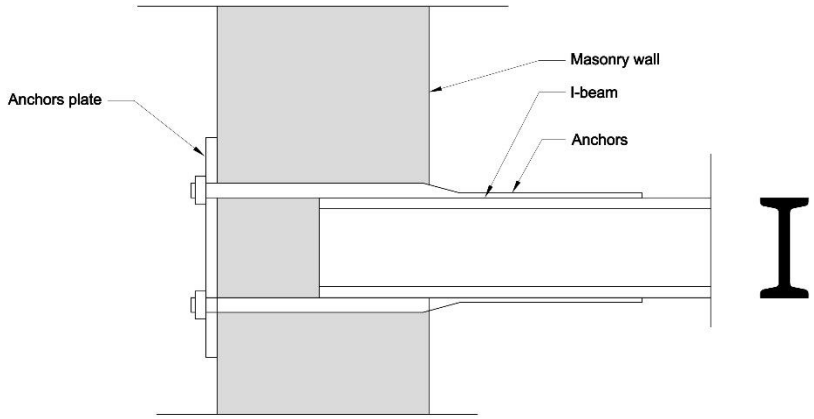

Figure 4.3-3 Strengthening solution for I-beams

Bond beam strengthening would be the ideal system as it provides full confinement to the structure. For the case of masonry walls, the steel ties can be inserted in the bed joints to avoid aesthetic issues.

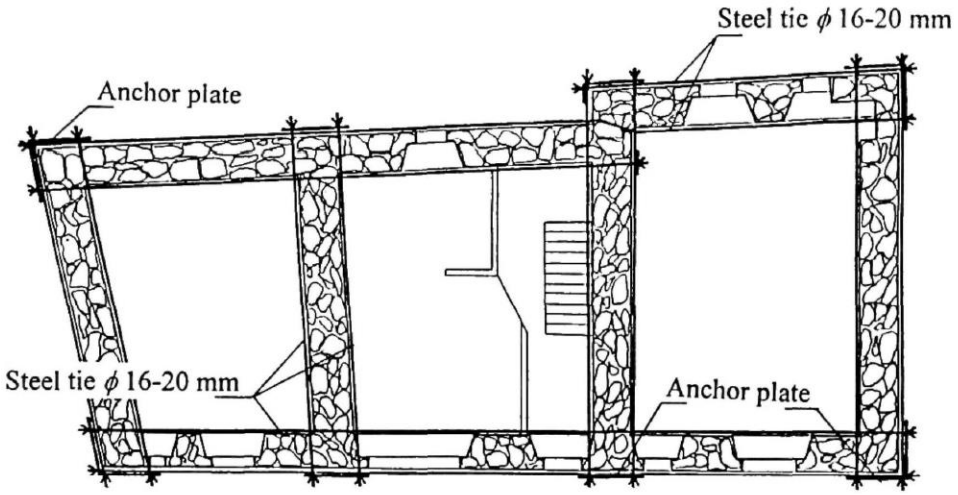

Figure 4.3-4 Position of steel ties in plan (Tomaževič, 1999).

6. CONCLUSIONS

6.1 Summary of the results

The report presents the vulnerability index analysis and nonlinear kinematic analysis of La Barceloneta in chapters three and four, respectively. The damage index for corner buildings was higher compared to the attached buildings amongst a row. In addition, it was noticed that the vulnerability index of a 4-story corner building was equal with the vulnerability index of a 5-story attached building amongst a row. The same was true also when comparing 3-story corner buildings with 4-story attached buildings amongst a row. As stated in chapter 3 section 3 the values obtained from the vulnerability assessment are within the range of the vulnerability index values for the EMS-98 building typologies. For an earthquake of 500 years return period, six-story corner building would be expected to reach damage μ=1.67, while 6-story attached building amongst a row would reach damage μ=1.60,

Next, the Kinematic analysis was carried out. It was found that the level of damage will range between moderate and extensive. Some mechanism will experience damage level 1 while some others damage level 2. In particular, the vertical strip overturning according to calculations is the weakest mechanism and the expected damage level is Dk=4. If this scenario happens then the whole building will probably collapse as this is the wall that supports the floors. The elements with the highest capacity in respect to overturning are those in the main facade with the implication of orthogonal walls. For local failures both categories; corner buildings and attached buildings amongst a row result being at risk since the vertical strip overturning mechanism is present at all the buildings

6.2 The vulnerability of la Barceloneta house

6.3 Comparison of analysis methods

Some conclusions were obtained from the seismic assessment of la Barceloneta through vulnerability index method and kinematic limit analysis. Vulnerability index method is a qualitative approach, strongly influenced by the opinion of the field experts whereas kinematic limit analysis is more rigid method as it takes into consideration the geometry and material properties to assess the capacity of the structure. During the application of the kinematic limit analysis careful selection and determination of the local mechanisms is required, otherwise the results might be in correct.

In the end, the vulnerability index is used to define a parameter and a percentage of the expected damage while kinematic analysis is used to exactly define the expected damage in a specific part. The vulnerability index can be considered as a technique for preliminary assessment that helps the administrators to efficiently allocate the budged in order to increase the safety in a specific region. While, the kinematic limit analysis is used to assess the capacity of the building and as a consequence in the strengthening design.
Furthermore, the vulnerability index is a much faster technique and can be used for large - scale assessment, while kinematic analysis requires more time and in - deep understanding of the structure. However, kinematic limit analysis has proven to be a plausible technic also for the analysis of historical centres. Calvi (1999) applied this method for the evaluation of the historic centre of Catania and obtain very good results.

7. ANNEXES

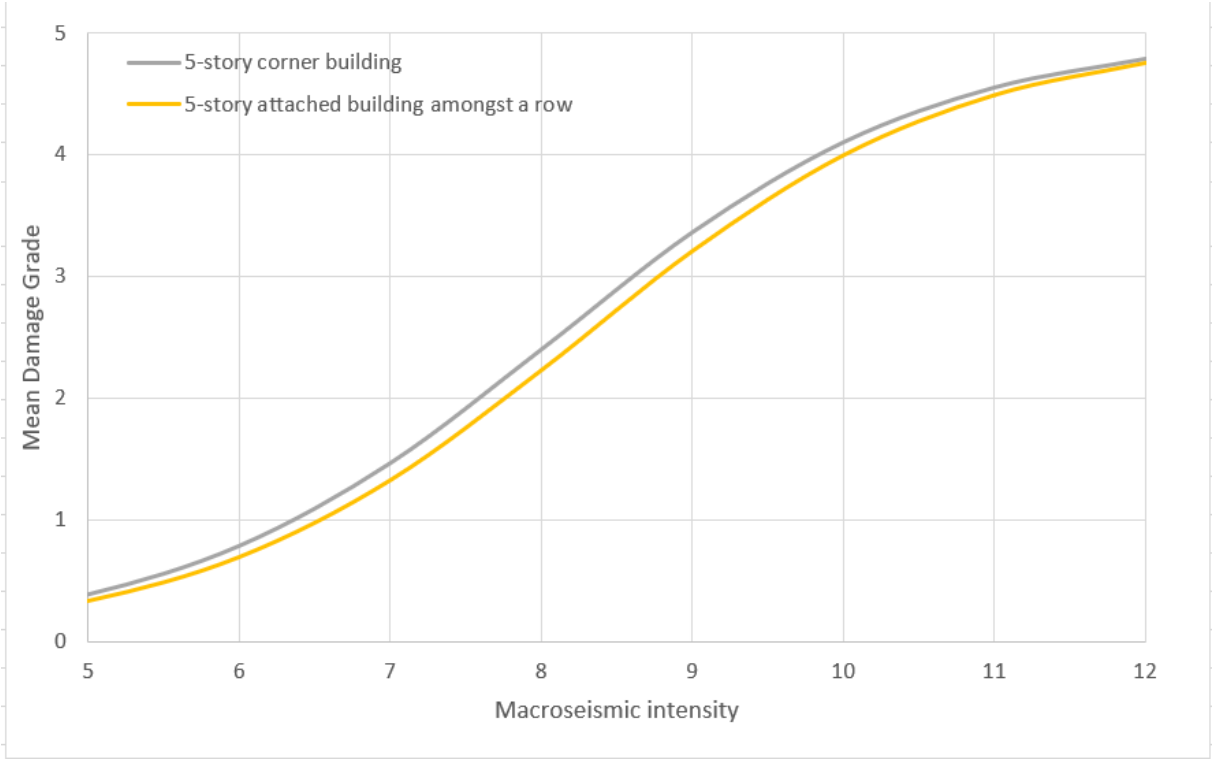

Figure 6.3-1 Macroseismic method, expected damage graph for 4-story buildings

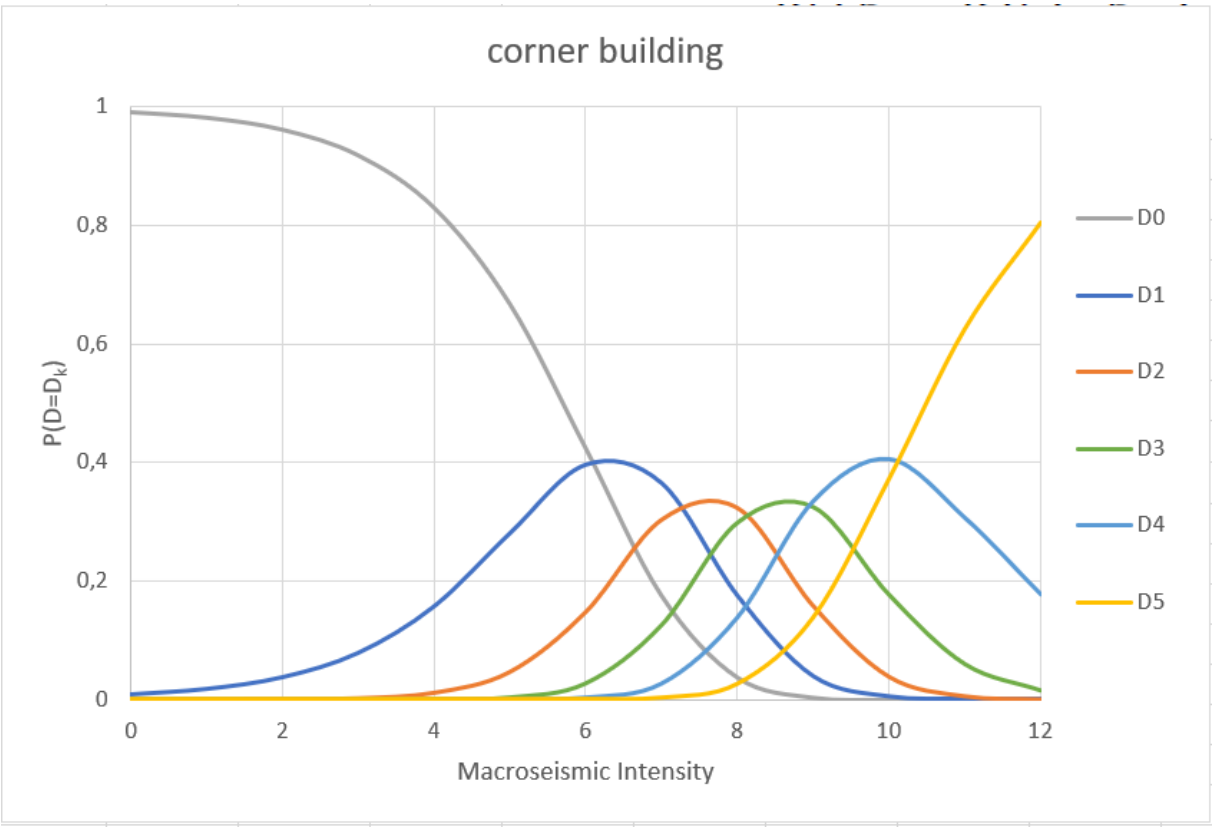

Figure 6.3-2 La Barceloneta, 5-story corner building; probability of each damage level

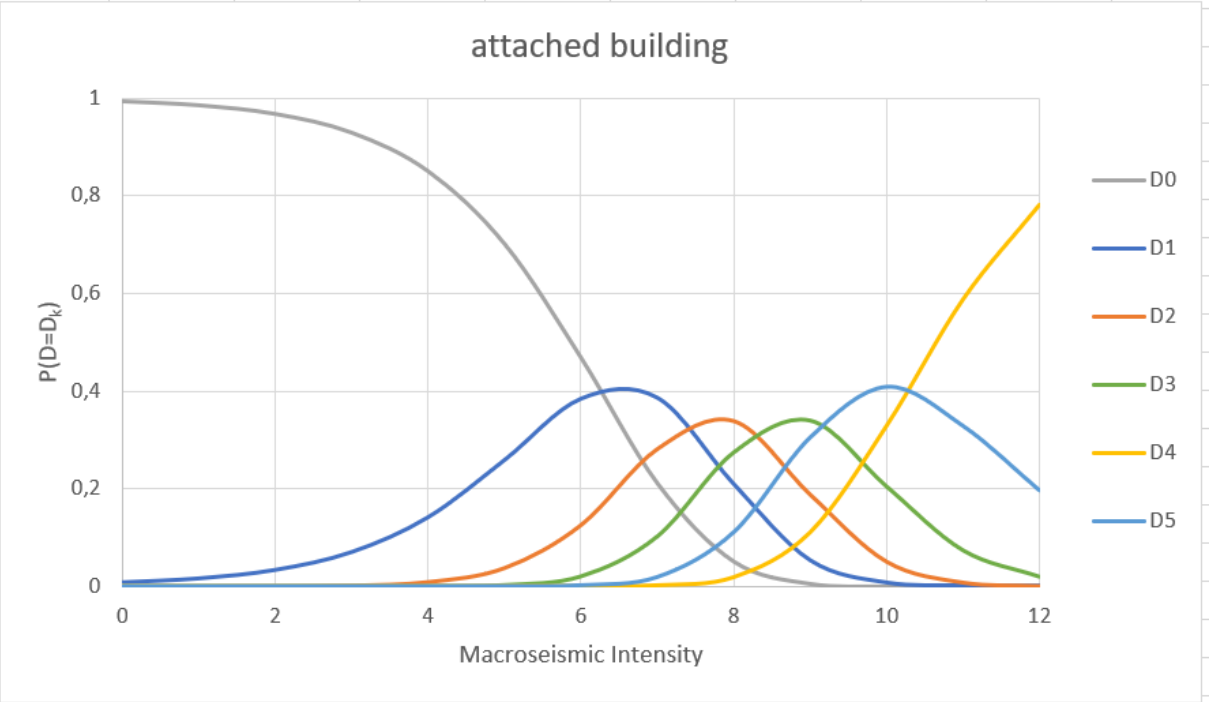

Figure 6.3-3 La Barceloneta, 5-story attached building; probability of each damage level

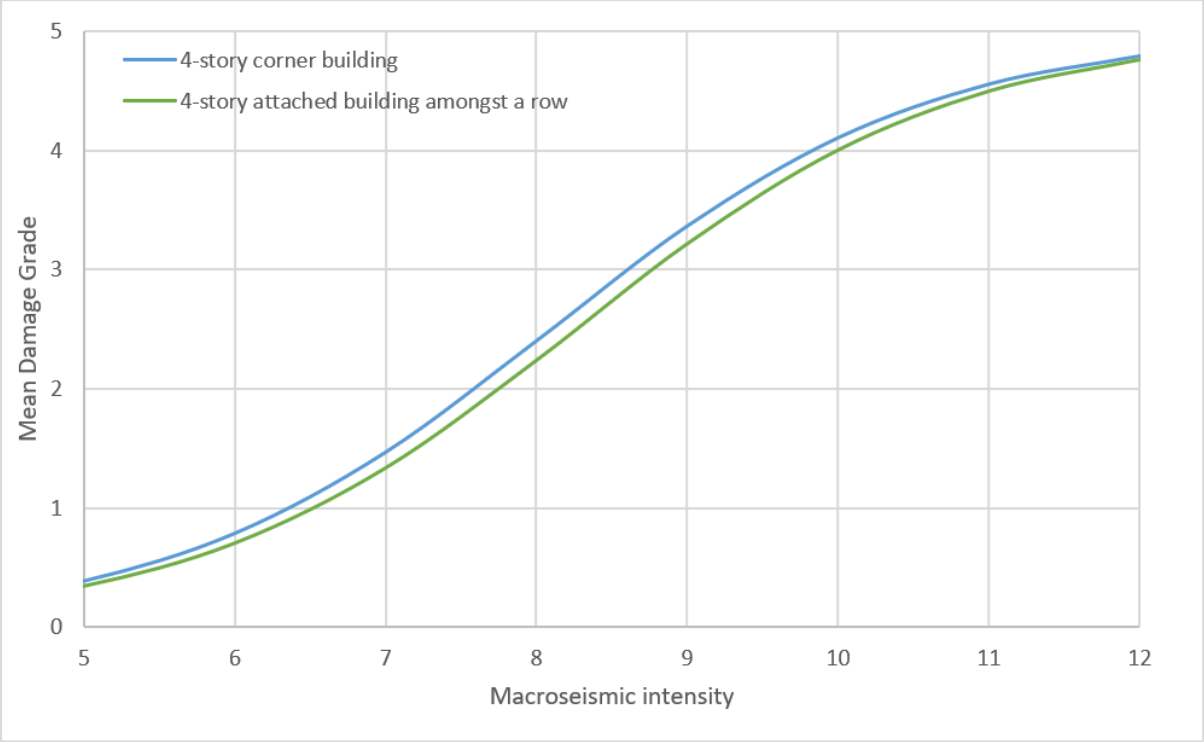

Figure 6.3-4 Macroseismic method, expected damage graph for 4-story buildings

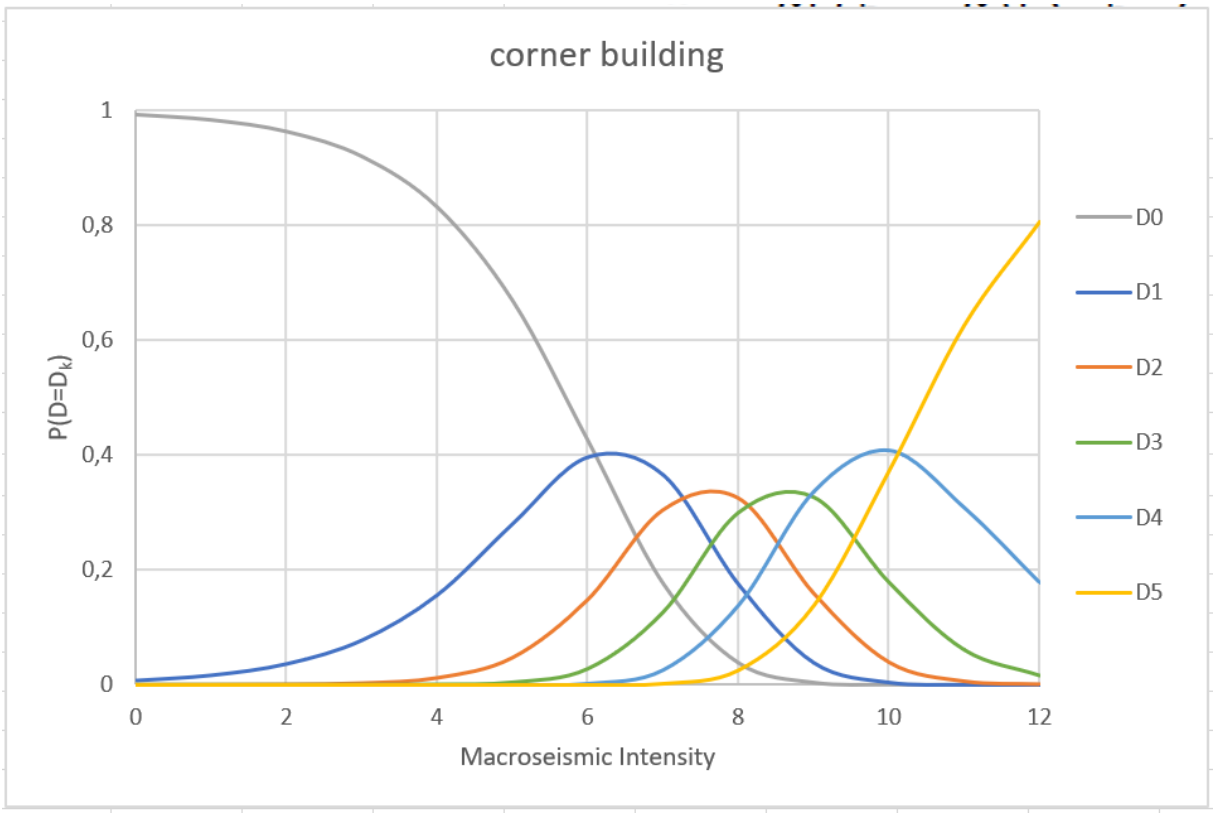

Figure 6.3-5 La Barceloneta, 4-story corner building; probability of each damage level

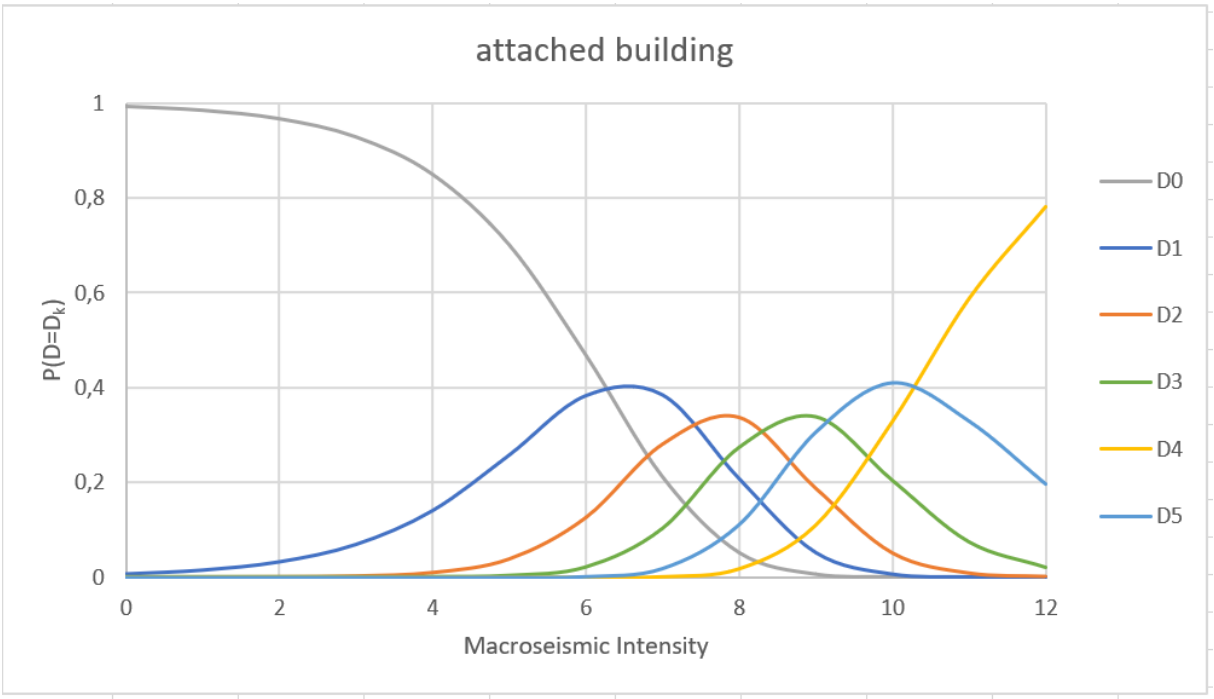

Figure 6.3-6 La Barceloneta, 4-story attached building; probability of each damage level

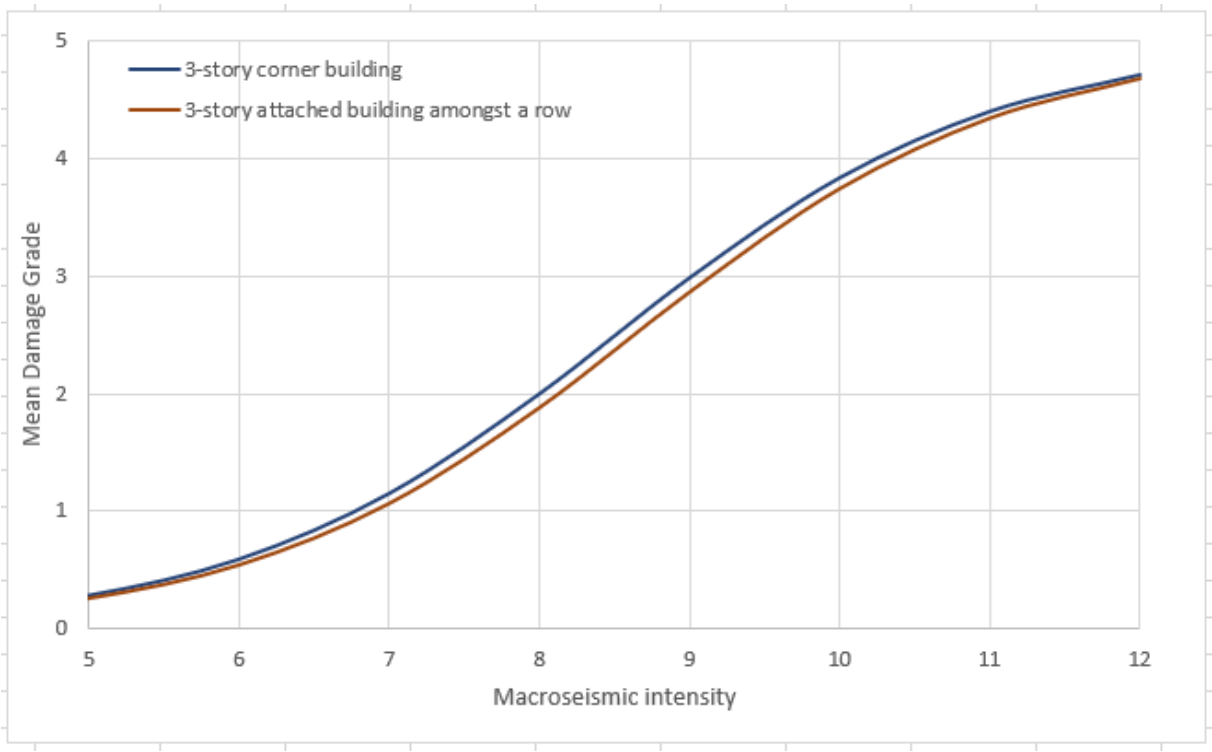

Figure 6.3-7 Macroseismic method, expected damage graph for 3 story buildings

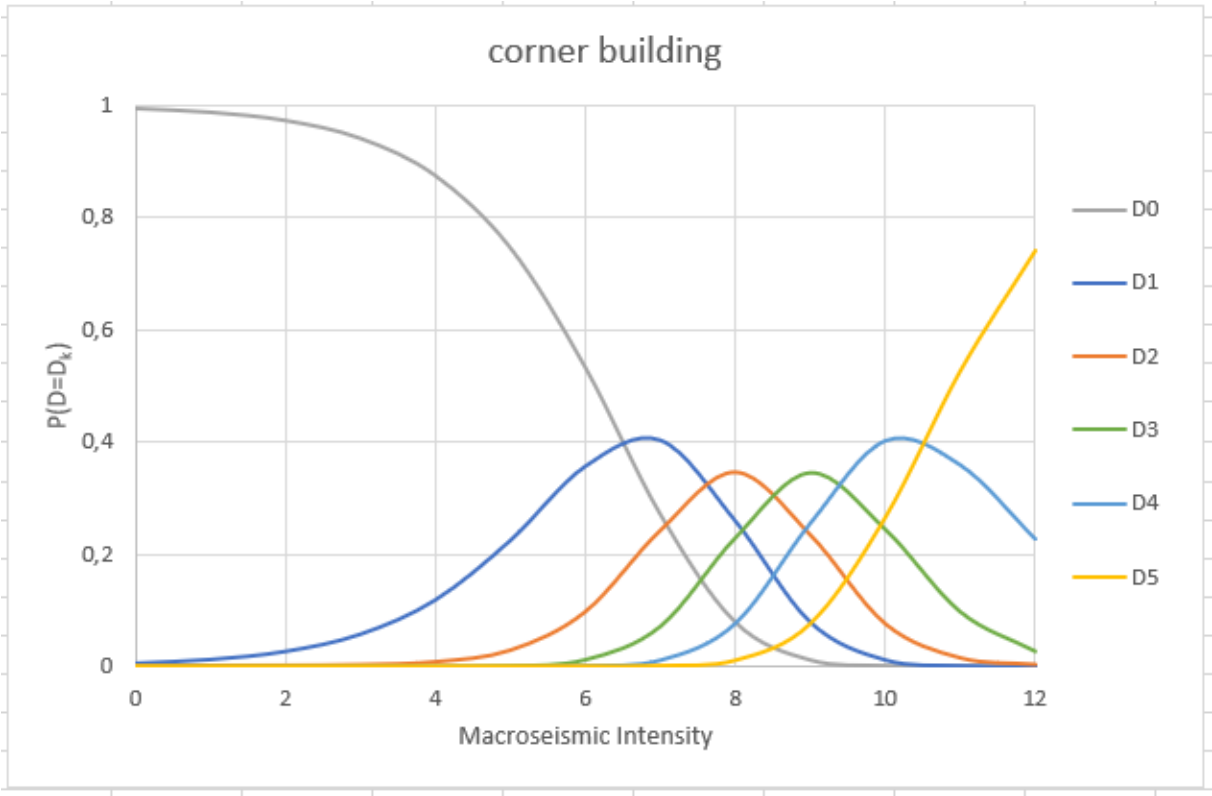

Figure 6.3-8 La Barceloneta, 3-story corner building; probability of each damage level

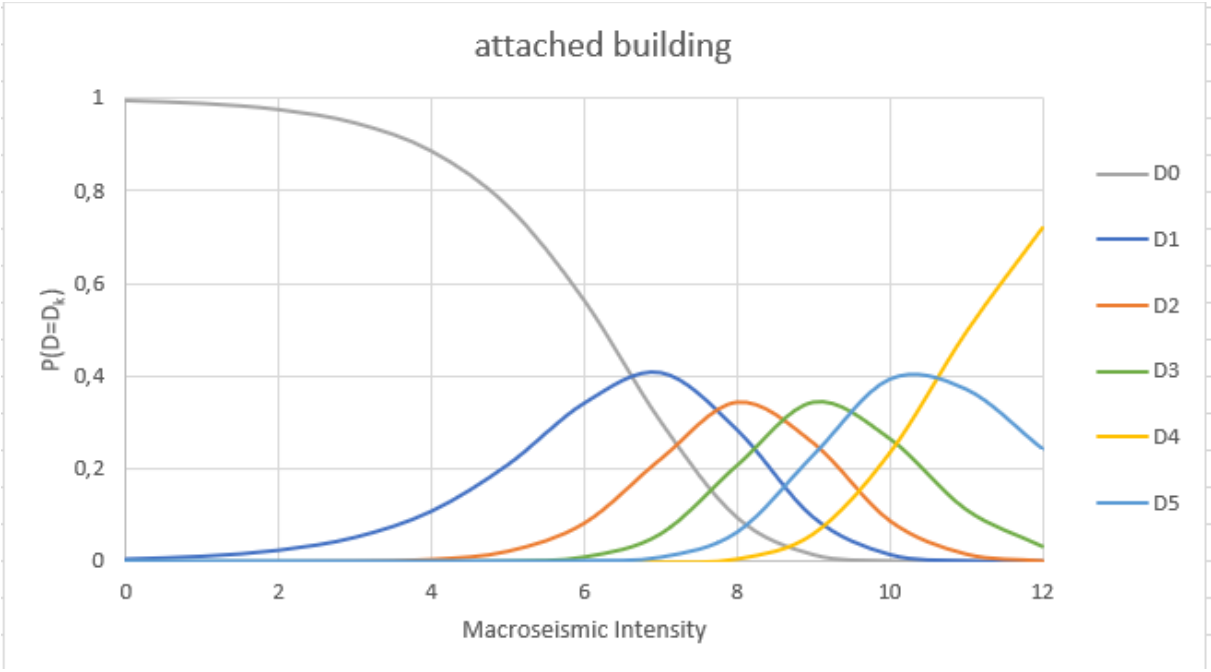

Figure 6.3-9 La Barceloneta, 3-story attached building; probability of each damage level

8. REFERENCES

ASCE, SEI 41, 06 (2007) Seismic Rehabilitation of Existing Buildings. American Society of Civil Engineers, Reston, VA

Aslam, M.; Godden, W.G.; Scalise, D.T. Earthquake Rocking Response of Rigid Bodies. *J. Struct. Div.* **1980**, *106*, 377–392.

ATC-13 (1985) Earthquake damage evaluation data for California. Applied Technology Council, RedwoodCity, California

ATC-21 (1988) Rapid visual screening of building for potential seismic hazards: a handbook. Applied Technology Council, FEMA 145, Redwood City, California

ATC-40 (1996) Seismic evaluation and retrofit of concrete buildings, Technical report, ATC-40. Applied Technology Council, Redwood City, California

Barbat AH, Carreño ML, Pujades LG, Lantada N, Cardona OD, Murulanda MC (2010) Seismic vulnerability and risk evaluation methods for urban areas. A review with application to a pilot area. Struct Infrastruct Eng 6(1–2):17–38

Bernardini A, Giovinazzi S, Lagomarsino S, Parodi S (2007) Vulnerabilità e previsione di danno a scala territoriale secondo una metodologia macrosismica coerente con la scala EMS-98. ANIDIS, XII Convegno Nazionale l’ingegneria sismica in Italia, 10 a 14 Giugno, Pisa
Caicedo C, Barbat AH, Canas JA, Aguiar R (1994) Vulnerabilidad sísmica de edificios, Monografía CIMNEIS-6. Barcelona; 1994

Cardona, O.D. (2001) Estimación holística del riesgo sísmico utilizando sistemas dinámicos complejos. Universidade Politécnica de Cataluña. PhD Thesis, Barcelona, Spain

Calvi GM (1999) A displacement-based approach for vulnerability evaluation of classes of buildings. J Earthq Eng 3(3):411–438

Coburn AW, Spence R (2002) Earthquake protection. Wiley, Chichester, England

D’Ayala D, Speranza E (2003) Definition of Collapse Mechanisms and Seismic Vulnerability of Historic Masonry Buildings. Earthq Spectra 19(3):479–509

D’AyalaD(2005) Force and displacement-based vulnerability assessment for traditional buildings. Bull Earthq Eng 3:235–265 McGuire RK (2004) Seismic hazard and risk analysis, EERI Monography. Earthquake Engineering Research Institute, Oakland, CA

Doherty K, Griffith MC, Lam NTK, Wilson JL (2002) Displacement-based analysis for out-of-plane bending of seismically loaded unreinforced masonry walls. Earthq Eng Struct Dynam 31(4):833–850

EN 1998-1 (2004) Eurocode 8: Design of structures for earthquake resistance—Part 1: General rules, seismic actions, and rules for buildings. CEN (European Committee for Standardization), Brussels, Belgium

Fajfar P (1999) Capacity spectrum method based on inelastic demand spectra. Earthq Eng Struct Dynam 28(9):979–993

FEMA 273 (1996) NEHRP guidelines for the seismic rehabilitation of buildings. Federal Emergency Management Agency, Washington DC

FEMA 178 (1992) NEHRP handbook for the seismic evaluation of existing buildings. Federal Emergency Management Agency, Washington, DC

Freeman SA (1998) Development and use of capacity spectrum method. Proceedings of 6th U.S. National Conference on Earthquake Engineering, Seattle, CD-Rom, Paper #269, EERI, Oakland, Ca

Griffith MC, Lam NTK, Wilson JL, Doherty K (2004) Experimental investigation of unreinforced brick masonry wall in flexure. J Struct Eng (ASCE) 130(3):423–432

GriffithMC, MagenesG, Melis G, Picchi L (2003) Evaluation of out-of-plane stability of unreinforced masonry walls subjected to seismic excitation. J Earthq Eng 7(S1):141–169.

Gruppo Nazionale per la Difesa dai Terremoti–GNDT-SSN (1994) Scheda di esposizione e vulnerabilità e di rilevamento danni di primo livello e secondo livello (muratura e cemento armato). Gruppo Nazionale per la Difesa dai Terremoti: Roma

Grünthal G (1998) European macroseismic scale. Centre Européen de Géodynamique et de Séismologie: Luxembourg. vol 15

Giovinazzi S, Lagomarsino S (2004) A macroseismic model for the vulnerability assessment of buildings. In: Proceedings of 13th world conference on earthquake engineering. Vancouver: Canada

Giovinazzi S (2005) The vulnerability assessment and damage scenario in seismic risk analysis. PhD Thesis, International doctorate, University of Florence, Technical University of Carolo-Wilhelmina

HAZUS MH (1999) Earthquake loss estimation methodology—technical and user manuals. Federal Emergency Management Agency, Washington, D.C

LESSLOSS (2007) European research project for risk mitigation for earthquakes and landslides (2004–2007); Website: http://www.lessloss.org/main/index.php (last viewed December 2007)

Housner, G.W. The behavior of inverted pendulum structures during earthquakes. *Bull. Seismol. Soc. Am.* **1963**, *53*, 403–417.

Ishiyama, Y. Motion of rigid bodies and criteria for overturning by earthquake excitations. *Earthq. Eng. Struct. Dyn.* **1982**, *10*, 635–650.

Jokilehto, J. 2010. Notes on the Definition and Safeguarding of HUL. City & Time 4 (3): 4. [online] url: http://www.ct.cecibr.org.

Istruzioni per l’applicazione dell’«Aggiornamento delle “Norme tecniche per le costruzioni”» di cui al decreto ministeriale 17 gennaio 2018. Gazzeta Ufficiale, MINISTERO DELLE INFRASTRUTTURE E DEI TRASPORTI, REPUBBLICA ITALIANA

Lagomarsino S, Resemini S (2009) The assessment of damage limitation state in the seismic analysis of monumental buildings. Earthq Spectra 25(2):323–346

Lagomarsino, S., & Podesta, S. (2004b). Seismic vulnerability of ancient churches: II. Statistical Analysis of Surveyed Data and Methods for Risk Analysis. *Earthquake Spectra*, *20*(2), 395–412

Luca Pelà (2018) New Trends and Challenges in Large-Scale and Urban Assessment of Seismic Risk in Historical Centres, International Journal of Architectural Heritage, 12:7-8, 1051-1054,

Makris, N. A half-century of rocking isolation. *Earthq. Struct.* **2014**, *7*, 1187–1221.

Makris N, Konstantinidis D (2001) The rocking spectrum and the shortcomings of design guidelines. Report No. PEER-01/07, Pacific Earthquake Engineering Research Center, Berkeley, CA

Makris N, KonstantinidisD(2003) The rocking spectrum and the limitations of practical design methodologies. Earthq Eng Struct Dyn 32(2):265–289

Modena, C., Valluzzi, M. R., da Porto, F., & Casarin, F. (2011). Structural Aspects of The Conservation of Historic Masonry Constructions in Seismic Areas: Remedial Measures and Emergency Actions. *International Journal of Architectural Heritage: Conservation, Analysis, and Restoration*, *5:4-5*, 539–558. https://doi.org/10.1080/15583058.2011.569632

Milutinovic, Z. V., & Trendafilosk, G. S. (2004). *WP4 Vulnerability of current buildings*. https://doi.org/10.1007/978-1-4020-3608-8_23

Ministerial Circular of Infrastructure and Transport. I*nstructions for the application of the New Technical Rules for Constructions (M.D. 14/01/08)*; M.C. n. 617, published on 02/02/09, Official Gazette of the Italian Republic n. 47, February 26. Available online: http://www.gazzettaufficiale.it/eli/gu/2009/02/26/47/so/27/sg/pdf

NCSE-02 (2002) “Normativa de Construcción Sismorresistente Española”. Real Decreto 997/2002. Boletín Oficial del Estado No 244 del 11 de Octubre de 2002.

NTC. (2018). Aggiornamento delle “Norme tecniche per le costruzioni.” *Gazzetta Ufficiale DellaRepubblica Italiana*, 1–198.

NTC. (2019). Istruzioni per l’applicazione dell’≪Aggiornamento delle “Norme tecniche per le costruzioni”≫ di cui al decreto ministeriale 17 gennaio 2018. *Gazzetta Ufficiale Della Repubblica Italiana*.

Priestly MJN, Evison RJ, Carr AJ (1978) Seismic response of structures free to rock on their foundations. Bull N Z Nat Soc Earthq Eng 11(3):141–150

RISK-UE Project (2004). An advanced approach to earthquake risk scenarios, with applications to different European cities; Website: http://www.risk-ue.net (last viewed December 2007)

Speranza E (2003) An integrated method for the assessment of the seismic vulnerability of historic buildings. PhD Thesis. University of Bath

Sergio Lagomarsino Seismic (2014) assessment of rocking masonry structures. Bull Earthquake Eng (2015) 13:97–128

Smith, W. (2005). The challenge of earthquake risk assessment, Seism. Res. Lett., 76, p. 415–416.

UNDP/UNIDO (1985) Project RER/79/015. Post-earthquake damage evaluation and Strength Assessment of Buildings under Seismic Condition. UNDP, Vienna

Vicente RS (2008) Strategies and methodologies for urban rehabilitation interventions. The vulnerability assessment and risk evaluation of the old city centre of Coimbra. PhD Thesis, University of Aveiro (in Portuguese)

Vicente RS, Varum H, Mendes da Silva JAR (2005) Seismic vulnerability assessment of buildings in the old city centre of Coimbra. In: Proceedings of the international conference 250th anniversary of the 1755 Lisbon earthquake, 1st–4th November, pp 206–213